AD_____

Contract Number DAMD17-96-C-6088

TITLE: Production and Enzyme Engineering of Human Acetylcholinesterase and Its Mutant Derivatives

PRINCIPAL INVESTIGATOR: Avigdor Shafferman, Ph.D.

CONTRACTING ORGANIZATION: Israel Institute for Biological Research
7045 Ness-Ziona Israel

REPORT DATE: June 1998

TYPE OF REPORT: Midterm

PREPARED FOR: U.S. Army Medical Research and Materiel Command
Fort Detrick, Maryland 21702-5012

REPORT DOCUMENTATION PAGE

Form Approved
OMB No. 0704-0188

1. AGENCY USE ONLY *(Leave blank)*	2. REPORT DATE	3. REPORT TYPE AND DATES COVERED
	June 1998	Midterm (16 Sep 96 - 16 Feb 98)

4. TITLE AND SUBTITLE
Production and Enzyme Engineering of Human Acetylcholinesterase and Its Mutant Derivatives

5. FUNDING NUMBERS
DAMD17-96-C-6088

6. AUTHOR(S)
Avigdor Shafferman, Ph.D.

7. PERFORMING ORGANIZATION NAME(S) AND ADDRESS(ES)
Israel Institute for Biological Research
7045 Ness-Ziona Israel

8. PERFORMING ORGANIZATION REPORT NUMBER

9. SPONSORING/MONITORING AGENCY NAME(S) AND ADDRESS(ES)
U.S. Army Medical Research and Materiel Command
Fort Detrick, Maryland 21702-5012

10. SPONSORING/MONITORING AGENCY REPORT NUMBER

11. SUPPLEMENTARY NOTES

12a. DISTRIBUTION / AVAILABILITY STATEMENT
Approved for public release; distribution unlimited

12b. DISTRIBUTION CODE

13. ABSTRACT *(Maximum 200*

The research is directed towards design of pharmacologically useful bio-scavengers against organophosphate poisoning, by : a. structure-reactivity studies of human acetylcholinesterase (HuAChE) and its mutant derivatives with various covalent and noncovalent ligands including CW agents; b. studies on molecular surface properties of HuAChE derivatives affecting biosynthesis, stability and clearance. Combination of recombinant DNA technology, kinetic studies , molecular modeling, x-ray crystallography and electro-spray MS methods are employed to identify the residues involved in direct interactions with phosphates and phosphonates and in the subsequent reactivation or aging processes. Our findings allow to define the structural determinants in the active center facilitating the bio-scavenging and provide clear directions for design of optimal bioscavengers which will combine advantageous properties of phosphylation, reactivation and aging via targeting mutations at specific residues. In the past we have demonstrated that a control over the number of vacant sialic acid attachment sites may improve the enzyme residence time in the bloodstream. Here we report that indeed by engineering cells expressing high levels of both recombinant HuAChE and recombinant 2,6-sialyltransferase we were able to extend significantly the residence time of the HuAChE bioscavenger.

14. SUBJECT TERMS	15. NUMBER OF PAGES
Human Acetylcholinesterase, Enzyme Engineering, Mutagenesis, Molecular Modeling, Organophosphorus Inhibitors, CW Agents, Pharmacokinetics, Bioscavengers, Glycosylation, Sialylation	159
	16. PRICE CODE

17. SECURITY CLASSIFICATION OF REPORT	18. SECURITY CLASSIFICATION OF THIS PAGE	19. SECURITY CLASSIFICATION OF ABSTRACT	20. LIMITATION OF ABSTRACT
Unclassified	Unclassified	Unclassified	Unlimited

FOREWORD

Opinions, interpretations, conclusions and recommendations are those of the author and are not necessarily endorsed by the US Army.

_____ Where copyrighted material is quoted, permission has been obtained to use such material.

_____ Where material from documents designated for limited distribution is quoted, permission has been obtained to use the material.

_____ Citations of commercial organizations and trade names in this report do not constitute an official Department of Army endorsement or approval of the products or services of these organizations.

____X___ In conducting research using animals, the investigator(s) adhered to the "Guide for the Care and Use of Laboratory Animals," prepared by the Committee on Care and Use of Laboratory Animals of the Israel Institute for Biological Research.

_____ For the protection of human subjects, the investigator(s) adhered to policies of applicable Federal Law 45 CFR 46.

_____ In conducting research utilizing recombinant DNA technology, the investigator(s) adhered to current guidelines promulgated by the National Institutes of Health.

_____ In the conduct of research utilizing recombinant DNA, the investigator(s) adhered to the NIH Guidelines for Research Involving Recombinant DNA Molecules.

_____ In the conduct of research involving hazardous organisms, the investigator(s) adhered to the CDC-NIH Guide for Biosafety Microbiological and Biomedical Laboratories.

11-6-98

PI - Signature Date

PRODUCTION AND ENZYME ENGINEERING OF HUMAN ACETYLCHOLINESTERASE AND ITS MUTANT DERIVATIVES

MIDTERM REPORT

BARUCH VELAN*
ARIE ORDENTLICH*
NAOMI ARIEL*
SHAUL REUVENI‡
YOFFI SEGALL#
DANA STEIN*
ARIE LAZAR‡
SARA COHEN*
ITAI MENDELSON*
DANA BERMAN*
DOV BARAK#
CHANOCH KRONMAN*
THEODOR CHITLARU*
TAMAR SERY*
NEHAMA ZELIGER*
LEA SILBERSTEIN‡
TAMAR BINO*
LEVANA MOTULA*
DINO MARCUS‡
SHIRLEY LAZAR*

AVIGDOR SHAFFERMAN*‡

We greatly appreciate the contribution of Mrs ESTHER HABERMAN≠ to the administrative management of the contract

*Department Of Biochemistry
#Department of Organic Chemistry
‡Department of Biotechnology
≠Division of Biology

CONTENTS

CONTENTS (Cont'd) Page

CONTENTS (Cont'd) Page

LIST OF FIGURES

LIST OF FIGURES (Cont'd) Page

LIST OF TABLES

I. General Introduction

The primary role of acetylcholinesterase (acetylcholine acetylhydrolase, 3.1.1.7 AChE), is the termination of impulse transmission in cholinergic synapses by rapid hydrolysis of the neurotransmitter acetylcholine (ACh). A second ACh hydrolysing enzyme butyrylcholinesterase (alcholine acyl hydrolase 3.1.1.8, BChE), often appears together with AChE in various tissues. BChE differs from AChE in its substrate specificity and in susceptibility to inhibitors. Several cholinesterase inhibitors remain of value as medicinal agents and pesticides while others possess the potential for use as chemical warfare agents. Some AChE inhibitors (e.g. phospholineiodide and physostigmine) are useful therapeutic agents in the treatment of glaucoma. In addition, the quaternary carbamates neostigmine and pyridostigmine are currently used for the treatment of myasthenia gravis (Taylor, 1990). Modifications in the levels of human brain AChE have been reported in several neurological and genetic disorders, such as Alzheimer disease (Coyle *et al.,* 1983) and Down's Syndrome (Yates *et al.,* 1980). Indeed the first drug approved recently by the FDA to treat Alzheimer disease is an AChE inhibitor - tacrine. Some organophosphorus (OP) inhibitors of ChEs such as malathion and diazinon, act as efficient insecticides and have been widely used in combating medfly and other agricultural pests. Other OP compounds, such as the nerve agents sarin and soman, inhibit AChE irreversibly by rapid phosphorylation of the serine residue in the enzyme active site. The acute toxicity of these nerve agents is elicited in motor and respiratory failure following inhibition of AChE in the peripheral and central nervous system. The current treatment regimes against nerve agent exposure are designed to protect life but are not able to prevent severe incapacitation. The use of exogenous scavengers such as AChE and BChE has been successfully demonstrated in animals (Wolf *et al.,* 1987; Raveh *et al.,* 1989; Broomfield *et al.,* 1991; Doctor *et al.,* 1992) for sequestration of highly toxic OPs before they reach their physiological target.

Elucidation of the primary structure of various cholinesterases (Schumacher *et al.,* 1986; Hall and Spierer 1986; Lockridge *et al.,* 1987; Prody *et al.,* 1987; Sikarov *et al.,* 1987; Chatonnet and Lockridge 1989; Olson *et al.,* 1990; De la Escalera *et al.,* 1990; Rachinsky *et al.,* 1990; Doctor *et al.,* 1990) and the recent solution of the crystal structure of a AChE (Sussman *et al.,* 1991) added new perspectives to cholinesterase research. Recently we developed (under U.S. contract no. DAMD17-89-C-9117) efficient mammalian expression systems for recombinant human AChE

(Velan *et al.* 1991a; Kronman *et al.* 1992). We also developed experimental systems for generating AChE mutants and methods for evaluation of their activity and conformation (Shafferman *et al.*, 1992a-d). All these developments provide the basis for identification of some of the critical elements of the active center such as the amino acids that constitute the "anionic" or the choline binding subsite, the acyl pocket and residues that determine specificity for the hydrophobic moiety of ligands and substrates, the peripheral anionic subsite (Ordentlich *et al.*, 1993a,b; Shafferman *et al.*, 1993; Ashani *et al.*, 1994; Barak *et al.*, 1994; Kronman *et al.*, 1994; Shafferman *et al.*, 1994; Barak *et al.*, 1995; Ordentlich *et al.*, 1995; Shafferman *et al.*, 1995; and see Figure 1). We are now involved in studies aimed at determinig how specific residues in the active center of human AChE (HuAChE) manifest the specificity towards different OP-inhibitors (Ordentlich *et al.*, 1995) and in demonstrating the ability to generate novel enzymes that are either more efficient in OP scavenging or highly resistant to the aging process (Ordentlich *et al.*, 1993b). We have begun the analysis of the role of oligosaccharide side chains and oligomerization in clearance of cholinesterases from the circulation (Kerem *et al.*, 1993; Velan *et al.*, 1993a,b; Shafferman *et al.*, 1994; Velan *et al.*, 1994; Kronman *et al.*, 1995; Velan *et al.*, 1995). All these studies provided the basis for the current research which is directed towards design of efficient OP-bioscavenger through manipulation of the biosynthetic pathways of production of recombinant human AChE and through further analysis and alterations of residues determining the functional characteristics of AChE.

This midterm report covers the progress in all these research areas. The first (section II) describes our current knowledge regarding the contribution of various subsites to reactivation of an OP-AChE conjugate. Sections III,IV and V are all related to novel aspects of the aging processes of OP-AChE conjugates. Section VI describes molecular dynamic studies related to the allosteric site of AChE - the omega loop. Section VII describes the studies which were aimed at testing some of the predictions from the theoretical studies described on section VI. Section VIII describes the progress made in elucidation of a post translation pathway determining the short residence time in circulation of recombinant AChE and the genetic manipulation of cells producing the enzyme which led to production of human AChE with improved pharmacokinetic profile. Section IX presents the main conclusions emerging from the studies described in previous sections and the main directions for future development of an AChE bioscavenger.

A.

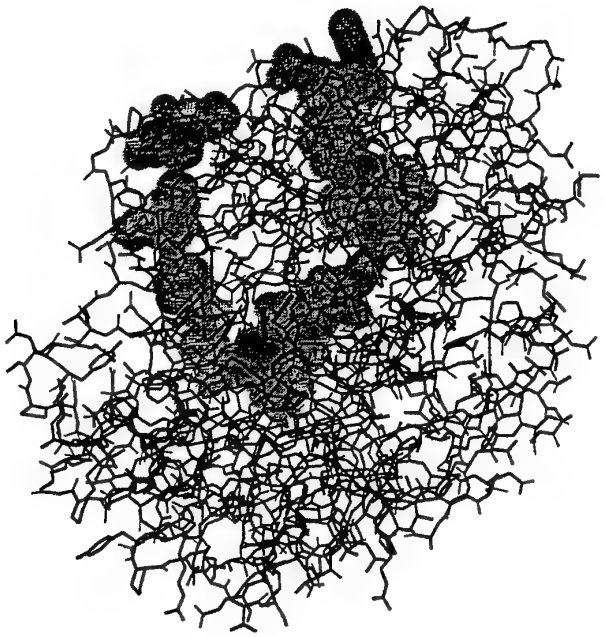

B.

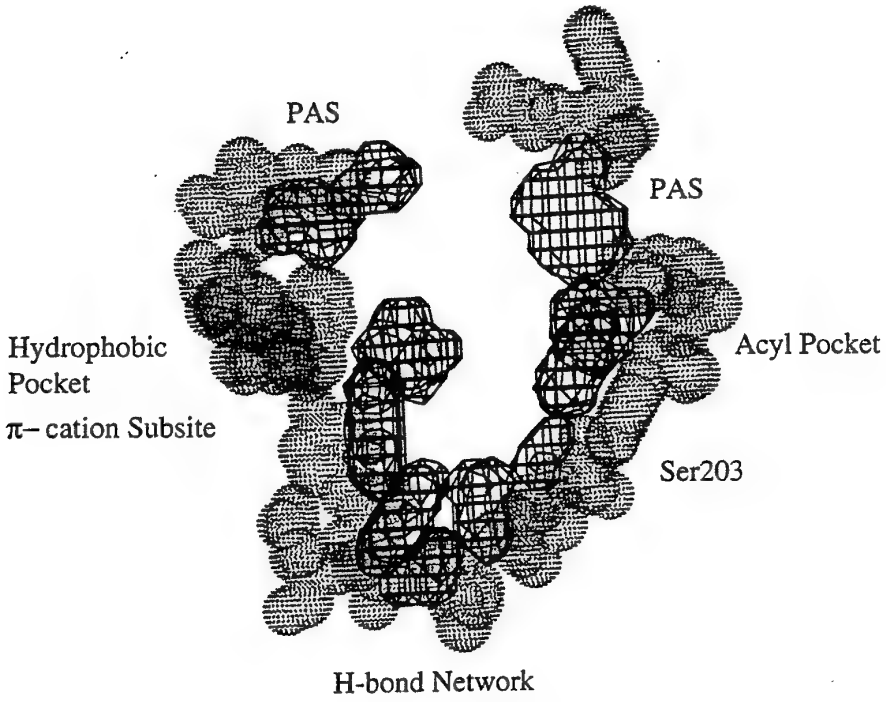

Fig.1 Functional Map of AChE Subsites. **A** - HuAChE molecular model. The gorge is denoted by a dot surface. **B**- The AChE functional subsites. The subsites are denoted by a grid surface. The catalytic triad: Ser203, His447, Glu334; π-cation subsite: Trp86; Acyl pocket: Phe295, Phe 297; Hydrophobic pocket: Tyr337, Phe338, (Trp86); H-bond network: Tyr133, Glu202, Glu450, Gly120, Gly448; PAS-Peripheral anionic subsite: Tyr72, Asp74, Tyr124, Trp286, Tyr341.

II. Reactivation of Diethylphosphoryl Adducts of Human Acetylcholinesterase and its Mutant Derivatives by Various Reactivators

INTRODUCTION

Acetylcholinesterase (AChE; EC 3.1.1.7) a key enzyme in cholinergic transmission is the major target of poisoning by organophosphorus agents through phosphylation at the catalytic serine. Inactivation of AChE leads to an overstimulation of cholinergic receptors and symptoms such as salivation, tremors and miosis, and at larger doses of the phosphylating agent, to respiratory paralysis and death (Chambers *et al.,* 1992). The phosphylated AChE may undergo spontaneous reactivation by hydrolytic displacement of the phosphyl moiety from the enzyme, however this is usually a slow and inefficient process of no practical significance (Aldridge and Reiner, 1972). Alternatively, such displacement can be readily accomplished by an appropriate nucleophile like fluoride or oximes to generate a reactivated enzyme molecule (Gray, 1984; Wilson *et al.,* 1992). Thus, AChE reactivation by certain oximes is an important part of the treatment in cases of human poisoning by organophosphorus derivatives like insecticides or warfare nerve agents (Ellin, 1982; Taylor, 1990). Despite the therapeutic significance of the oxime reactivators and notwithstanding the considerable effort invested in development of new derivatives, surprisingly little is known about the structure-activity relationship associated with the reactivation process. Reactivators like the monoquaternary 2-PAM (pyridine-2-aldoxime methyl iodide; the methanesulfonate salt is known as P2S) and the bisquaternary TMB-4 are particularly effective in reactivating phosphorylated AChEs and relatively ineffective in reactivating phosphonyl-conjugates (Rousseaux and Dua, 1989; Eyer *et al.,* 1992). On the other hand, HI-6 is more effective in reactivating phosphonylated AChEs which result from exposure to potent organophosphorus inhibitors such as sarin and soman (Rousseaux and Dua, 1989; Clement *et al.,* 1991). The apparent lack of correlation between the structural features of the reactivators and their reactivation efficiencies, is a major obstacle to development of novel advantageous oxime reactivators.

The resolution of the X-ray structure of AChE (Sussman *et al.*, 1991) together with extensive site-directed mutagenesis studies of recombinant enzyme molecules (Gibney *et al.*, 1990; Shafferman *et al.*, 1992b,c; Harel *et al.*, 1992; Vellom *et al.*, 1993; Ordentlich *et al.*, 1993a; Taylor and Radic, 1994; Barak *et al.*, 1994; Gnatt *et al.*, 1994; Ordentlich *et al.*, 1995) have opened a new avenue to investigate structure-function features of AChE reactivity. This has led to the dissection of the active center architecture (Vellom *et al.*, 1993; Taylor and Radic, 1994; Ordentlich *et al.*, 1995), analysis of the involvement of the periphery in HuAChE reactivity (Shafferman *et al.*, 1992c ; Barak *et al.*, 1994; Ordentlich *et al.*, 1995; Radic *et al.*, 1994) and examination of the phosphorylation (Ordentlich *et al.*, 1996), aging (Ordentlich *et al.*, 1993b) and reactivation (Ashani *et al.*, 1995) processes.

Here we report on the application of this approach to gain insight into the reactivation of phosphorylated HuAChE. We examine the reactivity of three structurally distinct reactivators towards phosphorylated HuAChE and selected derivatives of this enzyme, in which critical residues were replaced by site directed mutagenesis. The extensive kinetic studies unravel some of the characteristics of the reactivation process yet also indicate that the reactivity patterns of phosphylated HuAChE enzyme towards oxime reactivators are more complex than originally appreciated.

METHODS

Generation of HuAChE Mutants HuAChE mutants Y72A(*70*) (the numbers in parentheses refer to the positions of analogous residues in TcAChE according to the recommended nomenclature, Massoulie *et al.,* 1992) D74N(*72*), W86A(*84*), E202A, E202Q(*199*), W286A(*279*), F295A(*288*), F297A(*290*), Y337A, Y337F(*F330*), F338A(*331*), E450A(*443*) and the double mutant Y72A/W286A were generated as described previously (Shafferman *et al.,* 1992b,c; Ordentlich *et al.,* 1993a; Barak *et al.,* 1994; Ordentlich *et al.,* 1996). The HuAChEs were expressed in the human embryonal kidney 293 cell line (Velan *et al.,* 1991b; Kronman *et al.,* 1992). Stable recombinant cell clones expressing high levels of wild type (WT) and mutant AChEs were propagated in multitray systems (Lazar *et al.,* 1993), and enzymes were purified (over 90% purity) either by ligand affinity chromatography (Kronman *et al.,* 1992) or by fractionation on monoclonal antibody affinity columns (Barak *et al.,* 1995).

Analysis of AChE Activity All kinetic studies were carried out with acetylthiocholine iodide (ATC- Sigma) as substrate (Ellman *et al.,* 1961). Standard assays were performed in the presence of 0.2 mg/ml BSA, 0.3mM DTNB (5,5'-dithiobis(2-nitrobenzoic acid)) 50mM sodium-phosphate buffer pH-8.0 and 0.5 mM ATC or other concentrations, as indicated (the total solution volume was 100µl). The assays were carried out at 27°C and monitored by a Thermomax microplate reader (Molecular Devices). The inhibitor paraoxon:O,O-diethyl O-(4-nitrophenyl)-phosphate , and the reactivator 2-(hydroxyiminomethyl)-1-methylpyridinium chloride (2-PAM) were purchased from Sigma. The reactivators 1,3-bis(4'-hydroxyiminomethyl-1'-pyridinium)propane dibromide (TMB-4) and 1-(2'-hydroxyiminomethyl-1'-pyridinium)-3-(4''-carbamoyl-1''-pyridinium)-2-oxapropane dichloride (HI-6) were a gift from Dr. G. Amitai and Ms L. Raveh, Department of Pharmacology, IIBR (for chemical formulas see Fig.2).

Reactivation of Paraoxon - inhibited HuAChE Paraoxon was used to completely inhibit the AChEs as the preceding step to the reactivation assay. This organophosphate was selected since its AChE adduct does not undergo significant aging, a process which involves dealkylation of the phosphylated AChE leading to a non-reactivatable conjugate, within the time frame of the

reactivation experiments. The amounts of paraoxon required for inhibition of the various HuAChE enzymes were calculated by using the predetermined apparent bimolecular rate constants for the phosphorylation of WT HuAChE and of each of its mutants (Ordentlich *et al.*, 1996). Routinely, two identical aliquots of about three units of AChE in 0.1 ml were used. One was inhibited with paraoxon , and the other served as a control. Following inhibition , an aliquot of each of the reaction mixtures was diluted in buffer (50 mM phosphate buffer, pH 8.0, supplemented with 0.2 mg/ml of BSA), and assayed to verify inhibition (> 98%). Excess of unreacted inhibitor was immediately removed from the enzyme preparation by centrifugation through a 3 ml Sephadex G-15 spin column (3 min. spin at 2500 rpm).

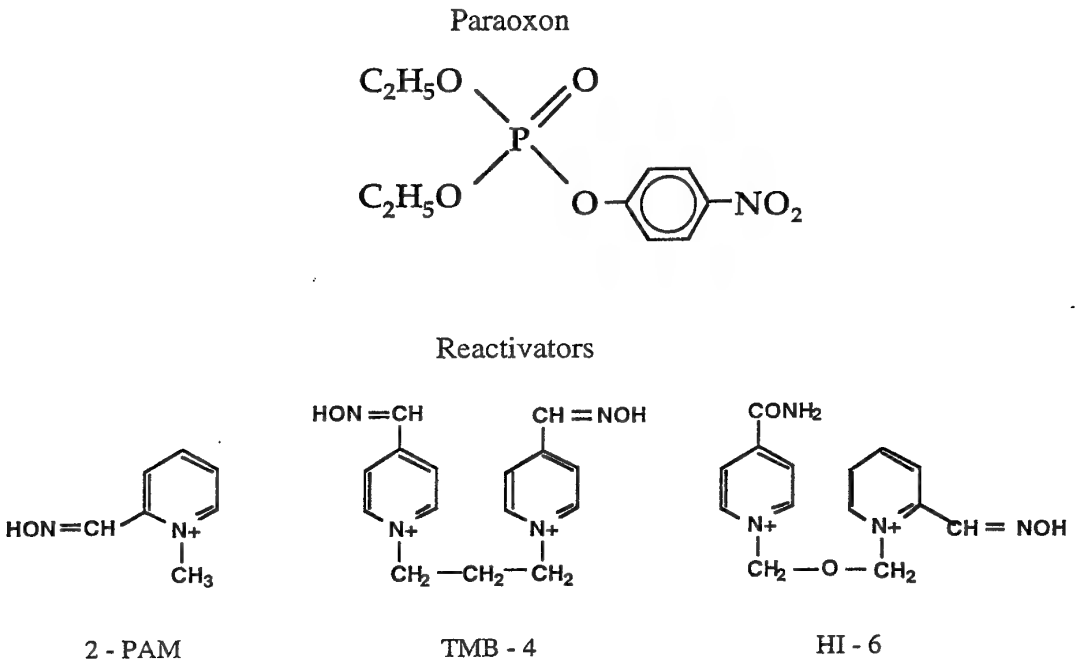

Fig. 2 Chemical formulas of the inhibitor and the reactivators used in this study.

The control noninhibited enzyme preparation was treated similarly. The flowthrough fractions containing the enzyme were diluted to a final working concentration of 0.3 unit/ml. In all cases, the spin column treatment proved to eliminate all inhibitory activity from the paraoxon treated samples , as verified by spiking with AChE . Reactivation reactions were initiated by the addition of the various oximes (concentrations ranging between 0.001 - 2.0 mM) to the paraoxon-free

enzyme solutions, in 50mM phosphate buffer pH 8.0, and were carried out at 27°C. Regeneration of AChE activity was monitored by diluting 10µl samples of the reactivation mixture into 100µl of the assay solution containing ATC and DTNB and the enzymatic reaction followed for 3-5 min., allowing for 7 to 11 time point readings. Control noninhibited enzyme preparations and samples without enzyme were treated similarly, and used for estimation of the expected enzyme activity at maximal reactivation and for monitoring the background readings respectively. The contribution of spontaneous reactivation was estimated by monitoring the enzymatic activity of paraoxon inhibited enzyme samples, in absence of reactivator.

Analysis of the Knetic Data According to Green and Smith (Green and Smith, 1958), the reactivation process can be kinetically described by the two steps shown in Scheme 1.

Scheme 1:

$$E(OP) + R \underset{k_{-1}}{\overset{k_1}{\rightleftharpoons}} E(OP).R \xrightarrow{k_2} E + R(OP)$$

In Scheme 1, E(OP) represents the inhibited enzyme, R the reactivator, E(OP)·R the intermediate complex, E the free enzyme and R(OP) the phosphorylated reactivator . All the reactivation experiments described here were performed under pseudo first order conditions with respect to the reactivator ([R]>> $[E(OP)]_0$).

According to Scheme 1, the time dependent change of phosphorylated enzyme concentration is provided by equation (1), where K_r can be considered as the dissociation constant of the complex E(OP)·R under the condition $k_{-1}>>k_2$. From equation (1), the relation between k_{obs} - the experimental rate constant of reactivation and the kinetic constants K_r and k_2, is described in equation (2).

$$(1) \quad \ln\frac{[E(OP)]_0}{[E(OP)]_t} = \left\{ \frac{\frac{k_2}{K_r}[R]}{1+\frac{[R]}{K_r}} \right\} t = k_{obs}t$$

$$(2) \quad \frac{1}{k_{obs}} = \frac{K_r}{k_2}\cdot\frac{1}{[R]} + \frac{1}{k_2} \qquad (3) \quad \ln\left(1-\frac{[E]_t}{[E]_4}\right) = -k_{obs}t$$

In these equations the subscripts 0, t and ∞ correspond to the respective values at zero time, at time t and after complete reactivation. Since $[E(OP)]_t = [(EOP)]_0 - [E]_t$, and since under conditions of complete reactivation $[E(OP)]_0 = [E]_\infty$, the concentrations in equation (1) can be expressed in terms of the reactivated enzyme (equation 3). Accordingly, values for the dissociation constant K_r and the dephosphorylation rate constant k_2 can be derived by determining k_{obs}, at different reactivator concentrations (according to equation 3), followed by plotting the double reciprocal relation of k_{obs} vs [R] (according to equation 2). From these linear plots one can determine the ratios K_r/k_2 from the slopes, which are equivalent to the reciprocal values of the apparent bimolecular rate constants of reactivation k_r, and values of k_2 from the y-intercepts. The kr constants have been also referred to as "bimolecular reaction constants" since they include equilibrium as well as rate constants (Main, 1964).

Treatment of Side Reactions Accompanying the Reactivation Reaction The relative difficulty in determining kinetic constants from the reactivation assay , is a consequence of the multiple reactions which may occur simultaneously and must be either eliminated, if possible, or considered in the evaluation of the data in order to avoid erroneous interpretation of the results.

Scheme 2:

a. $E + R \underset{}{\overset{K_{ox}}{\rightleftharpoons}} E.R$

b. $R + (OP) \longrightarrow R(OP)$

c. $R(OP) + E \longrightarrow E(OP) + R$

d. $S + R \longrightarrow$ hydrolysis products

e. $E(OP) \longrightarrow E + OP$

An underestimation of the reactivation rate due to a reversible inhibition by the reactivator (Scheme 2a), of the newly reactivated free enzyme was avoided by including identical concentrations of reactivator in the noninhibited control enzyme preparation. The phosphorylated reactivator R(OP) is a potential phosphorylating agent of the reactivated enzyme (Scheme 2b,c). The direct phosphorylation of the reactivator was avoided by efficient removal of the excess of paraoxon,

as described above. This allowed to minimize the formation of R(OP) during reactivation, to a concentration equivalent to that of the reactivated enzyme. To correct for possible hydrolysis of substrate ATC (S) due to oxime induced reaction (Scheme 2d), we included the appropriate blanks. Such correction was important mainly in case of diethylphosphoryl-W86A due to the high concentration of ATC needed to monitor the activity of the free enzyme. Spontaneous reactivation of the inhibited enzyme (Scheme 2e) was not observed in our experiments.

Determination of the Inhibition Constants of HuAChE Enzymes by Oxime Reactivators Values of the reversible inhibition constants (K_{ox}) were determined by monitoring the effects of various oxime concentrations on the rate of the enzymatic hydrolysis of ATC. For each concentration of oxime (in the range 0.1-0.8mM) the hydrolysis was carried out with various ATC concentrations (0.03-3.75mM) in phosphate buffer pH 8.0 containing 0.3mM DTNB. In each case the enzymatic reaction was monitored for 5 min., allowing for 11 time point readings within the Thermomax linear range (200mOD/min). Values of Kox were obtained from the double reciprocal plots of the slopes derived from Lineweaver-Burk plots versus the concentration of the inhibitor (Ordentlich *et al.*, 1995). In case of W86A, concentration of ATC was increased to 25mM resulting in high background product levels in presence of the reactivators. All activities were corrected for oxime -induced hydrolysis of ATC.

RESULTS

Kinetics of Reactivation of Paraoxon Inhibited HuAChE

The lack of a consistent structure-function relationship makes it difficult to formulate a reliable mechanistic scheme for the oxime induced reactivation reaction. The most frequently used reactivation model implicates formation of a noncovalent complex between the phosphylated enzyme and the reactivator, followed by a nucleophilic displacement of the phosphyl moiety (Scheme 1). Nevertheless, kinetic results from many reactivation studies provide only a partial support for this model (Harvey *et al.*, 1986). This may be a consequence of experimental difficulties due to the aging process and other side reactions which compete with the reactivation (see Scheme 2).

To evaluate the reactivation kinetics of phosphorylated HuAChE, and in particular of the phosphorylated mutants which are less amenable to reactivation, we have developed a reliable assay system in which these side reactions are either eliminated or corrected for (see Material and Methods). The reactivation process was monitored using HuAChE enzymes inhibited by paraoxon (see Fig.2). The resulting diethylphosphoryl-adducts are not susceptible to the aging process during the time course of the experiments (Aldridge and Reiner, 1972) and are achiral with respect to the phosphorous atom, and consequently should provide a homogenous population of reactivatable species.

To evaluate the effect of structural modifications of the enzyme on interaction with reactivators, three different oximes (Fig. 2) representing the monopyridinium (2-PAM) and bispyridinium (TMB-4 and HI-6) reactivator classes, were used. Among the two bispyridinium compounds, HI-6 represents the Hagedorn type reactivators known to be particularly reactive towards AChEs inhibited by phosphonates while TMB-4 is more effective in reactivation of phosphoryl-AChEs (Rousseaux and Dua, 1989; Eyer *et al.*, 1992; Clement *et al.*, 1991). This dependence of reactivation efficiency for the two structurally related oximes, upon the structure of the AChE-bound phosphyl moiety, is still not clearly understood (Eyer *et al.*, 1992).

Reactivation of phosphorylated HuAChE proceeds to completion with any of the oximes selected and curve fitting of the kinetic data (according to $E_t = E_\infty(1\text{-}e^{-tk_{obs}})$, see equation 3) exhibit a monoexponential dependence (Fig. 3A).

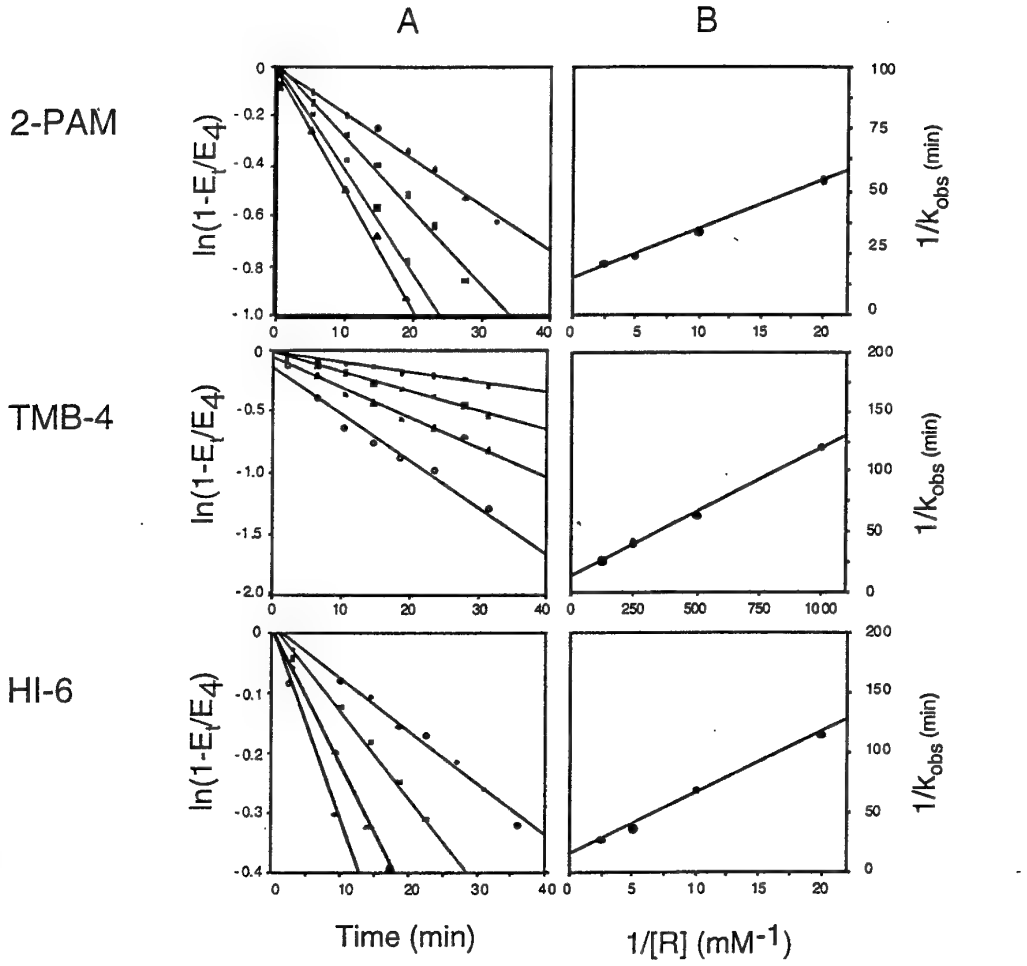

Fig. 3 Determination of the kinetic constants k_r, K_r and k_2 for reactivation of diethylphosphoryl-HuAChE by 2-PAM, TMB-4 and HI-6. A. Semilogarithmic plots of the relative concentrations of the reactivated enzyme vs reaction time, for four concentrations of reactivator in the following range: 2-PAM (0.05-0.4mM), TMB-4 (0.001-0.008mM), HI-6 (0.05-0.4mM). Values of k_{obs} were estimated from the slopes. **B.** Double reciprocal plots of k_{obs} vs reactivator concentration (see equation 2), yielding the values of K_r/k_2 ($1/k_r$) from the slopes and values of $1/k_2$ from the y-intercepts.

The same kinetic behavior has been observed for adducts in which reactivation is efficient as well as for cases where the reaction is very slow as exemplified by the oxime induced reactivation reactions of phosphorylated D74N, E202Q and W86A HuAChEs (Fig. 4). The kinetics profiles, observed for reactivation of diethylphosphoryl-adducts of all the HuAChE mutants tested in this study were linear (r= 0.965-0.998) indicating that the population of reactivatable species is indeed homogeneous and that the assay conditions, selected by us, effectively eliminate interference from

competing reactions (see Scheme 2). We note that nonlinear behaviour was experienced only when using exceedingly high concentrations of reactivator. Such linear behavior supports also the proposed reactivation kinetic scheme (Scheme 1) under the conditions studied, and therefore the values of k_r, K_r and k_2 can serve as an adequate measure of the enzyme reactivity characteristics towards the reactivators examined.

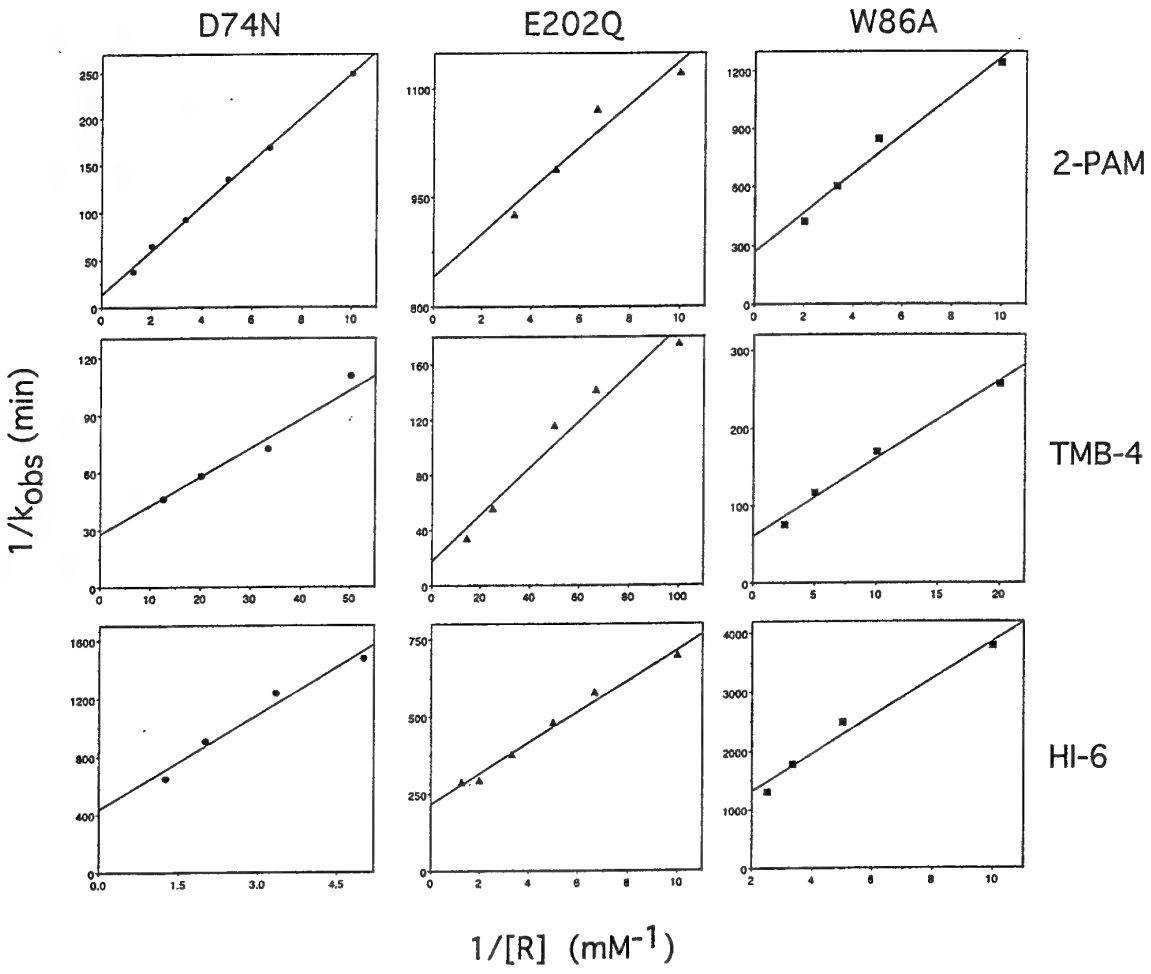

Fig. 4 Representative double reciprocal plots of k_{obs} vs reactivator concentration for selected HuAChE mutant derivatives. Reactivation of phosphorylated HuAChE enzymes mutated at the H-bond network (E202Q), the active center anionic subsite (W86A) and the PAS (D74N), by the reactivators 2-PAM, TMB-4 and HI-6, are shown.

The oxime reactivators are also inhibitors of the nonphosphorylated HuAChE enzymes, presumably by binding at the active center through interactions of the charged pyridinium moieties (Whiteley and Ngwenya, 1995). In order to compare the affinities of the free and diethylphosphoryl-HuAChEs toward the reactivators, as well as to correct for the reversible inhibition of the reactivated enzyme (see Methods), the inhibition constants K_{ox} have been evaluated. The affinity of the diethylphosphoryl-HuAChE enzymes toward the reactivators is approximated by the values of K_r. According to Scheme 1 $K_r = (k_{-1}+k_2)/k_1$, however since the measured values of k_2 are within the range 0.065-6.5min^{-1} (see Tables 1-3) it follows that $k_{-1}>>k_2$ or that $K_r \approx k_{-1}/k_2$ (k_{-1} is estimated to be in the range of 10^4-10^6 min^{-1} based on the assumption that the association proceeds at close to diffusion controlled rates, and on the measured values of K_r).

Table 1: Kinetic constants[a] for reactivation by 2-PAM

Enzyme	k_r($M^{-1}min^{-1}$)	k_2x10^2 (min^{-1})	K_r(mM)	Kox(mM)
WT	460±70	6.0 ±0.82	0.13±0.01	0.28±0.03
W86A	10±4	0.3 ±0.08	0.3 ±0.07	>2*
F295A	180±27	1.0 ±0.15	0.06±0.02	1.0 ±0.15
F297A	134±43	3.0 ±0.9	0.21±0.1	0.9 ±0.05
Y337A	220±39	6.0 ±0.15	0.27±0.04	0.76±0.05
Y337F	510±150	2.5 ±0.7	0.05±0.02	1.0 ±0.2
F338A	180±29	5.4 ±0.35	0.30±0.06	0.59±0.17
E202A	15±5	1.2 ±0.22	0.80±0.22	0.44±0.08
E202Q	41±5	0.16±0.04	0.04±0.01	0.46±0.04
E450A	60±25	0.4 ±0.09	0.07±0.03	1.0 ±0.03
Y72A	80±27	0.8 ±0.18	0.1 ±0.02	0.63±0.1
W286A	55±12	0.8 ±0.15	0.14±0.02	0.43±0.05
Y72A/W286A ±0.0060.67±0.07		100±16	1.0 ±0.2	0 . 1
D74N	47±7	7.0 ±0.73	1.5 ±0.11	1.2 ±0.08

a Mean±S.E. (n= at least four determinations); values of the apparent bimolecular rate constants of reactivation kr and of the first order rate constants k2 and were obtained from the slopes and y-intercepts of the double reciprocal relations of kobs vs [R]; Kr values were calculated from the ratios Kr=k2/kr for each determination and the corresponding S.E values represent deviations from the calculated mean; inhibition constants of the free enzymes by the reactivators Kox were derived from Lineweaver-Burk plots (see Methods).

* Only the lower limit could be estimated due to high background (see Methods).

Examination of the values of K_{ox} and K_r for the free and the diethylphosphoryl-HuAChE revealed that while the affinity of TMB-4 towards the phosphorylated enzyme is 30-fold higher than that toward the free HuAChE, the opposite was true for HI-6, with the affinity towards the phosphorylated enzyme being 16-fold lower. For 2-PAM the corresponding affinities were comparable (as reported also for P2S, see Main, 1964). Moreover the affinity of TMB-4 toward the phosphorylated HuAChE was much higher than those of either 2-PAM or HI-6, accounting for the superior efficiency of TMB-4 as reactivator since the values of k_2 were comparable for the three oximes.

Effect of Amino Acid Replacements at the Active Center on Reactivation

The selection of HuAChE mutants for the study was based primarily on the assumption that the reactivators interact with the enzyme at its active center.Accordingly, mutants carrying substitution of residues constituting the hydrophobic pocket (Trp-86, Tyr-337, Phe-338), residues of the acyl pocket (Phe-295, Phe-297) and residues implicated in the hydrogen bond network (Glu-202, Glu-450) (Harel *et al.,* 1992; Vellom *et al.,* 1993; Ordentlich *et al.,* 1993a; Taylor and Radic, 1994; Gnatt *et al.,* 1994; Ordentlich *et al.,* 1995), were investigated.

The tryptophan at position 86 is involved in stabilization of the charge in the enzyme substrate (Michaelis Menten) complex, and its replacement results in a drastic loss of affinity toward charged AChE ligands such as edrophonium or decamethonium (Ordentlich *et al.,* 1993a; Ordentlich *et al.,* 1995). It could be therefore expected that this residue would interact with the charged pyridinium moieties of the oxime reactivators, especially since in the recently resolved x-ray structure of 2-pyridinium aldoxime-TcAChE complex (Sussman, J. personal communication) the pyridinium moiety is stacked against the indole ring of Trp-84 (residue equivalent to Trp-86 in HuAChE). Indeed replacement of Trp-86 by alanine results in a considerable decrease in affinity of the nonphosphorylated W86A HuAChE toward all three reactivators tested, as demonstrated by the corresponding values of K_{ox} (Tables 1-3). In contrast, and quite surprisingly, the effects of this mutation on the affinity of the diethylphosphoryl-W86A towards 2-PAM and HI-6, relative to those of the phosphorylated wild type HuAChE, are negligible. For all the three reactivators a decrease in capacity to reactivate the phosphorylated W86A enzyme, relative to the wild type HuAChE, is evident from the respective values of k_r values. However, for 2-PAM and HI-6 this

Table 2: Kinetic constants[a] for reactivation by TMB-4

Enzyme	$k_r(M^{-1}min^{-1})$	k_2x10^2 (min^{-1})	K_r(mM)	Kox(mM)
WT	10000±1420	6.0 ±0.55	0.007±0.0008	0.21±0.03
W86A	150±25	3.1 ±0.07	0.2 ±0.03	>2*
F295A	610±62	0.3 ±0.045	0.005±0.002	0.11±0.02
F297A	1200±190	3.6 ±1.8	0.03 ±0.013	0.73±0.1
Y337A	3400±360	3.0 ±0.5	0.009±0.003	0.06±0.018
Y337F	8000±1250	3.0 ±0.6	0.004±0.001	0.32±0.08
F338A	3100±460	0.9 ±0.17	0.003±0.0009	0.17±0.022
E202A	170±17	0.32±0.09	0.018±0.007	0.18±0.02
E202Q	580±25	4.0 ±1	0.07 ±0.02	0.20±0.03
E450A	340±80	1.0 ±0.3	0.03 ±0.008	0.39±0.002
Y72A	460±56	4.4 ±0.3	0.1 ±0.01	0.3 ±0.04
W286A	360±20	4.0 ±0.6	0.11 ±0.009	0.26±0.023
Y72A/W286A	50±19	3.0 ±0.7	0.6 ±0.15	1.10±0.3
D74N	660±32	4.6 ±1.3	0.07 ±0.02	0.57±0.12

Table 3: Kinetic constants[a] for reactivation by HI-6

Enzyme	$k_r(M^{-1}min^{-1})$	k_2x10^2 (min^{-1})	K_r(mM)	Kox(mM)
WT	170±46	6.0 ±0.2	0.35±0.1	0.022 ±0.004
W86A	7±3	0.4 ±0.2	0.55±0.15	>2*
F295A	520±20	2.6 ±1.0	0.05±0.005	0.19 ±0.006
F297A	22±5			
Y337A	120±15	2.4 ±0.28	0.2 ±0.03	0.14 ±0.02
Y337F	113±52	4.0 ±1.2	0.34±0.13	0.12 ±0.02
F338A	80±20	0.55 ±0.05	0.07±0.02	0.044±0.004
E202A	5±1	0.065±0.03	0.13±0.05	0.05 ±0.001
E202Q	19±10	0.45 ±0.12	0.22±0.12	0.05 ±0.008
E450A	4±0.3	0.056±0.01	0.14±0.006	0.39 ±0.01
Y72A	24±8	1.2 ±0.2	0.5 ±0.15	0.06 ±0.01
W286A	24±5	4.7 ±2.0	2.0 ±0.5	0.4 ±0.03
Y72A/W286A	24±3	5.8 ±0.4	2.4 ±0.46	0.51 ±0.06
D74N	5±2	0.25 ±0.07	0.5 ±0.2	0.92 ±0.1

[a],* See footnotes for Table 1

is mainly due to decrease in k_2, while for TMB-4, it is predominantly an outcome of impaired binding to the diethylphosphoryl-W86A HuAChE. Nevertheless one should note that the affinity of diethylphosphoryl-W86A toward TMB-4 is still larger than that of the corresponding nonphosphorylated enzyme.

Residues Phe-338 and Tyr-337 together with Trp-86 are believed to constitute the hydrophobic pocket, accommodating one of the alkoxy substituents of the phosphoryl moiety and also the leaving group in paraoxon-HuAChE Michaelis complex (Ordentlich *et al.,* 1996). Due to its location, above the phosphorous and opposite the P-Oγ-Ser-203 bond, this subsite could play a role in the juxtaposing the nucleophilic moiety of the reactivator with the phosphoryl moiety. Contrary to this prediction, neither substitution of Tyr-337 nor of Phe-338 by alanine had a major effect on the bimolecular reactivation rate constants or on the affinity of the non-phosphorylated enzymes towards the reactivators (Table 1-3). The only effects worth noting are related to the affinities of the phosphorylated F338A mutant for both TMB-4 and HI-6, which are higher than the corresponding values for the wild type enzyme. However this affinity increase is not reflected in the k_r values since a concomitant decrease in k_2 is observed for the same two reactivators.

Residues Phe-295 and Phe-297 were shown to constitute the binding site for the acyl moiety of AChE substrates and for the alkoxy group of the organophosphorus inhibitors (Vellom *et al.,* 1993; Ordentlich *et al.,* 1993a; Ordentlich *et al.,* 1995). Substitution at these positions resulted in different changes of the reactivation rate constants, for the different reactivators (Tables 1-3). Replacement of Phe-297 by alanine resulted in a moderate decrease in affinity towards all the reactivators tested, by both the phosphorylated and the free enzymes. The reactions of diethylphosphoryl-F295A HuAChE with 2-PAM and TMB-4 reveal a significant decrease in the bimolecular rate constants of reactivation resulting only from reduced values of k_2. This is not the case for HI-6, where surprisingly a 7-fold increase of affinity toward the phosphorylated enzyme was observed (Tables 1-3). Consequently a 3-fold increase of the corresponding value of kr was observed although the decrease in the value of k_2 is comparable to that of 2-PAM. The non-uniform effects of replacement at position 295 could result from the relative positioning of the diethylphosphoryl moiety in the phosphorylated F295A enzyme.

The precise positioning of the Glu-202 carboxylate is an important feature of the functional

architecture of the HuAChE active center (Ordentlich *et al.,* 1995; Ordentlich *et al.,* 1996). Such positioning is achieved through an H-bond network spanning the cross section of the active site gorge, and including residues Glu-450, Tyr-133 and the backbone amide oxygens of Gly-122 and Gly-448. Perturbation of this architecture by replacement of residues E202 (by alanine or glutamine) and E450 (by alanine) results in a substantial reduction in the reactivity of the phosphorylated enzymes towards all three reactivators as compared to the wild type. In most cases this decrease is a reflection of the lower corresponding k_2 values, suggesting that the perturbation of the active center geometry affects mainly the nucleophilic process. Less pronounced effects can be observed on the affinity of both the phosphorylated and the non-phosphorylated enzymes towards the reactivitors tested. This behavior is markedly different from the previously observed effects of replacing Glu-202 and Glu-450 on the reactivity of HuAChE enzymes toward organophosphates, where affinity rather than nucleophilic efficiency was affected (Ordentlich *et al.,* 1993; Ordentlich *et al.,* 1995; Ordentlich *et al.,* 1996).

Effect of Amino Acid Replacements at the Peripheral Anionic Site (PAS) on Reactivation

Another binding subsite, the PAS, affecting the reactivity properties of the enzyme was mapped at the rim of the gorge, 20Å away from the active site (Barak *et al.,* 1994; Berman *et al.,* 1981; Hucho *et al.,* 1991; Radic *et al.,* 1991; Harel *et al.,* 1993). Bisquaternary AChE inhibitors bind to the enzyme by bridging the active center and the peripheral anionic site at the rim of the active site gorge (Harel *et al.,* 1993). TMB-4 and HI-6 are bisquaternary compounds and therefore could be expected to interact simultaneously with the active center and the PAS. In contrast, the monoquaternary 2-PAM is expected to interact only with the active center. Indeed, the affinities of 2-PAM to both the non-phosphorylated and the phosphorylated enzymes were not affected significantly by the PAS mutations Y72A W286A and Y72A/W286A (Table 1). Interestingly a similar pattern of mutational effects on affinity was observed for the bisquaternary HI-6. In contrast, the affinity towards TMB-4, remained relatively unaffected for the free enzymes, yet was significantly reduced for the phosphorylated enzymes (up to 100- fold in the double mutant Y72A/W286A). This reduction in affinity is the main reason for the pronounced reduction in the corresponding bimolecular rate constants of reactivation by TMB-4 (Table 2). In the case of HI-6,

some effects on k_r were also observed but these are much less pronounced and the underlying variability of K_r and k_2 are less uniform (Table 3). Quite surprisingly, PAS mutations led to a decrease k_r values for the reactivation by the monopyridinium reactivator 2-PAM. This reduction was not as high as for TMB-4 but larger than that for HI-6. As affinity towards 2-PAM does not change significantly upon PAS mutagenesis the effects on k_r are mainly due to variation of k_2 (Table 1). This observation is intriguing in view of the fact that replacements at positions 72 and 286 have not been observed to affect the chemical reactivity at the active center toward either substrates or covalent and noncovalent inhibitors (Barak *et al.,* 1994).

Unlike substitution of the other structural elements of the PAS, replacement of Asp-74 was shown to affect the binding of charged ligands to the AChE active center (Shafferman *et al.,* 1992c; Barak *et al.,* 1994). This mutation affects the nucleophilic reaction step by the oxime only in the case of HI-6, while the k_2 values for 2-PAM and TMB-4 are practically equivalent to those of the wild type enzyme. This observation underscores the differential effects of PAS mutations on the reactivity towards the individual reactivators, suggesting that the role of PAS in reactivation is more complex than was initially assumed based on the X-ray structure of the 2-PAM-AChE complex (Sussman J. personal communication).

DISCUSSION

Regeneration of AChE from its phosphoryl adducts, through reactions with oxime reactivators, proceed much faster than the analogous reactions for other phosphorylated enzymes or for low weight organophosphorus model compounds. Such rate acceleration strongly suggests the involvement of the AChE active center in accommodating the oxime reactivator and in facilitating the nucleophilic process. Investigation of the role of AChE active center, in interactions with substrates (Shafferman *et al.*, 1992c; Ordentlich *et al.*, 1993a; Taylor and Radic, 1994) as well as covalent and non- covalent inhibitors (Vellom *et al.*, 1993; Taylor and Radic, 1994; Barak *et al.*, 1994; Ordentlich *et al.*, 1996), has recently gained momentum with the advent of experimental approach combining data from X-ray crystallography, site directed mutagenesis, enzyme kinetics and molecular modeling. These studies allowed the elucidation of the functional architecture of the AChE active site gorge and could provide the basis for investigating the more complex interactions of phosphorylated AChE with oxime reactivators.

An adequate measure for probing the effect of mutagenesis on the reactivation process is through comparison of the respective values of the bimolecular rate constants of reactivation (k_r). Such comparison (Fig.5) reveals an apparently conserved trend in the effect of the different mutations on reactivation by the three oximes examined. Substitution of residues constituting the hydrophobic pocket (Tyr-337; Phe-338) had little effect on k_r values, while substitution of the H-bond network residues (Glu-202; Glu-450) and the anionic subside residue (Trp-86) resulted in significant decrease in k_r. Notably, the reactivation rate constants for the three oximes were also affected by replacement of residues at the PAS (Tyr-72,Asp-74, Trp 286). Although for most mutants, carrying residue replacements, at the various binding subsites of HuAChE, the variations of k_r values were similar for the three reactivators, closer examination of the kinetic characteristics (according to Scheme 1) indicated different effects for each reactivator .The kinetic description, which is supported by the linear relations of ln $(1-E_t/E_\infty)$ vs reaction time and of k_{obs} vs 1/[R], allows for the estimation of both the dissociation constants K_r and the rate constants k_2. Altogether, examination of the parameters (Tables 1-3; Fig. 6,7) indicates that the effects of

mutagenesis on the different steps of the reactivation process are more complex than may appear from the corresponding bimolecular rate constants (Fig. 5).

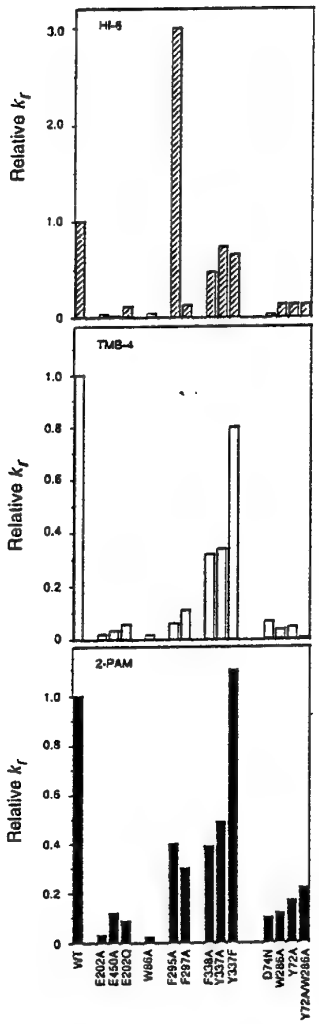

Fig.5 Relative values of the apparent bimolecular rete constants k_r for reactivation of paraoxon inhibited HuAChE and its mutant derivatives †.

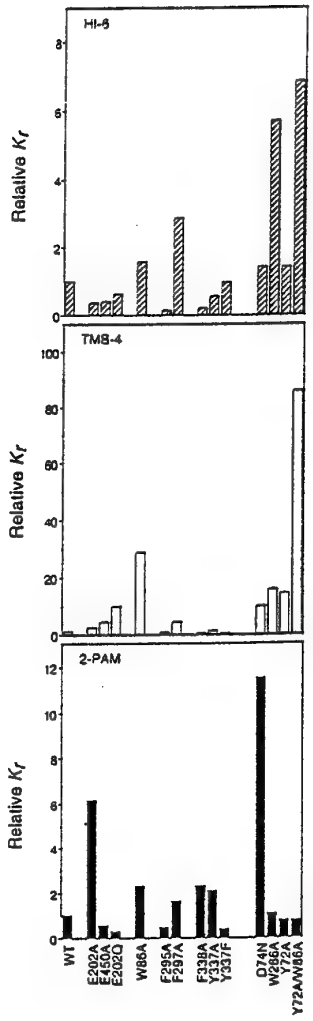

Fig.6 Relative values of the dissociation constants K_r for oxime reactivator complexes with diethyl phosphoryl-HuAChE and its mutant derivative †.

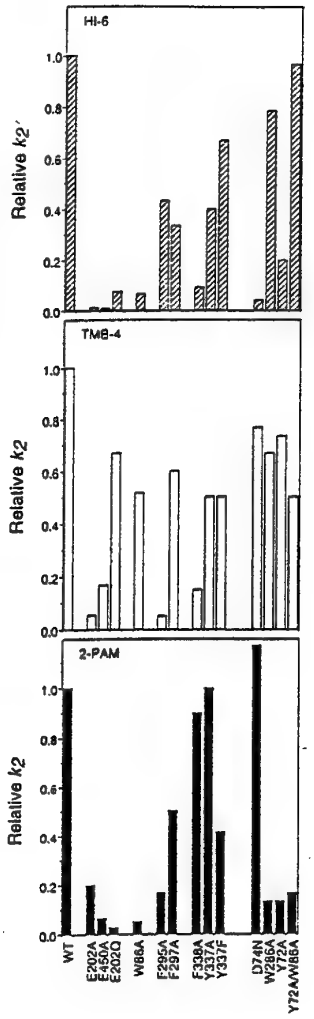

Fig.7 Relative values of the first order rate constants k_2 of reactions of oxime reactivator complexes with diethyl phosphoryl-HuAChE and its mutant derivative †.

† The enzymes are grouped according to the subsite at which residue replacement was made: H-bond network (E202A, E202Q, E450A); active center anionic subsite (W86A); acyl pocket (F295A, F297A); hydrophobic pocket (F338A, Y337A,Y337F) and the peripheral anionic site (D74N, W286A, Y72A. Y72A/W286A).

The role of the functional architecture of AChE active center in interaction with ligands is well established. This information is potentially instrumental to understanding the reactivation process

provided that the phosphylation of the active site serine does not have a dramatic effect on the structure of the active center. Previous studies have shown, for example, that binding of active center ligands like decidium is not affected by phosphylation of the active site serine (Berman and Decker, 1986b). One could expect therefore that the effects of mutagenesis on the affinity of the free and the phosphorylated enzymes towards the oxime reactivators (as reflected in the values of K_{ox} and K_r respectively) would be comparable. However, while the affinity of the free enzyme mutants were found to follow the structure-function patterns observed for positively charged non-covalent inhibitors (Ordentlich *et al.,* 1993a; Barak *et al.,* 1994), the corresponding affinities of the diethylphosphoryl adducts exhibited a marked variability, related to the structure of the specific reactivator. The most pronounced effect, on the affinity of the free enzymes was brought about by replacement of Trp-86, the anionic subsite at the AChE active center which is crucial for accommodation of charged ligands such as ATC, edrophonium and decamethonium (Ordentlich *et al.,* 1993a; Barak *et al.,* 1994). In addition, as for other charged ligands, mutagenesis at sites related to hydrophobic interactions (Tyr-337,Phe-338) or acyl pocket accommodation (Phe-295, Phe-297) on reactivator binding were less dramatic (except for F295A in TMB-4). Nevertheless comparison of the dissociation constants (K_r vs K_{ox}) indicates that the mutations affect differently affinity of the free and the phosphorylated enzymes towards different reactivators. The most striking difference is the negligible effect of Trp-86 replacement on the affinity of the phosphorylated enzyme towards 2-PAM and HI-6 as opposed to the observed decrease in affinity towards TMB-4. This would indicate that the alignment of the reactivators within the active center gorge of the phosphorylated enzyme is markedly different than in the free enzyme. Moreover, distinct oxime reactivators are accommodated differently in the active center. This is substantiated by several other observations: (a) Mutation at position 295 increases the affinity of the phosphorylated enzyme for HI-6 but not for the other reactivators studied. (b) Mutations at position 202 (E202A and E202Q) affect differently interactions with 2-PAM, HI-6 and TMB-4. (c) Substitution F338A results in an increase in affinity of the phosphorylated enzyme toward HI-6 which is not observed in the free enzyme.

Additional differences in the behavior of different reactivators are related to the effects of PAS mutations on oxime-AChE interactions. Replacements at positions 72 and 286 does not seem to affect the affinity of either the phosphorylated or the free enzymes towards 2-PAM, as expected

for a mono-charged derivative. Affinities towards the two bispyridinium reactivators are affected by mutations at these PAS positions, yet for HI-6 decrease in affinity is more pronounced in the free enzyme (~20 fold decrease) while for TMB-4 , the major effect is observed in the phosphorylated enzymes (18-100 fold). These observations suggest that the PAS could participate in accommodation of one of the charged pyridinium moieties, yet it appears that the two bispyridinium reactivators are differently oriented relative to the functional components of the active center gorge.

While the PAS appears to be involved in accommodation of the bisquaternary oxime reactivators, its effect on the actual reactivation reaction (as reflected by the rate constants k_2) is not straightforward. Replacements of residues Asp-74 and Tyr-72 lower the k_2 values for HI-6 while hardly affecting those for TMB-4. On the other hand, mutagenesis at the PAS affects the k_2 values for 2-PAM. The resemblance between the reactivity characteristics of 2-PAM and HI-6, as distinguished from these of TMB-4, are also manifested by the involvement of residue Trp-86 as well as of residues constituting the H-bond network (Glu-202, Glu-450) in the reactivation reaction. The apparent similarity in the reactivity pattern of 2-PAM and HI-6, could be related to the positioning of the oxime moiety on the pyridinium ring relative to the positively charged nitrogen. In 2-PAM and HI-6 the oxime moiety is at position-2 adjacent to the pyridinium nitrogen while in TMB-4 it is located at position-4 (Fig. 2).

Altogether, it is very difficult to rationalize the reactivation process using the previously established functional architecture of the AChE active center gorge (Ordentlich *et al.,* 1993a; Ordentlich *et al.,* 1995). Assuming that the overall gorge architecture is not altered significantly by the bound phosphoryl moiety, the observed structure-affinity relationships do not correspond to the defined array of binding elements, including the anionic and hydrophobic subsites as well as the acyl pocket, within the active center gorge. This may indicate that the structures of the reactivator-phosphorylated enzyme complexes are determined primarily by interactions other then those implicated in the corresponding complexes of the free enzyme. One such interaction can involve the oxime and the phosphoryl moieties. This interaction, which is instrumental in properly juxtaposing the two reacting elements, could involve some rearrangements of the gorge leading to abolishment of the defined binding subsites. These alterations should differ according to the different oxime structure and thus account for some of the oxime-specific effects of the

mutagenesis (Tables 1-3).

In conclusion, the experimental approach, utilizing site directed mutagenesis, which has been remarkably successful in elucidating the various aspects of AChE reactivity, appears to be less effective in the derivation of the structure-function profile for the reactivation process. One of the major problems in derivation of such profile is that the experimental observations cannot be rationalized in structural terms and are not amenable to molecular modeling since the nature and the extent of the conformational adjustment by the enzyme is not known and quite difficult to predict. In a recent study, various mutants of mouse-AChE were used to analyze reactivation by 2-PAM and HI-6 (Ashani *et al.,* 1995). The authors proposed a model of the phosphonylated AChE-HI-6 complex in which the positive charges of the bisquaternary reactivator were positioned near the indole moieties of Trp-86 and Trp-286, in the active center and the PAS respectively. However, such model may not be applicable to the corresponding reactivation of HuAChE conjugates since the value of the dissociation constant Kr, for the HI-6-W86A conjugate complex, is practically equivalent to that of the wild type HuAChE (Table 3). This is quite intriguing in view of the fact that the residue composition of the active site gorge in HuAChE and mouse AChE is identical (Gentry and Doctor, 1995).

The apparent inconsistency of the kinetic results with the expected structure-function pattern of AChE could indicate the inadequacy of the kinetic model currently employed for the reactivation process. Alternatively, the results presented in this study may implicate that interaction of the oxime with the bound phosphyl moieties is indeed the dominant characteristic of the phosphylated AChE-oxime reactivator complexes and/or that the binding modes of oxime to the phosphorylated and nonphosphorylated enzymes are considerably different. In such cases it is conceivable that reactivation rates could be manipulated by altering the size of the phosphorous alkyl substituents. Specifically, bulkier phosphyl moieties may confer a more restrictive binding environment to the oxime reactivator and thus reveal in more detail the structure function characteristics of the reactivation process.

III. Aging of Phosphylated Human Acetylcholinesterase: The Aromatic and Polar Residues: Trp86, Phe338, Asp74, Glu202 and Glu450 are Targets for Generation of HuAChE Bioscavengers Resistant to Aging.

INTRODUCTION

The inhibition of serine hydrolases such as cholinesterases (ChEs) by organophosphorus compounds involves phosphylation of the active site serine and the formation of a stable conjugate (Aldridge and Reiner,1972; Taylor, 1990). Although spontaneous hydrolytic cleavage of such conjugates is usually very slow, the enzymes can still be effectively reactivated through reaction with nucleophilic agents such as quaternary oximes or fluoride ion (Aldridge and Reiner,1972; Froede and Wilson, 1971). In certain cases, the ability to displace the phosphyl moiety decreases with time due to an unimolecular process termed "aging" (Scheme 3) (Hobbiger, 1955; Fleisher and Harris, 1965). This process, usually attributed to the loss of alkyl group from the phosphyl alkoxy substituent, is most pronounced for branched alkyl groups (Wilson *et al.*, 1992). The aging process of the phosphylated acetylcholinesterase prevents treatment and exacerbates the effects of human intoxication by organophosphorus agents, like certain insecticides and nerve agents (Taylor, 1990).

The rate determining step of the aging process is probably the alkyl-oxygen bond scission, resulting in formation of a carbonium ion, and a formal negative charge (see Scheme 4) in the conjugate (Benschop and Keijer, 1966 ; Michel *et al.*, 1967). Although the involvement of the enzyme in facilitating this process has been demonstrated long ago by the fact that aging does not occur in denatured phosphyl-AChE conjugate (Wilson, 1967), the specific role of the enzyme is

not well understood. Enzymatic acceleration of C-O bond breaking through generation of a carbonium ion is not unique to cholinesterases, however in other enzymes such as lysozyme, this reaction has a well defined catalytic function in the glycosyl transfer processes (Warshel, 1991). Stabilization of charge separation, leading to the formation of a carbonium ion, was recently proposed to involve the AChE active center and in particular residue Glu-202*(199)* (Qian and Kovach, 1993 ; Bencsura *et al.*, 1995). Such involvement of residue Glu-202 could be consistent with the observed effects of its replacement by glutamine, on the aging rate of the corresponding 2,3,3-trimethylpropyl methylphosphonyl conjugate (Ordentlich, *et al.*, 1993b; Saxena *et al.*, 1993). However, Ordentlich *et al.*, 1993a) have shown that the aging process was equally affected by replacement of residue Glu-450, which is remote from the phosphonyl moiety. Another unresolved issue related to aging is the profound resistance of the aged conjugates to reactivation. The proposed electrostatic barrier to a nucleophilic attack, due to the presence of additional negative charge (Amitai *et al.*, 1982) appears to be inconsistent with the reactivity properties of charged organophosphorus esters (Kirby and Younas, 1970; Segall *et al.*, 1993). Resistance to reactivation has been explained on the basis of conformational changes taking place following aging (Steinberg *et al.*, 1989; Masson *et al.*, 1994), yet comparison of the refined X-ray structures of aged and non-aged organophosphoryl conjugates of γ-chymotrypsin showed virtually no conformational difference in the protein backbone of the two structures (Harel *et al.*, 1991).

Scheme 3:

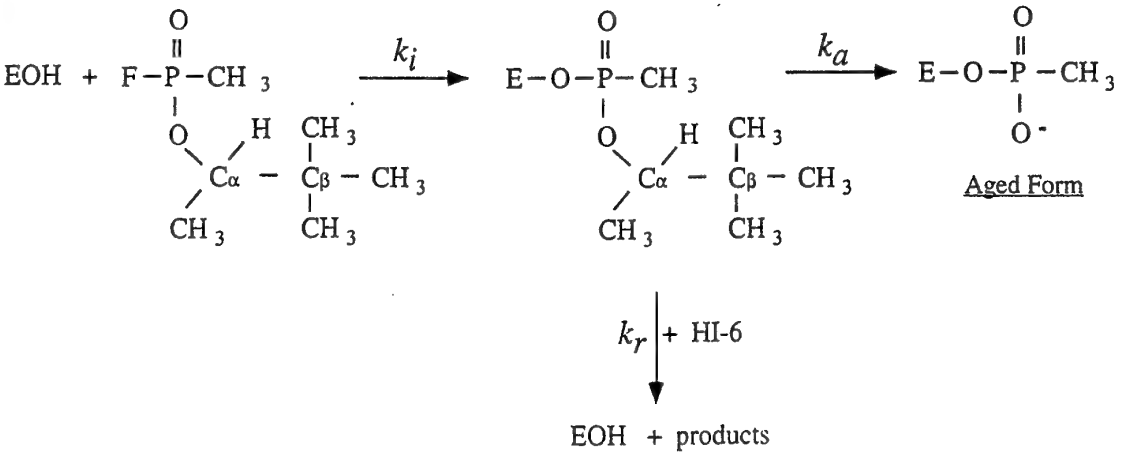

Scheme 4:

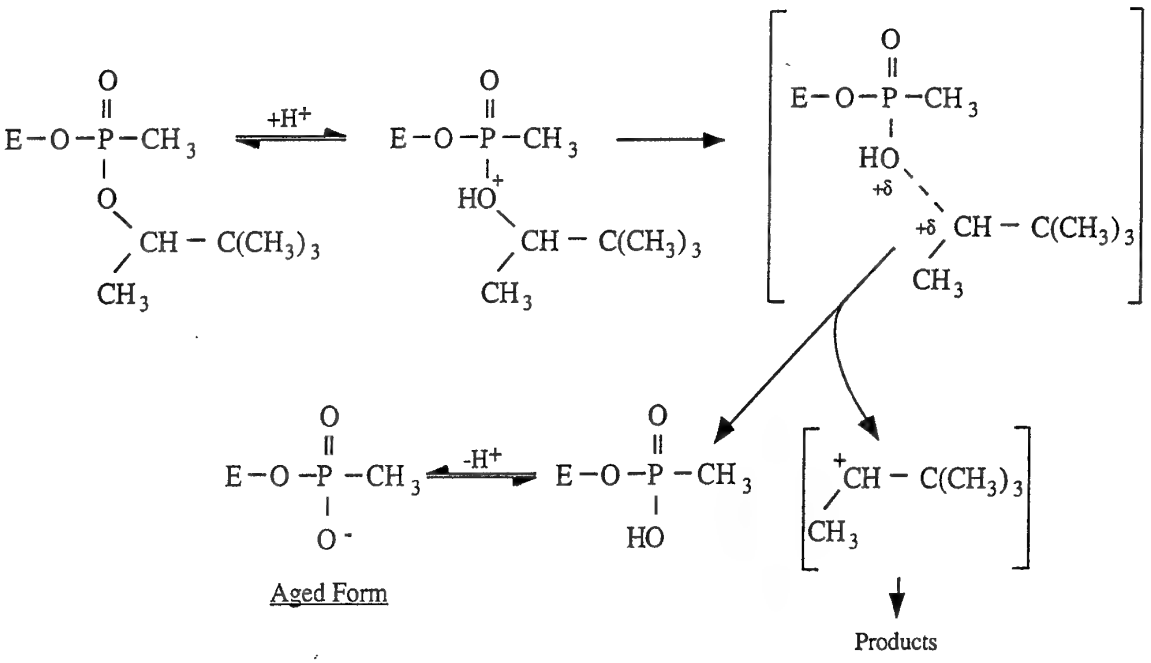

The role of the structure of the human acetylcholinesterase (HuAChE) active center in facilitating reactions with organophosphate inhibitors, was recently examined by combination of site directed mutagenesis and kinetic studies (Ordentlich *et al.,* 1996). This study identified some of the residues interacting directly with the ligands and suggested that the functional architecture of HuAChE active center has a major role in the stabilization of the enzyme-phosphate Michaelis complexes. The same active center residues may be involved in accelerating the aging process, and could explain the more efficient aging of the phosphyl conjugates of ChE's, as compared to the corresponding conjugates of other serine hydrolases (Van der Drift *et al.,* 1985; Grunwald *et al.,* 1989). Here we apply the combined approach of mutagenesis, kinetic studies and molecular modeling to identify the key residues in the active center of HuAChE contributing to the aging process and in particular to the carbonium ion formation.

METHODS

Materials. Acetylthiocholine iodide (ATC) and 5:5'-dithiobis (2-nitrobenzoic acid) (DTNB) were purchased from Sigma. Purified racemic mixture of 2,3,3-trimethylpropyl methylphosphonofluoridate (soman) and 7-[(ethoxymethylphosphinyl)oxy]-1-methyl-quinolinium iodide (MEPQ) were a gift from Dr. Y. Segall, and 1-(2-hydroxy-iminomethylpyridinium)-1-(4-carboxyimino-pyridinium) dimethylether dichloride (HI-6) was a gift from Dr. G. Amitai.

Production of Enzymes. Expression of recombinant HuAChE and its mutants in a human embryonal kidney derived 293 cell line (Shafferman *et al.,* 1992b; Velan *et al.,* 1991b; Kronman *et al.,* 1992), and generation of all the mutants was described previously (Ordentlich, *et al.,* 1993a,b; Shafferman *et al.,* 1992b,c; Ordentlich *et al.,* 1995). Stable recombinant cell clones expressing high levels of each of the mutants were established according to the procedure described previously (Kronman *et al.,* 1992). Enzymes were purified (over 90% purity) either by ligand affinity chromatography (Kronman *et al.,* 1992) or by fractionation on monoclonal antibody affinity column (Barak *et al.,* 1995).

Enzyme Activity Measurements and Active Site Titrations. Activity of HuAChE enzymes was assayed according to Ellman et al. (Ellman *et al.,* 1961) (in the presence of 0.1 mg/ml BSA, 0.3mM DTNB, 50mM sodium-phosphate buffer pH-8.0 and various concentrations of ATC), carried out at 27°C and monitored by a Thermomax microplate reader (Molecular Devices).

Active site titration of enzyme solutions was carried out in the presence of 0.1 mg/ml BSA in 50mM sodium-phosphate buffer pH 8.0, by adding various amounts of phosphonate inhibitors (MEPQ or soman). Inhibition was allowed to proceed to completion and the residual activity was plotted versus the concentration of inhibitor. MEPQ, a potent non-stereoselective inhibitor of ChEs (Levy and Ashani, 1986) reacting in a 1:1 ratio with various AChEs including the recombinant

HuAChE (Velan *et al.,* 1991b), was used as a standard for the active site titrations. The concentrations of the active site subunits of all the enzymes as determined by titration with MEPQ, were within ±10% from those measured by the specific enzyme linked immunosorbent assays (ELISA) (Shafferman *et al.,* 1992b). These values were used to determine the stoichiometry of the reactions of soman with the various HuAChE enzymes.

Measurements of Phosphonylation Rates. Kinetic measurements were carried out in at least four different concentrations of soman (I) and enzyme residual activity (E) at various times was monitored. The apparent bimolecular phosphonylation rate constants (ki) determined under pseudo-first order conditions were computed from the plot of slopes of ln(E) vs time at different inhibitor concentrations. Rate constants under second order conditions were determined from plots of $\ln\{E/[I_o-(E_o-E)]\}$ versus time.

Measurements of Aging Rates. The initial soman - inhibited enzymes were obtained under conditions where the rate of phosphonylation is much faster than the rate of aging ($ki[I_o] >> ka$) and with over 98% inhibition of the initial enzyme activity. The excess soman was rapidly removed either by column filtration (Sephadex, G-15) or by 1000 fold dilution, prior to reactivation. The reactivatable (non-aged soman - conjugate) fraction was determined by reactivation with 0.5 mM HI-6 under conditions where the rate of reactivation is higher than the rate of aging ($kr[HI-6]>ka$). The activity of the reactivated enzyme (Er) was routinely corrected for the inhibitory effect of the reactivator (De Jong and Kossen, 1985). The first order rate constants of aging (ka) were determined from the slopes of ln(Er) vs. time.

The pH profiles of aging of HuAChE and of some of its aging resistant mutants were examined by using the following 50mM buffer solutions: bis-Tris propane at pH ranges 5.5- 9.0, Tris at pH ranges 7.0- 9.0 and succinate at pH ranges 4.6- 6.0. The rates of aging could not be measured below pH 5.5 due to technical limitations (mainly enzyme stability).

Molecular Modeling. Building and optimization of three-dimensional models of 2,3,3-trimethylpropyl methylphosphono-HuAChE conjugates were performed on a Silicon Graphics workstation IRIS 70/GT using SYBYL modeling software (Tripos Inc.).The initial models were constructed as described before for the 2-propyl analogs (Barak *et al.*, 1992). The models were optimized by molecular mechanics using the MAXMIN force field (and AMBER charge parameters for the enzyme) and zone refined, including 127 amino acids (15 Å substructure sphere around Oγ-Ser-203). Optimization of the initial models included restriction of the distance between the phosphonyl oxygen and the amide nitrogen atoms of residues Gly-121, Gly-122 which were relieved in the subsequent refinement.

RESULTS AND DISCUSSION

Effect of Selected HuAChE Mutations on Phosphonylation by 2,3,3-trimethylpropyl Methylphosphonofluoridate

Several residues of the hydrophobic alkoxy subsite and of the H-bond network in the HuAChE active center are involved in the phosphorylation process (Ordentlich *et al.,* 1996). It is generally assumed that the electronic and steric requirements for the inhibitory processes in AChEs should be quite similar for phosphates and for phosphonates. This assumption was tested here using selected HuAChE mutants and the phosphonylating agent 2,3,3-trimethylpropyl methylphosphonofluoridate (soman), which yields conjugates that undergo rapid aging. Investigation of this reaction was also of interest because of the known stereoselectivity of AChE toward soman diastereomers (Benschop and De Jong, 1988). Phosphonylation of different AChEs by the two P_S diastereoisomers was shown to be over 10^3-times faster than that by the two P_R diasteroisomers (Keijer and Wolring, 1969; Benschop *et al.,* 1984). Therefore, for all practical purposes, the stoichiometry of the reaction should be 1:2, provided that the HuAChE mutations do not affect the stereoselectivity toward soman. Titrations of the various HuAChE enzymes with MEPQ and soman resulted in stoichiometries of 1:1 and 1:2 respectively for all the enzymes examined. This result indicates that substitutions of residues of the H-bond network and of the hydrophobic alkoxy subsite, do not affect the stereochemistry of the enzyme-soman interaction. Such conclusion is consistent with the predictions from molecular modeling (Barak *et al.,* 1992) and with the recent suggestion that stereoselectivity of AChE toward phosphonates results mainly from interactions in the acyl pocket of the enzyme (Hosea *et al.,* 1995).

The hydrophobic alkoxy pocket for substrate in the AChE active center is defined by aromatic residues Trp-86, Tyr-337 and Phe-338 (Ordentlich *et al.,* 1993a). This pocket seems to have limited interaction with the alkoxy substituents of organophosphates like diisopropyl phosphorofluoridate (DFP) and diethyl phosphorofluoridate (Ordentlich *et al.,* 1996 and Table 4).

Table 4: Apparent bimolecular rate constants (k_i)[a] of phosphonylation and phosphorylation of HuAChE enzymes by soman and DFP.

HuAChEs	Soman k_i ($x10^{-4}xM^{-1}xmin^{-1}$)	DFP[b]
Wild Type	8600 ± 2000	14.0 ± 1.0
W86F	2510 ± 220	14.0 ± 1.3
W86A	540 ± 30	2.6 ± 0.1
Y337F	4800 ± 800	40 ± 10
Y337A	2950 ± 640	3.0 ± 0.2
F338A	9000 ± 3000	2.6 ± 0.2
Y133F	250 ± 30	1.4 ± 0.1
E202A	460 ± 250	0.9 ± 0.1
E202D	570 ± 100	0.8 ± 0.1
E202Q	310 ± 100	0.18 ± 0.06
E450A	120 ± 20	0.09 ± 0.03
D74N	3400 ± 600	19.7 ± 1.2

[a] Calculated from the pseudo first order rate constants. Values are mean of 3-4 independent measurements ± SD.
[b] The ki values of DFP for most of the mutants were determined recently (Ordentlich *et al.,* 1996) and are cited for comparison.

A comparable lack of effect, on the phosphonylation rates by soman, has been observed for replacements of residues Tyr-337 and Phe-338 (Table 4). On the other hand, replacement of Trp-86 by alanine resulted in a 16-fold decrease of the phosphonylation rate whereas replacement by phenylalanine led to a smaller decrease in the rate (3.4-fold relative to the wild type), implying a role for this aromatic residue in stabilizing the bulky 2,3,3-trimethylpropoxy substituent.

The H-bond network (Ordentlich, *et al.,* 1993b; ,Ordentlich *et al.,* 1995) which has been suggested to contribute to the stabilization of the active center functional architecture, appears to be dependent on the precise positioning of Glu-202, Glu-450 and Tyr-133 (Fig. 8A). Indeed, substitutions of Glu-202 by acidic or neutral residue as well as replacements of residues Tyr-133 by phenylalanine and Glu-450 by alanine, caused a 15-28-fold reduction in the respective phosphonylation rates, relative to the wild type (Table 4). This reactivity pattern is analogous to that observed for the corresponding phosphorylation reactions with DFP.

The peripheral anionic site residue Asp-74 was shown to be a key element involved in the allosteric interactions between the active center and the remote enzyme exterior (Shafferman *et al.*, 1992b,c; Barak *et al.*, 1994). Therefore, it was of interest to monitor the effect of its replacement on the phosphonylation and the aging processes. The phosphylation rates of D74N enzyme by soman and DFP were practically equivalent to those of the wild type HuAChE (Table 4), indicating that the allosteric modulation of AChE activity may not contribute to the phosphylation processes.

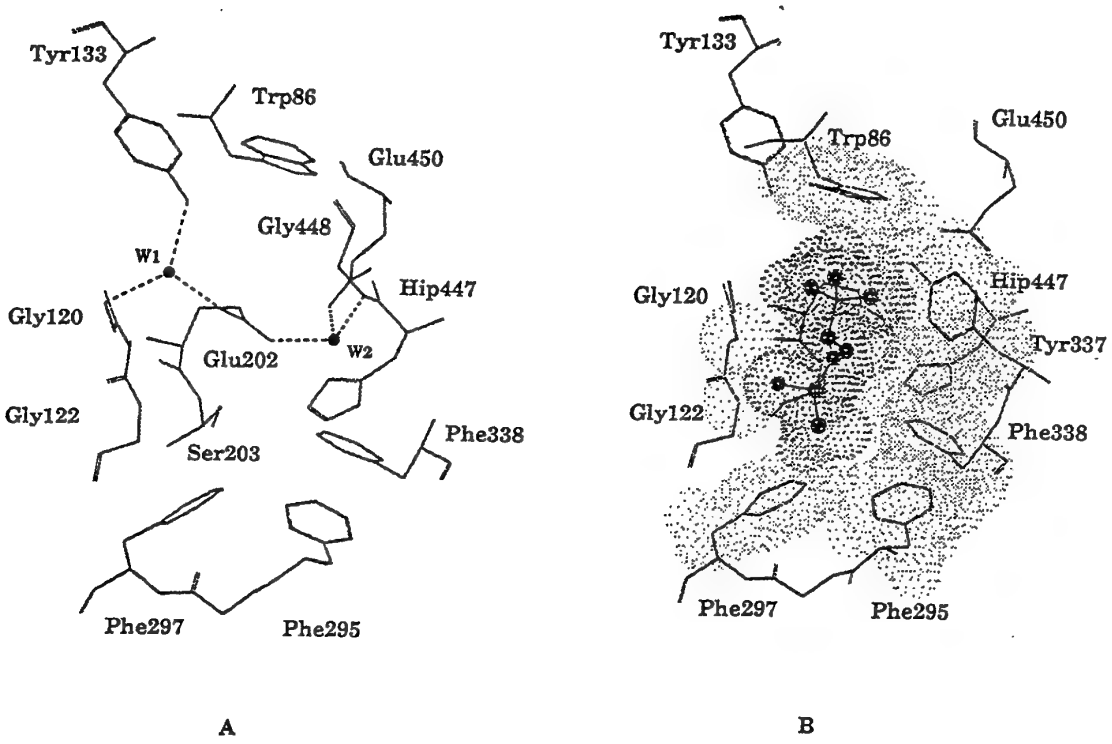

Fig. 8 Energy optimized models of the active center in the unligated and in the 2,3,3-trimethylpropyl-methylphosphonylated HuAChE states. In the unoccupied active center (panel **A**), the involvement of residues Glu-202; Glu-450 and Tyr-133 in the H-bond network, through waters w_1 and w_2, is shown (for distances within the network see Ordentlich et al., 1993b). In the phosphonyl conjugate (panel **B**), the relative orientation of the phosphorus substituents versus residues Trp-86 and Phe-338 of the alkoxy pocket and residues of the H-bond network are shown. The shape complementarity is shown by the corresponding van der Waals volumes. The hydrogens are omitted for clarity.

In conclusion, examination of the phosphonylation reactions with soman appear to support the assumption, regarding the similarity of the electronic and steric requirements for the phosphorylation and phosphonylation processes, as exemplified by the comparable inhibition patterns for the various mutants with soman and DFP (Table 4). Yet, as could be expected, the presence of a larger alkoxy substituent on the phosphyl moiety allows for somewhat better mapping of the interactions of this moiety with the residues of the hydrophobic alkoxy subsite.

Aging of Phosphonylated HuAChE and Selected Mutants

The aging processes of the 2,3,3-trimethylpropyl methylphosphonyl conjugates of HuAChE enzymes were monitored by measuring the reactivatable fraction of the conjugate in presence of the potent oxime reactivator HI-6 (see Scheme 3) (Roussaux and Dua, 1989). Under the experimental conditions used, a substantial regeneration of the enzymatic activity was observed even for the conjugate of the wild type HuAChE where the aging was fairly rapid. The exponential time courses, for aging of *all* the phosphonyl conjugates examined here, were consistent with the first order kinetics and with a single homogeneous population of reacting species.

Mutations of the H-bond network. The involvement of residue Glu-202 in the aging process was already demonstrated through the effect of its replacement by glutamine (Ordentlich, *et al.,* 1993b; Saxena *et al.,* 1993). The observed 150-fold decrease in the rate of aging, relative to the wild type HuAChE, due to this mutation (Ordentlich, *et al.,* 1993b), was attributed to the removal of the charged carboxylate moiety from the vicinity of the evolving carbonium ion (Bencsura *et al.,* 1995). However, the replacement of residue Glu-450, which is 9Å away from the catalytic serine, by alanine (Table 5) also resulted in a significant reduction in the rate of aging. This was explained by an H-bond network involving residues Glu-202 and Glu-450 as well as Tyr-133 (see Fig. 8A) that determines the orientation of the Glu-202 carboxylate (Ordentlich, *et al.,* 1993b). Indeed, we find that removal of the hydroxyl group, through replacement of Tyr-133 by phenylalanine resulted in a decrease of the rate of aging which is remarkably similar to that observed for the E450A enzyme (Table 5). Since in the E450A or in the Y133F enzymes the carboxylate of Glu-202 is still present within the active center manifold and only its position is

presumably affected, it appears that the role of Glu-202 in facilitating the hydrolytic activity as well as the aging process, is strongly dependent on its exact location and orientation.

To further examine the role of Glu-202, we have tested the consequences of shortening the acidic side chain, through substitution of the glutamic acid by the polar protic aspartate, or of its replacement by the nonpolar residue, alanine. The rates of aging for the two corresponding phosphonyl-conjugates are nearly equivalent to that of the E202Q enzyme (Table 5). These results suggest that Glu-202 exerts its effect either through: (a) a negative electric field, which is strongly dependent upon distance, and which stabilizes the positive charge on either the phosphonyl moiety or on the imidazolium moiety of His-447, or (b) involvement in either a proton transfer or a hydrogen-bonding interactions with the phosphonyl moiety.

Table 5: Rate constants of aging (k_a) of soman - inhibited HuAChE enzymes at pH 8.0[a].

HuAChEs	k_a ($x10^3 x min^{-1}$)	Ratio (WT/Mutant)
Wild Type	110 ± 45	1
W86F	4.5 ± 1.5	24
W86A	< 0.1[b]	>1000[b]
Y337F	40 ± 3.5	3
Y337A	160 ± 70	0.7
F338A	0.7 ± 0.4	157
Y133F	4.0 ± 0.9	28
E202A	0.33 ± 0.05	333
E202D	0.7 ± 0.1	155
E202Q	0.8 ± 0.3	138
E450A	4.6 ± 1.6	24
D74N	7.1 ± 2.1	15

[a] Values of the first order rate constants are average of at least three independent experiments determined at 24 °C.

[b] Aging reaction could not be detected after 96 hours.

The participation of Glu-199 in TcAChE (equivalent to Glu-202 in HuAChE) in general acid catalysis has been previously suggested for the reactions of AChE with certain substrates (Selwood *et al.,* 1993). A recent computational study has further suggested that Glu-202, rather than His-447, may be involved in the protonation necessary to induce the aging process (Bencsura *et al.,*1995). To explore such possibility, the pH - rate profiles of aging were determined for the 2,3,3-trimethylpropyl methylphosphonyl conjugates of the wild type and the E202Q HuAChEs as well as of an additional mutant, in which the H-bond network was not perturbed. As already reported for other AChEs (Michel *et al.,* 1967; Keijer *et al.,* 1974; Berman and Decker, 1986a), the rates of aging for the wild type HuAChE and the two mutant enzymes increase with decreasing pH (Table 6, Fig. 9). Due to experimental limitations the rates of aging could not be measured below pH 5.5 precluding the completion of the titration curves for determination of pKa values. We therefore compared the efficiency index of aging for each mutant, as a function of pH (Fig. 9). Efficiency index was calculated as the ratio of rate constant at any given pH and of the rate constant at pH 5.5. Although the actual rates of aging, at a given pH, are 100-fold lower for F338A and E202Q relative to the wild type enzyme (Table 6), all the three enzymes show a very similar dependence of their efficiency indices on pH (Fig. 9). This similarity suggests that Glu-202 is not directly involved in proton transfer relevant to the aging process.

Table 6: Enhancement of the rates of aging[a] for soman inhibited HuAChE enzymes with decrease of pH

HuAChEs	k_a ($x10^3 x min^{-1}$) pH 8[b]	pH 7	pH 6
Wild Type	110 ±45	370 ± 85	1660 ± 200
W86A	< 0.1	0.2 ± 0.05	0.5 ± 0.1
E202Q	0.8 ± 0.3	2.3 ± 0.9	6.4 ± 0.8
F338A	0.7 ± 0.4	2.2 ± 0.2	9.6 ± 1.6

[a] All first order rate constants determined at 24 °C in at least three independent experiments ± SD.
[b] Values cited from Table 5.

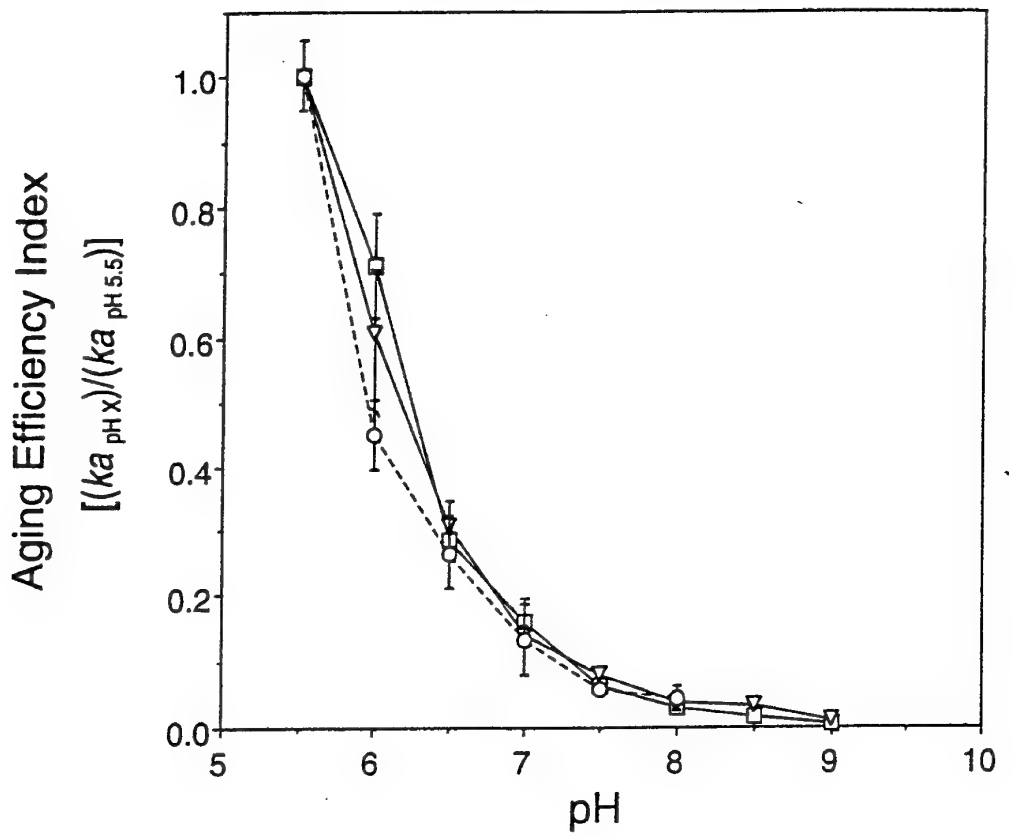

Fig. 9 Dependence of the efficiency indices of aging of the soman-inhibited HuAChE enzymes on pH. The value of efficiency index for each enzyme is defined as the ratio between the first order rate constant of aging at a given pH and the corresponding values at pH 5.5, for the wild type HuAChE (O), E202Q HuAChE (□) and F338A HuAChE (▽).

Mutants of the Hydrophobic Akoxy Pocket. In view of the hydrophobic nature of the 2,3,3-trimethylpropoxy substituent of the phosphonyl moiety and the plasticity of the HuAChE active center, the possible effect of interactions with several aromatic residues (Trp-86; Tyr-337; Phe-338) of the hydrophobic alkoxy subsite, on the aging process was examined. Molecular models (Fig. 8B) indicate that residue Tyr-337 is not involved in interactions with the phosphonyl moiety. This prediction is experimentally confirmed by the observation that replacements of Tyr-337 by alanine or phenylalanine resulted in only a marginal effect on the rates of phosphonylation and aging, relative to the wild type HuAChE (Tables 4, 5).

As in the case of residue Tyr-337, molecular models of the 2,3,3-trimethylpropyl methylphosphono-HuAChE indicate that the aromatic side chain of residue Phe-338 is remote from

the phosphonyl alkoxy group in both the Michaelis complexes (with the P_SC_S and P_SC_R soman diastereomers) and in the resulting covalent conjugates. This conclusion is supported by the finding that the phosphylation rate of F338A by soman is equivalent to that of the wild type enzyme. Nevertheless, replacement of residue Phe-338 by alanine has resulted in almost a 160-fold decrease in the rate of aging (Table 5), demonstrating the involvement of this aromatic amino acid in the aging process. Since this pronounced effect cannot be attributed to a direct interaction of residue Phe-338 with the alkoxy group, it may originate from a structural perturbation that induces a change of the mechanism of aging. Such possibility seems unlikely in view of the similar pH-rate profiles of aging, for the phosphonyl conjugates of F338A and of the wild type HuAChE (Fig. 9). Alternatively, the replacement of Phe-338 may affect the process of proton-transfer to the phosphonyl moiety, through a local perturbation that affects the relative position of the proton donating group (see below and Fig. 10).

The potential participation of residue Trp-86 in the aging process of the 2,3,3-trimethylpropyl methylphosphono-HuAChE, was suggested by both molecular models of the conjugates and the observed differential effects of replacement of residue Trp-86 by alanine and by phenylalanine, on the phosphonylation rates by soman (Table 4). The most dramatic effect on the rate of aging has been observed for the phosphonyl conjugate of W86A HuAChE. For this conjugate, at pH 8, no dealkylation reaction could be detected for several days, indicating that the rate of aging was at least 1000-fold lower than for the wild type enzyme. In attempt to determine whether the W86A conjugate was still capable of undergoing aging, measurements were carried out under low pH conditions which were shown to accelerate aging in other mutants (Fig. 9). Indeed, at pH 7 and pH 6 a slow dealkylation processes could be observed with rate constants 1,850 and 3,300-fold lower respectively than the corresponding values for the wild type enzyme (Table 6). Assuming that this ratio is maintained at pH 8, then the calculated value of half life time for the 2,3,3-trimethylpropyl methylphosphonyl conjugate of the W86A enzyme should be 7.6 -15 days as compared to 6.3 minutes for the wild type HuAChE. Unlike the case of the W86A conjugate, the aging process for the 2,3,3-trimethylpropyl methylphosphono-W86F HuAChE could be monitored at pH 8, with rate constant 25-fold lower than that of the wild type enzyme. These findings underscore the crucial role of aromatic residue at position 86 in the aging of the 2,3,3-trimethylpropyl methyl phosphonyl conjugates of AChEs.

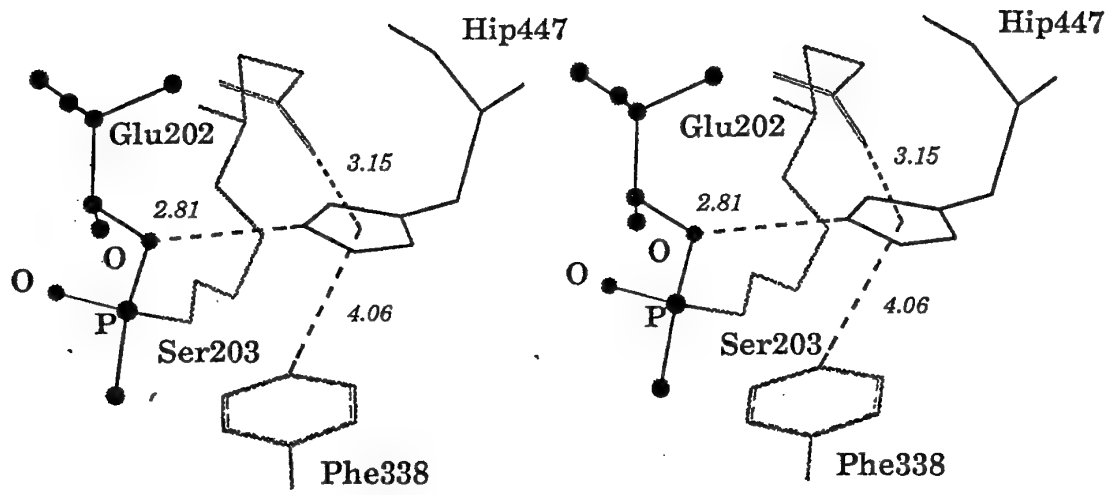

Fig. 10 Stereoview of the proposed orientation of His-447 imidazolium group versus the alkoxy oxygen of the phosphonyl moiety. The 2,3,3-trimethylpropyl methylphosphonyl moiety is shown as balls and sticks and hydrogen atoms are not displayed. The interaction distances (Å) from the centroid of the protonated histidine (Hip-447) imidazolium ring to $O^{\varepsilon 1}$(Glu-202) and the C^{ξ}(Phe-338) are shown in dashed lines. These interactions contribute to the stabilization of both the charge of the imidazolium moiety and its positioning proximal to the alkoxy oxygen, as shown by the corresponding distance $N^{\varepsilon 1}$(Hip-447)-O-alkyl.

Mutant of the Peripheral Anionic Site. Although residue Asp-74 is remote from the active center, its substitution by asparagine was already shown to affect the accommodation of the charged trimethylammonium group in the active center since it lowered the affinity of HuAChE toward ligands like ATC or edrophonium (Shafferman *et al.*, 1992b,c; Barak *et al.*, 1994). On the other hand, such replacement had no effect on the affinity toward the noncharged substrate TB (unpublished results) or toward soman and DFP (Table 4). As was the case of the charged ligands, the mutation Asp74Asn resulted in a 15-fold decrease in the rate of aging of the D74N conjugate with soman. These results may imply that interactions of the active center with a positive charge is part of the aging process of 2,3,3-trimethylpropyl methylphosphonyl conjugates, operating by stabilization of the carbonium ion via the 'anionic' subsite in the active center (Trp-86).

How does AChE Catalyze the Process of Aging?

The generally accepted mechanism of aging involves protonation of the phosphonyl moiety at the alkoxy oxygen, followed by the C-O bond scission and formation of a carbonium ion (Scheme 4). This view is supported by results from experiments with radiolabelled organophosphorus inhibitors (Wilson *et al.,* 1992; Keijer *et al.,* 1974), kinetic correlations with unimolecular solvolysis reactions (Benschop and Keijer, 1966) , crystallographic structures of the related aged conjugates of chymotrypsin (Harel *et al.,* 1991) and by NMR studies of the aging products in AChE (Segall *et al.,* 1993). Although there is evidence that the aging process is facilitated by intermolecular interactions of the phosphonyl moiety with structural elements of the AChE active center, the mechanism of the catalysis is not clear and many, seemingly conflicting, results can be found in the literature. In particular, it is not clear whether the enzyme is catalytically involved in the step of protonation, in that of carbonium ion formation or in both steps.

The efficiency of the protonation step should depend mainly on the proper juxtaposition of the alkoxy group oxygen relative to the potential proton donors in the active center. According to the molecular models of phosphonyl-HuAChE conjugates, the only acidic groups within H-bond distance from the alkoxy oxygen, are those of residues Glu-202 and the catalytic triad His-447 (Shafferman *et al.,* 1992b; Gibney *et al.,* 1990; Sussman *et al.,* 1991). As already indicated, the pH-rate profile of the E202Q conjugate is not consistent with the action of residue Glu-202 as a proton donor. For residue Hip-447 (the protonated form of His-447), the models show (Fig. 10) that formation of a short distance N^{ε}-O-alkyl hydrogen-bond (2.81Å) is possible through motion of the imidazolium moiety from the vicinity of the O^{γ}-Ser-203 to a position near the alkoxy oxygen (Fig. 11). Such stable H-bond may be essential for facilitating the protonation of the alkoxy oxygen and for maintaining a *sufficient steady state concentration* of the oxonium reactive species for the dealkylation to take place. As shown in Fig. 10, formation of the N^{ε}-O-alkyl H-bond places the imidazolium ring within a cation-π interaction distance (4.06 Å) from the phenyl group of residue Phe-338, and within a short distance (3.15 Å) from the negative $O^{\varepsilon 1}$ of the Glu-202 carboxylate.

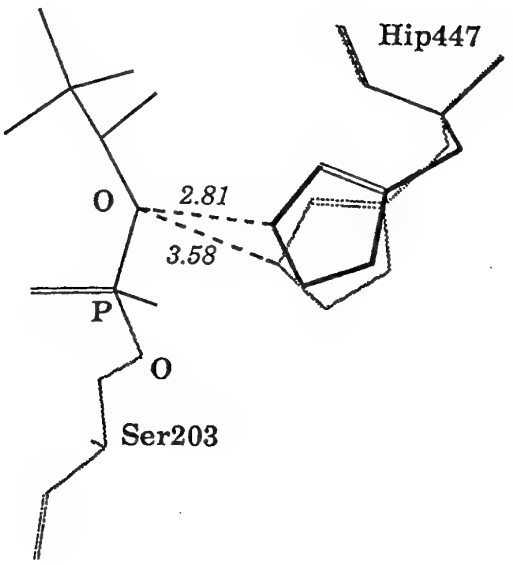

Fig. 11 Significance of conformational mobility of the side chain of His-447 to the catalysis of phosphonyl conjugates dealkylation - an analogy to substrate hydrolysis. The conformation of the protonated histidine (Hip-447) side chain (χ1=167; χ2=89; χ3=-179), marked by heavy line, is probably involved in the proton transfer to the phosphonyl moiety, maintaining a high steady state concentration of the oxonium species. Analogous conformational state of Hip-447 is involved in the choline release from the ACh-AChE tetrahedral intermediate. The alternative, less stable conformation in the phosphonylated enzyme (light line, χ1=-176; χ2=73; χ3=-177), where the immidazolium moiety forms H-bond with O$^{\gamma}$-Ser-203, is analogous to that involved in the release of the enzyme from the hydrated acetyl enzyme. In reaction with substrate, the motion towards O$^{\gamma}$-Ser-203 may be induced by the deprotonation of the immidazolium (through elimination of choline) whereas in phosphonate conjugates such motion is retarded since the alkoxy substituent is not a leaving group.

The participation of residues Glu-202 and Phe-338 in the stabilization of the imidazolium positive charge and in its proper juxtaposition versus the phosphonyl moiety, is consistent with the effects of HuAChE mutagenesis of these residues, on the rates of aging. Such preferential stabilization of the protonated form of histidine, through cation-π interaction with an adjacent aromatic residue, has been already established in barnase (Loewenthal *et al.,* 1992). It should be noted that the motion of His-447 imidazole moiety between the two positions, proximal to O$^{\gamma}$-Ser-203 and to the alkoxy oxygen (Fig. 11), is actually an integral part of the catalytic machinery in serine hydrolases,

operating in both the acylation and the deacylation steps respectively (Nakagawa *et al.*, 1993). During the acylation of AChE by ACh, this imidazole participates in proton transfer from O^{γ}-Ser-203 while the transition of the tetrahedral intermediate into the acyl enzyme is assisted by proton transfer from the imidazolium to the choline oxygen. The latter is analogous to the protonation step of the alkoxy oxygen of phosphonyl conjugates and the formation of the oxonium ion, during the aging process (Fig. 11). Unlike the case of the choline moiety in the substrate, the alkoxy substituent of phosphonates is not a leaving group. Therefore the stabilized N^{ε}-O-alkyl hydrogen bond in the phosphonyl conjugates may restrict the motion of the imidazolium, preventing the protonation of O^{γ}-Ser-203 (indeed in this conformation the distance O^{γ}-Ser-203 - N^{ε} (Hip-447) is 3.45Å, see Fig. 10). Thus, one of the reasons for the hydrolytic stability of phosphyl-AChE conjugates, and in particular that of their aged forms, may be the lack of protonation of O^{γ}-Ser-203, which is necessary for elimination of the enzyme from the conjugate (Qian and Kovach, 1993; Bencsura *et al.*,1995). The proposed localization of the imidazolium moiety relative to the alkoxy oxygen, is also consistent with the well established (Berman and Decker, 1989) resistance of conjugates with the P_R phosphorus configuration to dealkylation. According to the corresponding molecular model (not shown), the N^{ε}-atom of the imidazolium is too remote from the alkoxy oxygen (4.3 Å) to form a stable H-bond, precluding the formation of oxonium and consequently the dealkylation reaction of the P_R phosphonyl AChE conjugates.

The mechanistic hypothesis presented above, suggests that AChE is catalytically involved in the aging process through one of its basic functional features, and consists mainly of accommodating the reactive oxonium species via the catalytic triad residue His-447. Such mechanism should operate for all the P_S phosphonyl conjugates, irrespective of the nature of the alkyl group in the alkoxy moiety. Indeed, the rate constants of aging for various alkyl methylphosphono-AChE conjugates have shown a good correlation with those for solvolysis of the corresponding alkyl tosylates (Benschop and Keijer, 1966; Benschop *et al.*, 1967), demonstrating an equivalent effect of the alkyl structure on both reactions. Furthermore, the activation energy for the dealkylation reaction of cycloheptyl methylphosphono-AChE was found to be comparable to that for solvolysis of the cycloheptyl tosylate (Berman and Decker, 1986a). These results suggest that in all these

cases the AChE is not involved in the charge separation and carbonium ion formation step. However, the aging of two outstanding AChE phosphonyl conjugates, carrying the 2,3,3-trimethylpropyl (Benschop *et al.,* 1967) and the 2,2-dimethylcyclohexyl (Benschop, personal communication) alkyl groups, is much faster than could have been expected from the correlation between the rates of aging and solvolysis. We note that the two alkyl groups share a common branching pattern of a secondary C_α and a tertiary C_β main chain carbon atoms (see Scheme 3). A clue for understanding the unique efficiency of AChEs, in facilitating the dealkylation step of such branched alkoxy groups in the phosphonyl-HuAChE conjugates is provided in this study. We propose that the key element for the unique enzymatic acceleration of dealkylation of the branched alkoxy substituents on the phosphonyl adducts, may be due to the interaction of the 2,3,3-trimethylpropoxy group with residue Trp-86. Stabilization of the carbonium ion on the C_α of the 2,3,3-trimethylpropyl moiety, through hyperconjugation with the adjacent alkyl groups, imparts a partial positive character to the C_β methyl substituents. The aromatic moiety of the Trp-86 may contribute to the stabilization of this partial positive charge, thereby facilitating the charge separation process. Such interaction is analogous to the well established cation-π interaction of residue Trp-86 with the trimethylammonium substituents of ligands like edrophonium or the substrate acetylcholine (Ordentlich *et al.,* 1993a; Harel *et al.,* 1993). The dramatic 1,850-3,300-fold decrease in the rate of aging for the 2,3,3-trimethylpropyl methylphosphono-W86A conjugate, compared to the wild type HuAChE conjugate, can be rationalized by the absence of this stabilizing effect. A comparable decrease in affinity (4,000-15,000-fold) was observed for the W86A enzyme toward the bisquaternary ligands BW284C51 and decamethonium (Ordentlich *et al.,* 1995; Barak *et al.,* 1994), whereas the affinities toward the noncharged bulky ligands like the m-tertbutyl trifluoroacetophenone (Radic *et al.,* 1995) and soman (Table 4) are only moderately affected (about 20-fold) by such replacement. Moreover, the 25-fold decrease of the aging rate constant, for the 2,3,3-trimethylpropyl methylphosphono-W86F conjugate, is quite similar to the effect of replacing the indole moiety by a phenyl group on the inhibition constant by the charged, active center reversible inhibitors, edrophonium, decamethonium and BW284C51 (Ordentlich *et al.,* 1995). These comparisons further underscore the importance of the positive charge stabilization by Trp-86, to the reactivity of AChE toward substrates and other active center ligand.

The enhanced capacity of tryptophane to interact with positively charged species, as compared to phenylalanine, is a result of the much larger negative electrostatic potential provided by the indole moiety (Dougherty, 1996). The involvement of aromatic residues, revealed in this study, in the aging of soman-inhibited AChEs clarifies the *absence* of a comparable acceleration effects on aging for soman-inhibited serine hydrolases like chymotrypsin, where no aromatic residue adjacent to the phosphonyl alkoxy group can be found.

Finally, the enzymatic involvement in acceleration of both the protonation and the carbonium ion formation steps may account for the rapid aging of soman-inhibited AChEs as compared to other phosphyl conjugates of cholinesterases. It is also consistent with the measured solvent isotope effects of aging for 2-propyl- and 2,3,3-trimethylpropyl-methylphosphono-AChE conjugates (k^H/k^D ratio of 1.2 and 1.6 respectively (Qian and Kovach, 1993; Kovach and Bennet, 1990) which indicate that for the latter, both steps (protonation and dealkylation) contribute to the overall rate of aging. According to this view it may be expected that for most AChE phosphonyl conjugates, where acceleration of the dealkylation step is limited, the substitution of residue equivalent to Trp-86 will have less significant on the rates of aging.

Implications for Design of Future OP-HuAChE Bioscavenger

The results from the present study provide some clues for potential manipulations of target amino acids in the design of a novel OP-HuAChE bioscavenger which will not undergo rapid aging as native AChE enzymes.These residues include : elements of the H-bond network - Glu202, Glu450, and Tyr133; residues constituting the hydrophobic alkoxy pocket - Phe338 or Trp86 and surprisingly even Asp74 which belong to the peripheral anionic subsite located at the entrance to the active center gorge. However selection criteria for target amino acids should obviously include also the effect of such mutations on the efficiency of phosphylation reactions. Accordingly and on the basis of studies reported above for soman and carried out recently (Ordentlich et al 1995) with several organophosphates it appears that the H-bond network elements are essential for efficient phosphylation. It seems therefore that the future OP-AChE bioscavenger should retain the H-bond network residues intact in spite of the contribution of their mutations to a phenotype more resistant to aging. Other amino acids mentioned above and combination thereof should be evaluated in the future in combination with mutations that are optimal for phosphylation.

IV. Aging is a Biocatalytic Process Involving Stabilization of a Carbocation Intermediate by Trp86

INTRODUCTION

The cation-π interaction is currently receiving considerable attention as a new type of binding force that is important in the function of biological systems like selectivity of ion channels (Kumpf and Dougherty, 1993), monoamine neurotransmitters interactions with their membranal receptors (Trumpp-Kallmeyer *et al.*, 1992; Norvall *et al.*, 1992; Schwartz, 1994; Hucho *et al.*,1996) and enzyme recognition of substrates and inhibitors (Ortiz *et al.*, 1992; Raine *et al.*,1995; Lin and Johnson, 1995). In particular, the involvement of residue Trp86 at the active center of human acetylcholinesterase (HuAChE; Shafferman *et al.*, 1992d; Ordentlich *et al.*, 1993a; Ordentlich *et al.*, 1995; Barak *et al.*, 1995) and corresponding tryptophanes in other AChEs (Weise *et al.*, 1990; Sussman *et al.*, 1991; Harel *et al.*, 1993; Radic *et al.*, 1995; Harel *et al.*, 1996), in accommodating the quaternary ammonium moieties of acetylcholine and of several covalent and noncovalent inhibitors, is well documented. The stabilizing cation-π interaction has been extensively investigated in a variety of synthetic "host" systems (Dougherty and Staufer, 1990; Méric *et al.*, 1993; Garel *et al.*, 1993) and is currently interpreted as a predominantly charge-quadrupole attraction between a positive charge and the "anionic" face of the aromatic ring, supplemented by dispersion attraction and polarization (Staufer *et al.*, 1990; Kim *et al.*, 1994; Chipot *et al.*, 1996). The involvement of aromatic residues , in stabilization of partially charged transition states for certain enzymatic processes mediated by carbocations or sulfonium ions, has been also suggested as a means to provide highly polar interaction loci which are compatible with the hydrophobic environments of the enzyme active centers (McCurdy *et al.*, 1992; Dougherty, 1996). However, a direct experimental evidence for such involvement is not yet available.

METHODS

Materials - Acetylthiocholine iodide (ATC) and 5:5'-dithiobis (2-nitrobenzoic acid) (DTNB) were purchased from Sigma. Phosphonyl conjugates of the HuAChE enzymes were obtained using purified racemic mixtures of 2,3,3-trimethylpropyl methylphosphonofluoridate (soman) and 2-propyl methylphosphonofluoridate (sarin; prepared from methylphosphonodifluoride following an accepted synthetic procedure, see Monard and Quinchon, 1961) or of 2-butyl methylphosphono-fluoridate (IBMPF) and 2,3-dimethylpropyl methylphosphonofluoridate (DMPF) both a gift from Dr. H. Benschop (Prins Maurits Laboratory TNO, Netherlands). 1-(2-hydroxy-iminomethylpyridinium)-1-(4-carboxyimino-pyridinium) dimethylether dichloride (HI-6) was a gift from Dr. G. Amitai.

Production of Enzymes- Expression of recombinant HuAChE and its mutants in a human embryonal kidney derived 293 cell line (Shafferman *et al.*, 1992b; Velan *et al.*, 1991a; Kronman *et al.*, 1992) and generation of all the mutants was described previously (Ordentlich *et al.*, 1993a,b; Shafferman *et al.*, 1992b,c; Ordentlich *et al.*, 1995). Stable recombinant cell clones expressing high levels of each of the mutants were established according to the procedure described previously (Kronman *et al.*, 1992). Enzymes were purified (over 90% purity) either by ligand affinity chromatography (Kronman *et al.*, 1992) or by fractionation on monoclonal antibody affinity column (Barak *et al.*,1995).

Enzyme Activity Measurements and Active Site Titrations- Activity of HuAChE enzymes was assayed according to Ellman *et al.* (1961) (in the presence of 0.1 mg/ml BSA, 0.3mM DTNB, 50mM sodium-phosphate buffer pH-8.0 and various concentrations of ATC), carried out at 27°C and monitored by a Thermomax microplate reader (Molecular Devices).

Active site titration of enzyme solutions was carried out in the presence of 0.1 mg/ml BSA in 50mM sodium-phosphate buffer pH 8.0, by adding various amounts of phosphonate inhibitors (MEPQ or soman). Inhibition was allowed to proceed to completion and the residual activity was plotted versus the concentration of inhibitor. MEPQ, a potent non-stereoselective inhibitor of ChEs (Levy and Ashani, 1986) reacting in a 1:1 ratio with various AChEs including the recombinant

HuAChE (Velan *et al.*,1991b), was used as a standard for the active site titrations. The concentrations of the active site subunits of all the enzymes as determined by titration with MEPQ, were within ±10% from those measured by the specific enzyme linked immunosorbent assays (ELISA; Shafferman *et al.*, 1992b). These values were used to determine the stoichiometry of the reactions of soman with the various HuAChE enzymes.

Measurements of Aging Rates- The conjugates of the wild type (WT) the W86F and the W86A HuAChEs were obtained from phosphonylation of the respective enzymes as described before (Ordentlich *et al.*, 1995). The reactions were carried out under conditions where the rate of phosphonylation is much faster than the rate of aging ($ki[I_o] >> ka$) and with over 98% inhibition of the initial enzyme activity. The excess phosphonate was rapidly removed either by column filtration (Sephadex, G-15) or by 1000 fold dilution, prior to reactivation. The reactivatable (non-aged phosphonyl conjugate) fraction was determined by reactivation with 0.5 mM HI-6 under conditions where the rate of reactivation is higher than the rate of aging ($kr[HI-6]>ka$). The activity of the reactivated enzyme (Er) was routinely corrected for the inhibitory effect of the reactivator (De Jong and Kossen, 1985). The first order rate constants of aging (ka) were determined from the slopes of ln(Er) vs. time.

Under the experimental conditions used (pH=7.0; temp=37 °C), a substantial regeneration of the enzymatic activity was observed even for the WT-soman conjugate for which the aging is fairly rapid. Although the conjugates are presumably each a mixture of two diastereomers, in most cases monoexponential aging kinetics have been observed. In the cases of W86F-IBMPF and W86F-DMPF conjugates, where the biexponential kinetic behaviour becomes evident, the rate constant corresponding to the faster reaction has been cited.

RESULTS AND DISCUSSION

In section III we reported that replacement of residue Trp86 in HuAChE by alanine resulted in a dramatic decrease (over 10^3-fold) in the dealkylation rate of 1,2,2 trimethyl propyl methylphosphonofluoridate (soman) inhibited enzyme. This process, known also as 'aging', involves scission of the alkyl-oxygen bond through formation of a carbocation (Benschop and Keijer , 1966; Benschop *et al.*, 1967; Michel *et al.*, 1967; Cadogan *et al.*, 1969) resulting in a substantial formation of alkenes and a formal negative charge in the conjugate (see Scheme 5). The participation of HuAChE in the aging process was hypothesized (see section III) to involve the stabilization of partial positive charges of the C_β methyl substituents, imparted through hyperconjugation with the evolving carbocation on the C_α of the 1,2,2-trimethylpropyl moiety, by cation-π interaction with the indole ring of the active center residue Trp86 (Fig. 12). If this idea is correct then the extent of methylation at the alkoxy C_β of the phosphono-conjugate should be of a crucial importance to the facility of aging, since these methyl groups may mediate both the delocalization of the evolving positive charge and its accommodation in the enzymatic environment. Furthermore, replacement of Trp86 by another aromatic residue - phenylalanine - should still allow for the cation-π interaction, albeit its contribution to the carbocation accommodation may be lower (Kearney *et al.*,1993). Finally, one could also expect that in the absence of aromatic residue at position 86, the correlation between the rate of aging and branching at C_β of the alkoxy substituent should resemble that of limiting solvolysis reactions of analogous tosylates or phosphonates (Benschop *et al.*, 1967; Cadogan *et al.*, 1969).

These predictions were tested through examination of the kinetics of aging for twelve methylphosphonyl - HuAChE conjugates (see Scheme 5), differing in the number of methyl groups at C_β and in the nature of the residue at position 86 of the enzyme. The data (Table 7) are in accordance with all the above predictions and thus support the notion that HuAChE is involved in the mechanism of aging through cation-π interactions. To our knowledge this is the first actual demonstration of biocatalysis through cation-π stabilization of a carbocationic transition state.

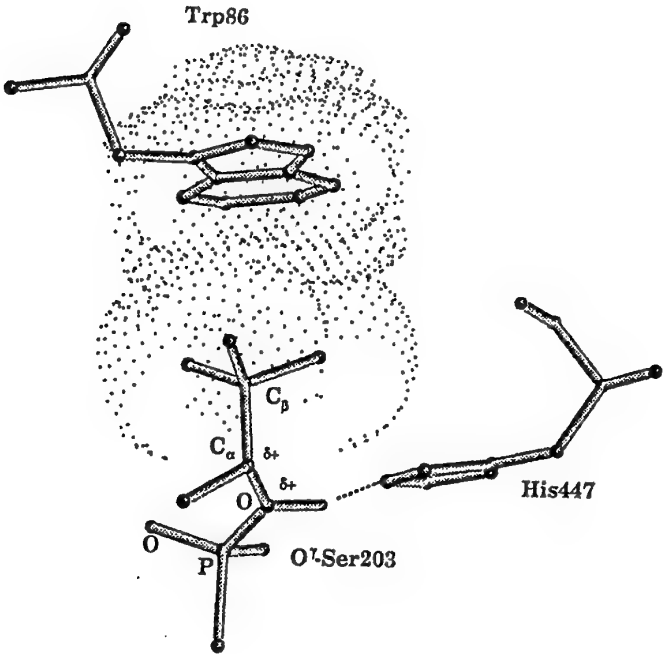

Fig. 12 Orientation of the protonated methylphosphonyl moiety in WT-soman conjugate relative to the residues presumably involved in the catalysis of aging. The catalytic triad residue His447 is probably involved in proton transfer to the phosphonyl moiety, maintaining a sufficient steady-state concentration of the oxonium reactive species for the dealkylation to take place (see section III). The methylphosphonyl C_β methyl substituents and the indole group of residue Trp86 exhibit a tight matching of their van der Waals syrfaces and are favorably juxtaposed for the development of the stabilizing cation-π interaction, during the charge separation (O-C_α bond breaking) step. The positive charge on C_α is dispersed through partial overlap of the empty p-orbital of C_α and the σ C_β-CH_3 bonds (hyperconjugation).

For the conjugates of the wild type enzyme a progressive decrease in rates of aging was observed (from 0.675min^{-1} to 0.003min^{-1}) concomitant with a decrease in branching of the alkyl group of the methylphosphonyl moiety (see Scheme5 and Table 7). Examination of the effects due to amino acid replacements at position 86 of HuAChE, on the rates of aging of the corresponding methylphosphono-conjugates (compare those of WT and W86F in Table 7) shows that substitution Trp—>Phe results in a moderate and uniform decrease of the rates (13-16-fold), irrespective of the nature of the phosphonyl moiety. Similar decrease in affinities towards positively charged ligands (edrophonium, decamethonium; see Ordentlich *et al.*, 1993a) was also observed in the W86F

enzyme as compared to the wild type enzyme. This parallelism indicates that Phe86 may indeed participate in the aging process through carbocation stabilization. In addition, the constant ratio of the aging rates for the conjugates of the wild type and the W86F enzymes is consistent with the notion that tryptophane and phenylalanine play equivalent roles in the aging process, and that their relative contributions are determined only by the size of their respective π-electron systems (Kearney *et al.*, 1993). On the other hand, for the various alkyl substituents in the methylphosphono-conjugates, comparison of the ratio k_a^{WT}/k_a^{W86A} for soman, DMPF, IBMPF and sarin shows a decline from 1120 to 60 respectively. This decline demonstrates that the extent of involvement of residue Trp86 in WT, relative to Ala86 in W86A, in the aging process is stronger dependence upon the number of methyl groups at C_β of the phosphono alkoxy substituent.

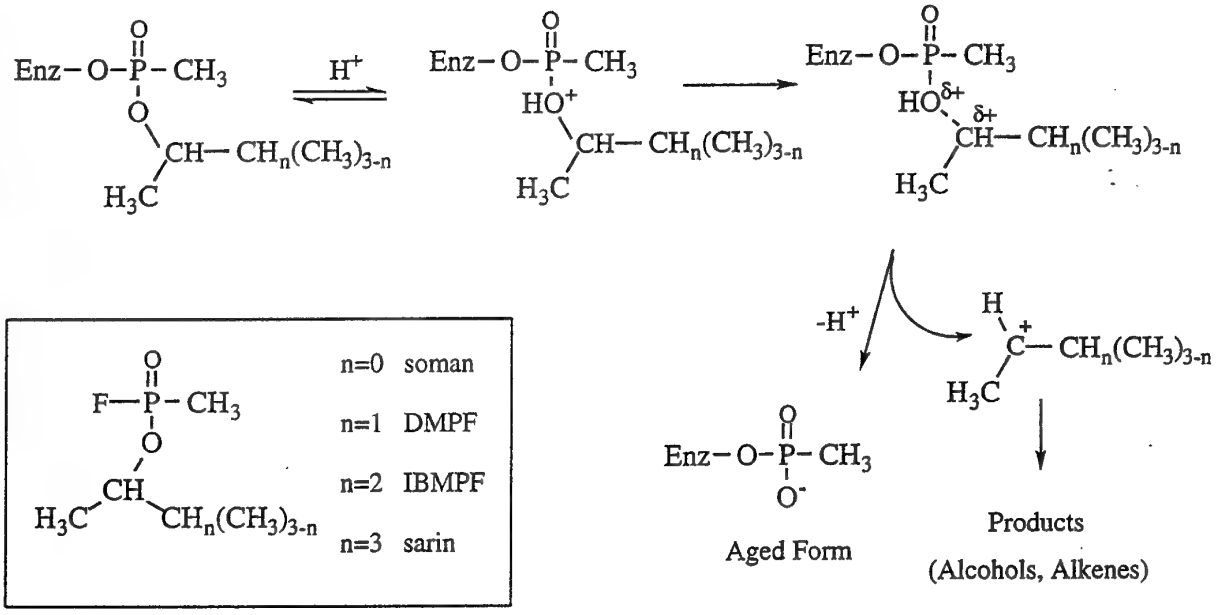

Scheme 5 Carbocation mechanism of the aging process in alkyl methylphosphono HuAChE conjugates

Table 7: Rate constants of aging (ka) of the alkyl methylphosphono conjugates of the HuAChE mutants at pH 7.0, 37°C

	phosphonyl			
enzyme	Soman	DMPF	IBMPF	Sarin
	ka ($x10^3 min^{-1}$)			
WT	675 ± 150	75 ± 15	30 ± 6	3.6 ±0.6
W86F	46 ± 6	5.9 ± 1	2.0 ±O.2	0.21±0.02
W86A	0.6±0.1	0.20±0.06	0.08±0.02	0.06±0.01

Aging of the W86A-soman conjugate is 10-fold faster than that of the W86A-sarin adduct (see Table 7), corresponding to a relatively small difference in the activation energies of the two reactions ($\Delta E^{\#}_{(W86A\text{-}sarin\text{-}(W86A\text{-}soman)}$= 1.42 Kcal/mol; see Fig. 13). A similar rate dependence on the C_β substitution has been observed for the analogous limiting solvolysis reactions of the corresponding alkyl brosylates (the rate constants of limiting formolysis for 2-butyl; 2,3-dimethylpropyl and 2,3,3-trimethylpropyl p-bromobenzene-sulfonates, relative to the 2-propyl derivative are 2.5, 14 and 14 respectively - see Winstein and Marshall, 1952). This similarity suggests that the W86A enzyme does not participate in facilitation of the charge separation step and that the decrease in activation energy is mainly due to hyperconjugative effects. The protein environment may still have some effect since the geometry of the transition state of the W86A-sarin conjugate aging reaction appears to be somewhat different from that of the analogous solvolysis of 2,3,3-trimethylpropyl brosylate. The latter is probably similar to the resulting planar carbocation intermediate, since the data (Winstein and Marshall, 1952) show that solvolysis reactions of 2,3,3-trimethylpropyl and 2,3-dimethylpropyl brosylates proceed at the same rate. Such lack of contribution of the third C_β methyl substituent may be due to the planarity of the transition state, where gauche interactions force a methyl substituent into the nodal plane of the empty p-orbital of the evolving carbocation. In contrast, for the two enzymes bearing aromatic residues at position

86, the decrease in activation energy of dealkylation reaction of the WT-soman and W86F-soman conjugates, relative to the WT-sarin and W86F-sarin conjugates respectively ($\Delta E^{\#}_{(WT\text{-}sarin)\text{-}(WT\text{-}soman)} \approx \Delta E^{\#}_{(W86F\text{-}sarin)\text{-}(W86F\text{-}soman)} > 3.2$Kcal/mol; see Fig 13) is much larger. Such enzymatic acceleration appears to involve interaction with aromatic system since the values of $\Delta E^{\#}_{(WT\text{-}sarin)\text{-}(WT\text{-}soman)}$ and $\Delta E^{\#}_{(W86F\text{-}sarin)\text{-}(W86F\text{-}soman)}$ are practically equivalent irrespective of the aromatic residue at position 86. Note that such similarities in $\Delta E^{\#}$ values exist also for the pairs $\Delta E^{\#}_{(WT\text{-}IBMPF)\text{-}(WT\text{-}soman)}$ and $\Delta E^{\#}_{(W86F\text{-}IBMPF)\text{-}(W86F\text{-}soman)}$ or $\Delta E^{\#}_{(WT\text{-}DMPF)\text{-}(WT\text{-}soman)}$ and $\Delta E^{\#}_{(W86F\text{-}DMPF)\text{-}(W86F\text{-}soman)}$. On the other hand, the greater contributions of tryptophan in conjugates of the WT HuAChE as compared to phenylalanine in conjugates of the W86F enzyme, to the overall rate of aging (see Table 7 and inset Fig. 13) is consistent with the relative capacities for cation-π interactions of these two aromatic moieties (McCurdy *et al.*, 1992; Dougherty, 1996). Presentation of the kinetic data through the respective values of $\Delta E^{\#}$ (Fig. 13) for the entire series of WT and W86F adducts (relative to the WT-sarin and W86F-sarin conjugates respectively) demonstrates the extent of enzyme participation in the aging process as well as a clear correlation between the branching of the alkyl substituent. This correlation is consistent with the mechanistic hypothesis which relates the contribution of cation-π interactions to stabilization of transition state with the polarizabilities of the interacting partners (McCurdy *et al.*, 1992; Dougherty, 1996). Transition state polarizability of the aging process should be enhanced by dispersion of the evolving positive charge, and therefore by branching at the C_β of the phosphono alkyl group. Ultimately, this enhancement results in a uniquely high rate of aging of HuAChE conjugated with the 1,2,2-trimethylpropyl methylphosphonyl moiety, with a half life of 1 minute (pH 7, 37 °C, see Table 7). The correlation between branching at C_β of the alkyl phosphono substituent and the acceleration of the aging process can be also rationalized in terms of steric congestion at the active center (Benschop *et al.*, 1967). However such explanation is inconsistent with the nearly identical $\Delta E^{\#}$ values for the WT and W86F series of conjugates bearing aromatic moieties of considerably different volume and shape.

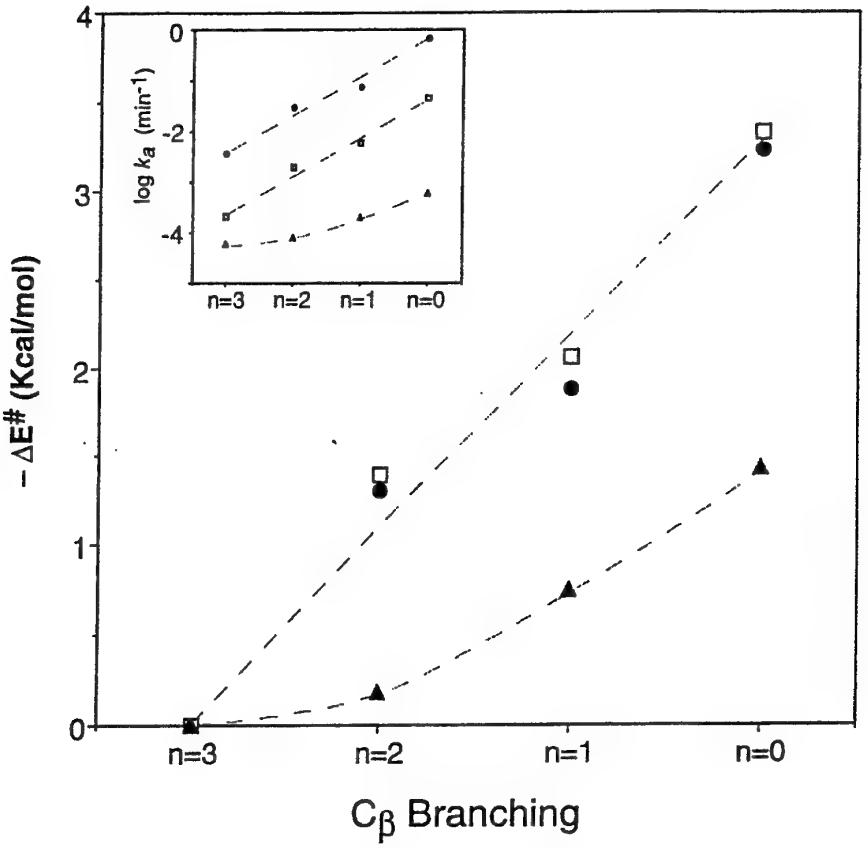

Fig. 13 Differences in activation energy of aging, between the alkyl methylphosphono conjugates of WT, W86F and W86A HuAChEs and the corresponding 2-propyl methylphosphono-HuAChEs. **WT** (●), **W86F** (□) and **W86A** (▲), as a function of the number (n) of methyl substituents at C_β (see Scheme 5). Values of ΔE# were calculated from Arrhenius equation (R=1.99·10^{-3} Kcal·mole^{-1}·K^{-1}; T=310 °K) assuming a constant frequency factor. The correlation between the rate constants of aging and C_β branching is shown in the inset.

Carbocationic transition states may be stabilized through polar interactions with acidic residues, like those encountered in the enzymatic glycosyl transfer reactions (Warshel, 1991). On the other hand, nature appears to use aromatic moieties as "hydrophobic negative charges" for polar interactions in apolar environments like membrane-bound receptors and protein interiors (McCurdy *et al.*, 1992; Dougherty, 1996). The recently proposed guidance of carbocation formation during the enzymatic cyclization of squalene, by aromatic residues is an example of the possible utilization of such interactions in biocatalysis (Shi *et al.*, 1994). Yet, recognition of cation-π interactions as

one of the noncovalent forces contributing to catalytic activity is mostly speculative, due to the absence of structural data for any of the relevant enzymes (Dougherty, 1996). On the other hand, for the system studies here we can rely on the 3D structure of the closely related enzyme (*Torpedo californica* AChE) for which there is also information on some covalent and noncovalent adducts (Weise *et al.*, 1990; Sussman *et al.*, 1991; Harel *et al.*, 1993; Radic *et al.*, 1995; Harel *et al.*, 1996). This structural background together with the experimental findings regarding aging of methylphosphono-HuAChE conjugates strongly support the molecular mechanism of biocatalysis operating through cation-π interactions.

V. Use of Electrospray-Ionization Mass Spectrometry to Determine the Chemical Composition of Acetylcholinesterase Phosphonylation Products

INTRODUCTION

The catalytic power of acetylcholinesterase (AChE, EC 3.1.1.7), which is among the most efficient enzymes with turnover number of over 10^4 sec^{-1} (for recent reviews see Massoulie *et al.*, 1993; Taylor and Radic, 1994), is believed to be a consequence of the unique architecture of its active center (Gibney *et al.*, 1990; Sussman *et al.*,1991; Velan *et al.*,1991a; Shafferman *et al.*, 1992b,c; Radic *et al.*, 1992; Vellom *et al.*, 1993; Ordentlich *et al.*, 1993a; Radic *et al.*, 1993; Barak *et al.*, 1994 ; Gnatt *et al.*, 1994; Bourne, *et al.*, 1995; Ordentlich *et al.*,1995; Harel *et al.*, 1996). This architecture can also account for the marked stereospecificity toward certain alkyl methylphosphonofluoridates and methylphosphonothioates (Benschop and De Jong, 1988; Barak *et al.*, 1992; Hosea *et al.*, 1995). The phosphonylation is thought to proceed through an *in-line* displacement reaction at the phosphorus to form a stoichiometric (1:1) and stable conjugate through inversion of configuration around the phosphorus (Aldridge and Reiner, 1972; Main, 1976; Berman and Decker, 1989). The post-inhibitory behavior of phosphonyl-AChE adducts has been examined mainly through the facility of reactivation of the enzyme by reaction with nucleophilic agents such as quaternary oximes or fluoride ions (Taylor, 1990; Wilson, *et al.*, 1992). Nonreactivability of the adducts is usually associated with a unimolecular process which involves a loss of an alkyl group from the phosphonyl alkoxy substituent and is termed 'aging' (Benschop and Keijer, 1966; Michel *et al.*, 1967; Segall *et al.*, 1993; Ordentlich *et al.*, 1993b; see section III).

In certain cases resistance to reactivation of phosphonyl-AChE conjugates, like that of (P+)-cycloheptyl methylphosphono-AChE (Berman and Decker, 1989) , may not be due to the classical 'aging' mechanism. The non-reactivability in these cases can originate from the inability of the protein to regain the conformationally active form following inhibition, even though displacement of the phosphyl moiety from the active site serine has actually occurred (Thompson *et al.*, 1992). In addition, non-reactivability may in principle also occur through a path for the decomposition of phosphonyl - AChE adducts which is different from the classical 'aging' (Maglothin *et al.*, 1975 Mullner and Sund, 1980). One of the reasons for the difficulty to estimate the importance of those mechanisms to the reactivability of phosphonyl-AChE adducts, was that the variations in composition of these enzyme-adducts could not be determined.

Structures of several serine hydrolase phosphyl-conjugates were determined by x-ray crystallography (Kossiakoff and Spencer, 1980; Harel *et al.*, 1991; Derewanda *et al.*, 1992; Grochulski *et al.*, 1994). Such data are not available for cholinesterases and the nature of the corresponding phosphyl adducts can be inferred mainly from analogies to other hydrolases. To date, structures of aged cholinesterase-conjugates could be suggested only on the basis of capture of low molecular weight decomposition products (corresponding alkyl alcohol or alkene; see Michel *et al.*, 1967) and more recently by NMR studies (Segall *et al.*, 1993). Although these results are consistent with the commonly accepted structure of the aged phosphyl-AChE conjugate, an unequivocal evidence regarding its composition is not yet available.

Here we report that the chemical composition of certain phosphonyl - adducts of HuAChE can be directly measured by electrospray-ionization mass spectrometry (ESI-MS). In this method the molecular mass of HuAChE and its phosphonyl adducts has been measured accurately allowing also to monitor the post-inhibitory processes on a molecular level. In the absence of x-ray structures for the different phosphyl-cholinesterase conjugates, these mass spectrometric results represent a direct evidence for their chemical identity.

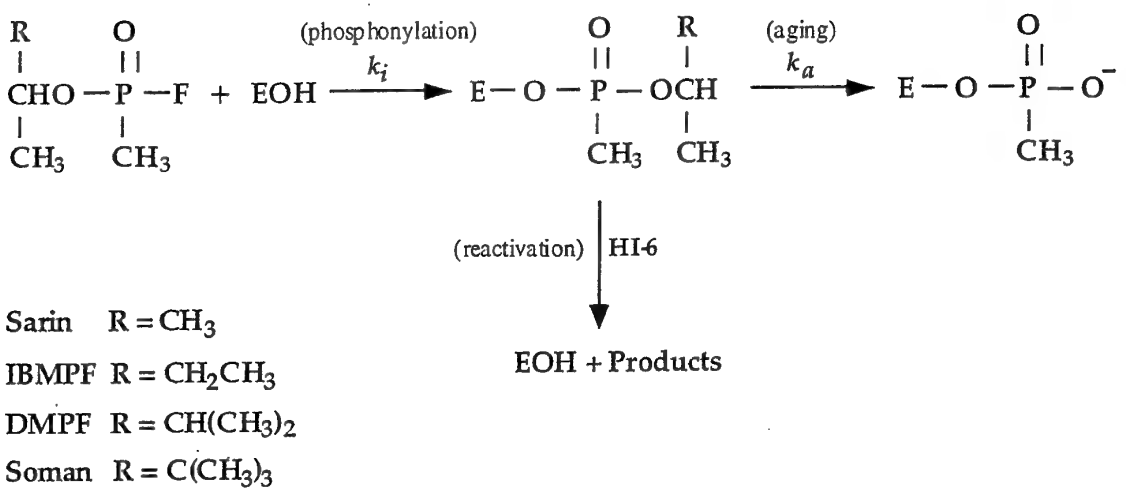

Scheme 6. Generation and 'aging' of phosphonylated AChE

METHODS

Enzymes Reagents and Inhibitors- Wild type (WT) recombinant HuAChE and its monomeric mutant C580A were expressed in 293 cells and purified as described before (Velan *et al.*, 1991a; Ordentlich *et al.*, 1993a). The monomeric C580S bacterially expressed enzyme (HuAChE-bac) was expressed in E. coli (Fischer *et al.*, 1993) with an N-terminus sequence Met-Glu-Gly-Arg-. Acetylthiocholine iodide (ATC) and 5:5'-dithiobis (2-nitrobenzoic acid) (DTNB) were purchased from Sigma. 1-(2-hydroxyimino-methylpyridinium)-1-(4-carboxyimino-pyridinium) dimethylether dichloride (HI-6) was a gift from Dr. G. Amitai. Preparation of the racemic mixtures of 2-propyl, 2-butyl and 1,2-dimethylpropyl methylphosphonofluoridates, used in this study, followed an accepted synthetic procedure using methylphosphonodifluoride (Monard and Quinchon, 1961) and the appropriate alcohol. The purified stereoisomers (C+P+) - and (C+P-) - 1,2,2-trimethylpropyl methylphosphono-fluoridates were isolated as described before (Benschop *et al.*, 1984).

Kinetic Studies- HuAChE activity was assayed according to Ellman et al., (1961) (in the presence of 0.1 mg/ml BSA, 0.3mM DTNB, 50mM sodium-phosphate buffer pH-8.0 and various concentrations of ATC), carried out at 27°C and monitored by a Thermomax microplate reader (Molecular Devices).

Measurements of phosphonylation rates, with the mammalian recombinant HuAChE, were carried out in at least four different concentrations of the alkyl methylphosphonofluoridates (I) and enzyme residual activity (E) at various times was monitored. The apparent bimolecular phosphonylation rate constants (ki) determined under pseudo-first order conditions were computed from the plot of slopes of ln(E) vs time at different inhibitor concentrations. Rate constants under second order conditions were determined from plots of $\ln\{E/[I_o-(E_o-E)]\}$ versus time (see section III).

The stabilities of the HuAChE phosphono-conjugates were evaluated under conditions where the rate of phosphonylation is much faster than the rate of aging ($ki[I_o] >> ka$, see scheme 1) and with over 98% inhibition of the initial enzyme activity. The excess inhibitor was rapidly removed either by column filtration (Sephadex, G-15) or by 1000 fold dilution, prior to reactivation. The reactivatable (non-aged methylphosphono-conjugate) fraction was determined by reactivation with 0.5 mM HI-6 under conditions where the rate of reactivation is higher than the rate of aging (see scheme 6 and section III).

Mass Spectrometric Analysis - Molecular mass measurements were carried out on a VG Platform mass spectrometer, which consists essentially of an electrospray ion source operating at atmospheric pressure followed by a quadrupole mass analyzer. Samples of HuAChE-bac and of the phosphonyl-HuAChE conjugates, prepared by mixing the enzyme (30-40pmol/µl) with an excess of appropriate phosphonofluoridate, were introduced directly into the ion source in a 50:50 acetonitrile-water solutions.The flow-rate of the sample solution into the ion source was 20 µl/min. The mass spectrometer was scanned, in positive ion mode, from m/z 500 to 1900 in 10 sec and several scans were summed to obtain the final spectrum. Mass-scale calibration employed the multiply charged ions from a separate introduction of myoglobin.

The multiply charged electrospray ionization mass spectra were converted to the true molecular

weight spectra using the VG MaxEnt algorithm of the MassLynx NT software. Molecular weight calculations of homogeneous samples were carried out over a mass range of 50000-80000 Da (see Fig. 14,16), whereas a narrower mass range (64000-66000 Da) was used for the case of 1,2-dimethylpropyl methylphosphono-HuAChE (see Fig. 15). At least 5 mass determinations were carried out for each of the molecular species reported, yielding every time exactly the same values (within the experimental resolution of 1Da) .

Similar experiments aimed to obtain molecular masses for either the wild type HuAChE or the monomeric C580A mutant, expressed in mammalian cells, were unsuccessful. Scanning in positive or negative ion modes and at higher resolution (peak width at half height ≤0.75 Da) failed to produce spectra in which discrete multiply charged species could be isolated.

RESULTS AND DISCUSSION

ESI-MS is a new mass spectrometric method that has been recently applied to the detection of covalent enzyme-substrate and enzyme-inhibitor complexes as well as for probing protein-ligand noncovalent interactions (Chait and Kent , 1992; Li *et al.*, 1993; Andersen *et al.*, 1996). One of its unique features is that the protein sample is introduced directly from solution, in its biologically active form, for mass spectrometry analysis. The ESI is not expected to facilitate chemical changes of covalent conjugates during the ionization process and therefore is suitable to monitor the post-inhibitory behavior of phosphyl-AChE adducts.

To examine the potential utility of ESI-MS to such study we attempted to determine the molecular mass of the HuAChE recombinant enzyme expressed in human embryonal 293 cells (Velan *et al.*, 1991a), by direct introduction into the ion source. However the resulting signal could not be resolved into discrete masses, indicating a mixture of molecular species which may originate from oligomerization and post-translational modifications of the protein (Massoulie *et al.*, 1993). To overcome this problem we measured, in the same manner, the mass spectrum of the C580A mutant enzyme, in which replacement of the C-terminal cysteine prevents oligomerization and the protein is monomeric (Massoulie *et al.*, 1993). In this case we still could not obtain a discrete molecular mass, probably due to the variable sugar composition of the enzyme glycosyl substituents and

variability of the glycosylation pattern (Velan *et al.*, 1994). Such variability appears to be characteristic to HuAChE's, where all the three potential N-glycosylation sites are utilized but not all the secreted molecules are fully glycosylated (Velan *et al.*, 1993a; Kronman *et al.*, 1995). Consequently, we decided to examine the monomeric form of HuAChE (C580S) expressed in *E. coli* (HuAChE-bac) which is not glycosylated. In the past it was demonstrated that oligomerization or the extent of glycosylation of HuAChE has practically no effect on either catalytic activity or on reactivity towards active center ligands (Kronman *et al.*, 1995). For the HuAChE-bac the molecular mass could indeed be determined by ESI-MS (see Fig 1A). The measured molecular mass (64700 Da) is consistent with that calculated (64695 Da) for a bacterial HuAChE (C580S) sequence containing methionine at the N-terminus.

Following the determination of HuAChE-bac molecular mass we examined the feasibility of measuring the composition of its phosphonyl-adducts. Since for some methylfluoro-phosphonates (like soman or DMPF, see scheme 6) the initial phosphonyl-HuAChE conjugate could be expected to undergo fairly rapid post-inhibitory transformations (Benschop *et al.*, 1967; Barak *et al.*, 1997), the mass spectrometric experiments had to be carried out immediately after the phosphonylation. In addition, the reaction had to be carried out under conditions where the phosphonylation reactions were rapid but the development of non-reactivability was relatively slow. To determine accurately these boundary conditions, the rates of HuAChE phosphonylation with the homologous series of alkyl methylphosphonofluoridates (soman, DMPF, IBMPF, sarin) and the stabilities of the corresponding phosphonyl-HuAChE conjugates were measured (see Table 8). The actual measurements were carried out by reacting the enzyme with excess diastereomeric mixtures of DMPF, IBMPF and sarin and subjecting the reaction solutions to mass spectrometric analysis 2-4 minutes after the reaction onset. On the other hand, in the case of soman, measurements were carried out with each of the purified diastereomers (C+P- and C+P+) since for the diastereomeric mixture only the aged product is expected to be formed within a few minutes after the phosphonylation (see Table 8, see section III).

T= 2-4 min

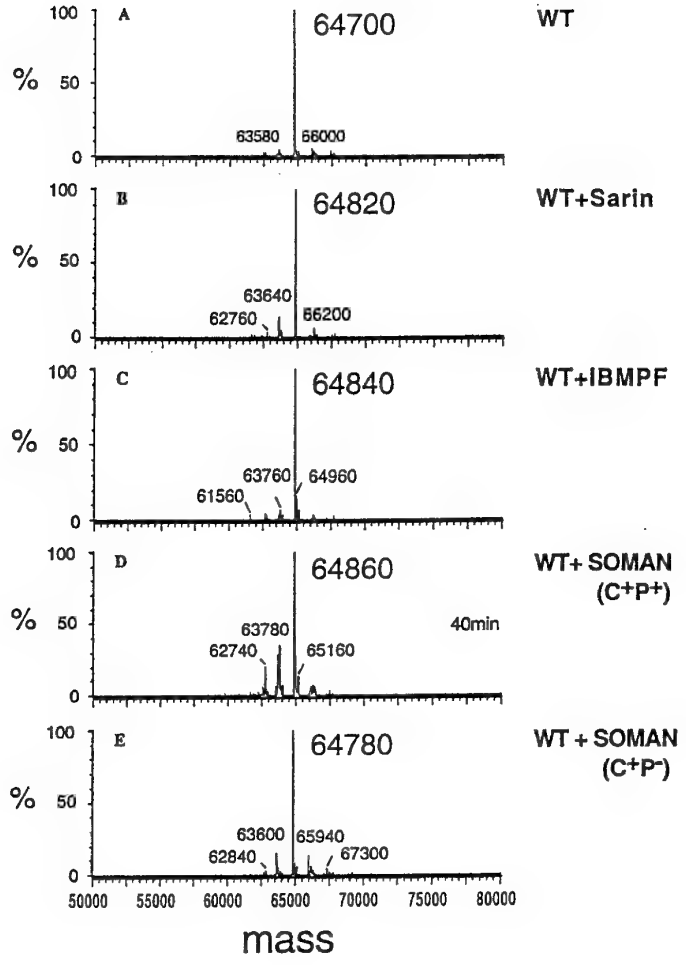

Fig.14 Positive - ion ESI-MS mass spectra of HuAChE-bac and of its alkyl methylphosphono - conjugates, after processing by VG MaxEnt software. Spectra of the adducts were measured within 2-4 min. of mixing the enzyme with excess of the phosphonylating agent, as shown in each of the panels: **A**. Free C580S HuAChE-bac (mass calculated from sequence 64695 Da); **B**. 2-propyl methylphosphono-HuAChE-bac (mass calculated 64821 Da); **C**. 2-butyl methylphosphono-HuAChE-bac (calculated 64835 Da); **D**. Product of phosphonylation with (C+P+)-1,2,2-trimethylpropyl methylphosphono-fluoridate (calculated 64863 Da), spectrum taken after 40 min. since in this case adduct formation is very slow; **E**. Product of phosphonylation with (C+P-)-1,2,2-trimethylpropyl methylphosphono-fluoridate (calculated 64778 Da for the aged adduct, see text and Fig. 16). The minor peaks in the spectra may reflect the inherent "noise" of the method. It should be pointed out that the peak height is a reflection of the precision as well as of the abundance of the corresponding molecular species in the sample.

The mass spectrometric results for some of the phosphonyl-HuAChE-bac adducts are presented in Fig. 14. For the isopropyl methylphosphonyl-HuAChE-bac (derived from reaction with sarin) the molecular mass (Fig. 14B) corresponds exactly to the sum of previously measured mass of the free enzyme and that of the phosphonyl moiety (64700+121). Mass measurement of the reaction product with IBMPF (Fig. 14C), which differs from sarin by one methyl group, gave a molecular mass of 64840 (compared to the calculated mass 64700+135). For the (P+)-1,2,2-trimethylpropyl methylphosphono-HuAChE-bac (Fig. 14D) the observed molecular mass - 64860 Da corresponds to an intact somanyl adduct (calculated 64700+163 Da), which is different by two and three methyl groups from the corresponding adducts of IBMPF and sarin respectively . These results demonstrate again the utility of the ESI-MS in monitoring chemical changes in enzymes like HuAChE and its accuracy in measuring such high molecular masses with deviations of ≤5 Da (corresponding to the precision of 0.01% achievable by this method; see Andersen *et al.,* 1996). Furthermore, in accordance with the kinetic results (see Table 8), intact (non-'aged') phosphonyl-HuAChE adducts were observed for all the cases where the development of non-reactivability was slow. On the other hand, for the phosphonylation product with the (C+P-)-stereoisomer of soman, only an entity with molecular mass of 64780 Da could be observed after 4 minutes (Fig. 14E). This molecular mass corresponds almost exactly to that calculated (64700+78 Da) of a dealkylated methylphosphonyl-HuAChE adduct resulting in the 'aging' process (see scheme 6). Assuming that the *progressive* non-reactivability of the other phosphonyl-adducts originates from analogous dealkylation mechanism, the same dealkylation product (64780 Da) should result in all cases (see scheme 6). This point is clearly demonstrated by the behavior of 1,2-dimethylpropyl methyl-phosphono-HuAChE-bac, where the time frame of the development of non-reactivability (Table 8) makes it possible to actually follow the process (see Fig. 15). Although the mass difference between the intact and aged adducts is too small to permit observation of two discrete masses, the molecular weight measured after 10 minutes - 64852 Da (calculated for the intact adduct 64700+149 Da, see Fig 15A) and that measured after 7.5 hours - 64780 Da (calculated 64700+78 Da, see Fig 15D), as well as the continuous shift of the average mass (Fig. 15B,C) all indicate the progression of the dealkylation process.

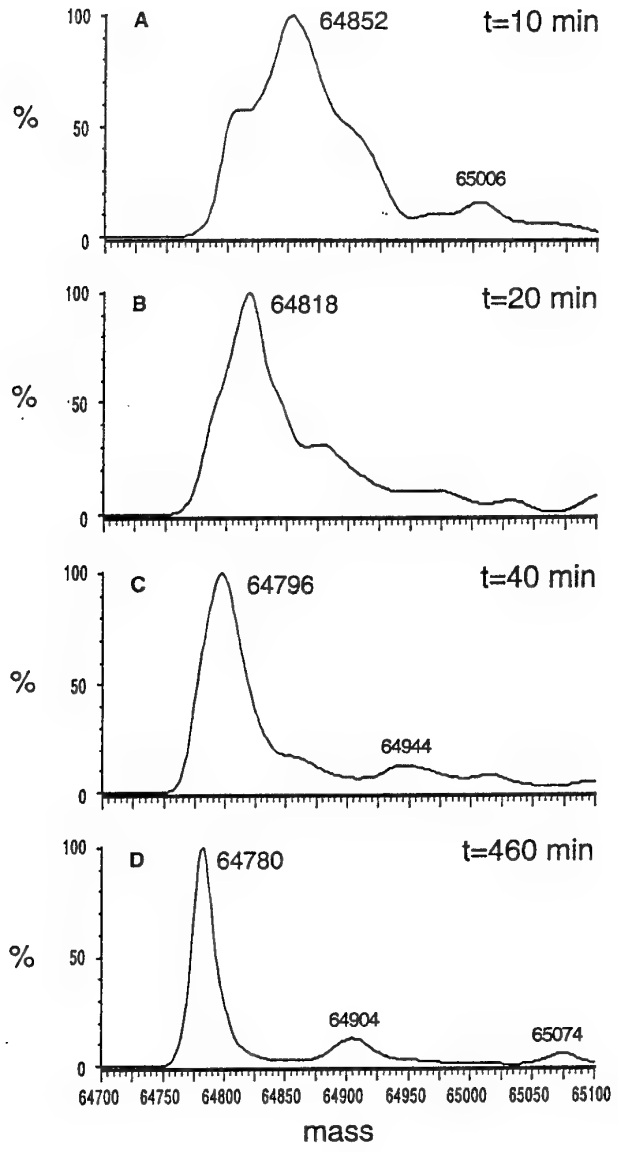

Fig. 15 Positive - ion ESI-MS mass spectra of the reaction mixture DMPF + HuAChE-bac sampled at different times after the reaction onset. Average molecular weight of the mixture components was obtained for each spectrum after processing by the VG MaxEnt software. Although the value after 10 minutes corresponds closely to that calculated for 1,2-dimethylpropyl methylphosphono-HuAChE-bac (64849 Da), the asymmetric shape of the peak indicates an additional component with a lower molecular mass. Both the shapes and the average values of the peaks, obtained after 20 and 40 minutes, suggest a gradual transition from a species with molecular weight of 64852 Da to one with molecular weight of 64780 Da (see also Fig. 16B).

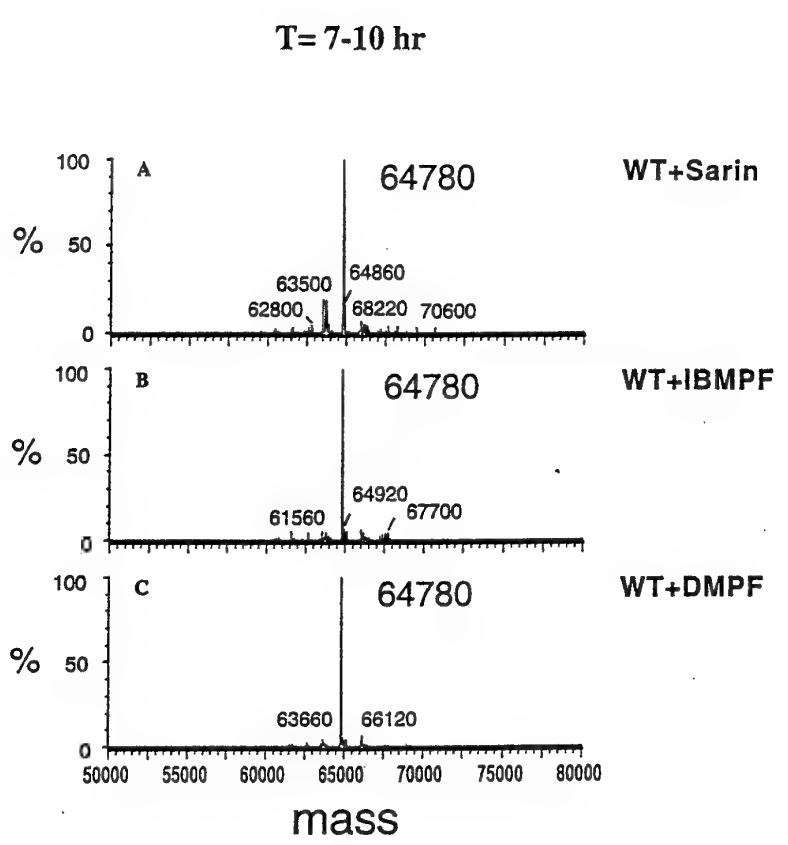

Fig. 16. Positive-ion ESI-MS mass spectra of phosphono-HuAChE-bac conjugates, 7-10 hrs after phosphonylation. For all the cases shown the molecular mass corresponds to a common product resulting from dealkylation the respective phosphonyl moieties (calculated 64778 Da). Note that these spectra are equivalent to that obtained for the phosphonylation product with (C+P) -1,2,2-trimethylpropyl methylphosphonofluoridate (see Fig. 14E)

The notion that aging results in a common product for all the methylphosphonyl-HuAChE conjugates is further supported by measuring the composition of the sarin and IBMPF adducts after 7-10hrs. In both cases the adducts underwent conversion to molecular entities with the same mass (64780 Da, see Fig. 16A,B) as those resulting from (P-)-soman-HuAChE and the DMPF-conjugates (see Fig. 14E and 16C). Since for all the adducts the time scale of this change is comparable to that of the kinetically observed aging process (Table 8), we can conclude that the aging indeed involves loss of alkyl group from the phosphonyl conjugate, as has been shown in the cases of trypsin (Kossiakoff and Spencer, 1980) and chymotrypsin (Harel *et al.,* 1991) Furthermore, no other molecular species could be observed, indicating that in case of phosphonyl

adducts, aging is the only mechanism responsible for non-reactivability. This point is further exemplified by both, the stability of the aged (P-)-soman-HuAChE adduct (Fig. 14E) and by the continuous change observed in the case of DMPF-HuAChE adduct, where the only masses observed correspond to the transition between the nonaged and the aged (dealkylated) forms. On the other hand, the molecular mass of the P(+)-soman-HuAChE adduct remained unchanged after 10 hrs, in agreement with the already reported stability of the (P+)-soman-AChE adducts (Keijer and Wolring, 1969).

Table 8: Rate constants of phosphonylation (k_i) and $t_{1/2}$ for aging of soman, DMPF, IBMPF or sarin - inhibited HuAChE enzymes at pH 8.0, 24 °C.

	Soman		DMPF	IBMPF	Sarin
	C(+)P(-)	C(+)P(+)			
k_i (x10^{-5} min^{-1} M^{-1})	1500	<0.05	2000	1400	230
$t_{1/2}$ (min)	6.3	>40 000	130	255	2300

The ability to observe and sometime even to monitor the chemical transitions of HuAChE covalent adducts by a direct determination of chemical composition may help to examine other cases where the post inhibitory behavior of the adducts is not clear. The fact that the current ESI-MS method is applicable to enzyme preparations that are either nonglycosylated or have a homogenous carbohydrate profile, should not limit its utility for investigating various aspects of HuAChE function. Such aspects include, for example, the reactivation properties of tabun-AChE adducts or the incomplete regeneration of enzymatic activity which is often observed following inhibition of HuAChE enzymes by the presumably reversible active center inhibitor - m-(N,N,N-trimethylammonio)-trifluoroacetophenone (Shafferman *et al.*, unpublished results). The findings also exemplify the great potential of ESI-MS and related mass spectrometric techniques to the study of structure - function and reactivity characteristics of enzymes.

VI. Simulation of Surface Loop Motion in Acetylcholinesterase: Implications on Catalytic Activity and Allosteric Modulation

INTRODUCTION

Acetylcholinesterase (AChE, E.C.3.1.1.7) is a serine hydrolase, whose function in the cholinergic synapse is the termination of impulse transmission by rapid hydrolysis of the neurotransmitter acetylcholine (ACh). In accordance with its biological function, AChE possesses unusually high catalytic activity, with rates approaching diffusion control (Rosenberry, 1975; Quinn, 1987). Allosteric modulation of this activity, through ligand binding to the peripheral anionic site (PAS), is one of the most intriguing aspects of the functional characteristics of AChE since the PAS is located about 20 Å away from the active center (Roufogalis and Quist, 1972; Rosenberry and Bernhard, 1972; Taylor and Lappi, 1975; Shaffermann *et al.*, 1992b,c; Radic *et al.*, 1993; Harel *et al.*, 1993; Barak *et al,* 1994). While evidence exists that PAS ligands (the natural substrate, inhibitors and divalent cations) affect the conformation of the active center (Berman *et al.*, 1981; Taylor and Radic, 1994), the molecular events involved in the allosteric signal transmission and the mechanism of conformational change are not known. Chemical affinity labelling (Weise *et al.*, 1990; Hucho *et al,*. 1991), site directed mutagenesis and kinetic studies together with molecular modeling, resulted in identification of the array of residues which constitute the PAS (Shaffermann *et al.*, 1992b,c; Ordentlich *et al.*, 1993a; Radic *et al.*, 1993; Harel *et al.*, 1993; Barak *et al.*, 1994). However, molecular models of AChE complexes with the PAS inhibitor propidium (Barak *et al.*, 1994) and in particular the recently published crystallographic structures of AChE-fasciculin complexes (Bourne *et al.*, 1995; Harel *et al.*, 1995) , indicate that binding results in physical obstruction of the access to the active center, contrary to the reactivity characteristics of the enzyme (Ordentlich *et al.*, 1993a; Radic *et al,*. 1995; Eastman *et al.*, 1995). This apparent inconsistency

can be resolved by assuming that the structure of the AChE-propidium adduct, in solution, allows substrate access to the active center. In fact, it was recently proposed that the inhibition of AChE catalytic activity by propidium operates via conformational transitions in the active center, involving mainly the anionic subsite Trp86*(84)* (Ordentlich *et al.*, 1995; Barak *et al.*, 1995). The path of signalling the incidence of propidium binding to the PAS, down to the active center, was proposed to include the conformational mobility of the disulfide surface loop (Cys69*(67)*-Cys96*(94)*) of human AChE (HuAChE), which constitutes the thin portion of the active center gorge lining and which contains residue Trp86 as well as residues of the PAS: Tyr72*(70)* and Asp74*(72)* (Barak *et al.*, 1995).

The disulfide loop (Cys69-Cys96) in HuAChE is a structural element conserved throughout the esterase/lipase family of hydrolytic enzymes, of wide phylogeneic origin and catalytic function, sharing the alpha/beta hydrolase fold (Ollis *et al.*, 1992; Cygler *et al.*, 1993; the $L_{b3,2}$ variable length loop). In the case of lipases, molecular simulations and x-ray crystallographic structures of free versus complexed structures show that the $L_{b3,2}$ loop is one of the most mobile structural elements of the enzyme (Norin *et al.*, 1993; Grochulski *et al.*, 1994), alternating between open and closed states. This motion has been implicated in the lipase interfacial activation and in substrate accommodation (van Tilbeurgh *et al.*, 1993). While the x-ray analyses of AChE and its adducts with specific ligands, provide no indication of the mobility of the $L_{b3,2}$ loop (Sussman, *et al.*, 1991; Harel *et al.*, 1993), the fact that the crystallographic dimensions of the active site gorge should preclude access of ACh and bulky active center ligands, suggests that some conformational adjustments may be essential for enzymatic activity (Axelsen *et al.*, 1994; Gilson *et al.*, 1994). Participation of the AChE $L_{b3,2}$ loop in such adjustment, is suggested by virtue of the evolutionary constraint on the conservation of this structural motif in the lipase/esterase family (Ollis *et al.*, 1992; Cygler *et al.*, 1993) and by the growing recognition of the role, played by surface loop mobility, in a variety of enzymatic systems (Kempner, 1993; Gerstein *et al.*, 1994; Fetrow, 1995). Properties related to the inherent flexibility of structural domains in proteins cannot be addressed by x-ray crystallography, therefore we used methods of molecular simulation to test the notion that conformational mobility of residue Trp86 is coupled to the PAS through the dynamic behavior of the $L_{b3,2}$ loop and that the loop motion affects the accessibility of the active center. High temperatures have been used to decrease the time required for conformational change and to allow

for a more comprehensive exploration of the conformational space accessible to the loop (Karplus *et al.*, 1992; Björksen *et al.*, 1994). Our findings indicate that the loop can assume a range of conformations differing from the initial HuAChE model structure (Barak *et al.*, 1992), through unwinding rather than through rigid lid motion, and that this conformational flexibility affects both the dimensions of the active site gorge and the positioning of the Trp86 side chain. Such a picture of dynamic behavior of the $L_{b3,2}$ loop is consistent with its proposed role in allosteric modulation of AChE catalytic activity (Barak *et al.*, 1995).

METHODS

Hardware, Software and Force-fields Used - All calculations (optimizations, molecular dynamics and simulated annealing) were performed on a SUN-Sparc10 workstation, using the AMBER 4.01 suite of programs (Pearlman *et al.* , 1991) with the all-atom parameter set (Weiner *et al.*, 1986). Trajectories were analyzed using the ANAL and CARNAL modules of AMBER , and the molecular modeling package SYBYL 6.03 (Tripos, 1994). Average structures were calculated using the MDANAL option of AMBER. Visualization, characterization and structure manipulations were carried out using SYBYL 6.03 running on an IRIS 4D/70GT workstation.

Simulation Protocol - Simulations were performed using a three-step protocol : Optimization of the solvated starting structure, simulated annealing and molecular dynamics followed by energy minimization. The main features of each step are described below.

Generation and Optimization of the Starting Structure - The starting conformation of the enzyme was the 3D-HuAChE model (Barak *et al.*, 1992) constructed by homology modeling to TcAChE (Sussman *et al.*, 1991). The optimized model was solvated through addition of a total of 619 water molecules comprising of: the TcAChE crystallographic water molecules , following superposition of the structures and assuming identical locations, (using the ADD option of AMBER) and a spherical cap of Monte-Carlo water (using the SOL option of AMBER), extending 25Å from multiple residues located on the $L_{b3,2}$ loop and gorge entrance, chosen to ensure filling of the gorge and appropriate solvation of the loop and the gorge entrance while maintaining the desired room temperature water density. Unfavorably placed waters were removed based on input steric and distance criteria. The water cap was restrained by a soft half harmonic potential to minimize water evaporation without affecting protein motion. In order to relax the water molecules, avoid spurious protein movements and maintain the initial structure close to the 3D model, the following consecutive optimizations were performed: A. optimization of the bulk solvent in a rigid protein environment. B. optimization of the protein. C. optimization of the solvated system (Laughton *et al.*, 1994). The HuAChE residues included in all optimizations and

simulations were selected using the belly option of AMBER and comprised of the $L_{b3,2}$ loop (res Cys69 to Cys96) as well as residues in and around the active site gorge - a total of 96 residues. Atoms defined by this option are included in the simulation whereas the rest of the atoms are frozen and the sole contribution of the frozen part of the molecule, is not calculated.

Simulated Annealing - The starting structure for the simulation protocol was the solvated optimized enzyme described above. The simulation protocol consisted of gradual heating of the enzyme to 1000°K, at a rate of 50°K/3ps (Brünger and Krukowski, 1990), and a molecular dynamics (MD) run at 1000°K (for 100ps). From different starting points at 1000°K, the system was slowly cooled down to 300°K at a rate of 50°K/3ps. Atoms were assigned velocities according to the maxwellian distribution at the appropriate temperature. The temperature was kept constant by separate coupling of the solute and solvent to an external water bath (Berendsen *et al.*, 1984) with a relaxation constant of 0.2ps. A constant dielectric function was used and non-bonded neighbors were truncated every 9 Å and this list was updated every 24fs. Covalent bond lengths were kept constant using the SHAKE algorithm (Ryckaert *et al.*, 1977) allowing for a time step of 2fs. Conformers (energy, velocity, coordinates) were sampled every 50 steps.Two different heating simulations were carried out and a total of seven cooling schedules were performed, from different stages of the 1000°K MD run.

Molecular Dynamics - Structural stability of the annealed conformers was assessed via constraint-free constant temperature molecular dynamics simulation at 300°K for 60 ps, the general conditions were as described in the previous section. The structures obtained from the last 2/3 of the molecular dynamics run were averaged. The averaged structures were optimized. The conformers were visualized and analyzed employing SYBYL modeling package, AMBER and CARNAL (see first section in experimental procedures). The structural and physicochemical properties of the individual conformers (i.e. gyration radius, root mean square distances - RMSD, dihedral-angles, energy, etc.) were compared to the optimized solvated starting structure.

RESULTS

Starting Structure - The HuAChE model (Barak *et al.*, 1992), built by homology modeling from the crystal structure of TcAChE (Sussman *et al.*, 1991), was chosen as the starting structure since the experimental studies pertaining to the role of $L_{b3,2}$ loop mobility in allosteric modulation of AChE, were carried out on HuAChE and its muteins (Shafferman *et al.*, 1992b,c; Barak *et al.*, 1994; Ordentlich *et al.*, 1995; Barak *et al.*, 1995). In view of the documented differences in reactivity between TcAChE and HuAChE, any attempt to correlate HuAChE reactivity with structural properties, should be based on the HuAChE rather than the TcAChE structure. All simulations were carried out on residues comprising the $L_{b3,2}$ cysteine loop, the active site gorge and surrounding secondary structure elements (96 residues), using the AMBER belly option (Pearlman *et al.*, 1991). Residues defined in the belly option are listed (Table 9) and are referred to according to their allocation to secondary structure elements (Cygler *et al.*, 1993).

In order to simulate realistic conditions in solution and to avoid spurious movements of the loop, the 3D model of HuAChE was solvated with water molecules filling the active site gorge cavity and capping the loop and gorge entrance. Optimization of the solvated HuAChE model demonstrated that the initial structure remains essentially unchanged, as judged by the small root mean square distances (not shown) and the minor changes in the radius of gyration, compared to the non-optimized model. Examination of the secondary structure elements (in comparison to both the 3D HuAChE model and the x-ray structure of TcAChE) also revealed that the initial structure was not significantly perturbed by the solvation procedure.

Preliminary constant temperature molecular dynamics (MD) simulations (300°K/60ps) of the solvated HuAChE, resulted in structures which were essentially equivalent to the starting structure (for details see Methods). During the time-frame of the MD simulation, only minor movements were observed, mostly within in the $L_{b3,2}$ loop region while for the protein core residues, included in the simulation, only minor adjustments of individual side-chains were observed. Similar observations were previously reported for TcAChE, by Axelsen *et al.*, (1994).

Table 9 : Listing of the residues included in the simulation according to allocation to the secondary structural elements in HuAChE

Residues	Type	Name	Belly residues
8-12	β–strand	b_1	
15-18	β–strand	b_2	
20-23	β–strand	β_0	
28–36	β–strand	β_1	
59–62	β–strand	b_3	
81-87	α-helix	$\alpha_{b3,2}$	69-96
98-104	β–strand	β_2	
112–119	β–strand	β_3	
			117-136
135–142	α-helix	$\alpha_{3,4}$	
145-150	β–strand	β_4	
-	α-helix	$\alpha^1_{4,5}$	
			151-158
171-186	α-helix	$\alpha^2_{4,5}$	
196-202	β–strand	β_5	
			200-214
203-214	α-helix	$\alpha_{5,6}$	
223-229	β–strand	β_6	
			223-229;
			233-237
241–255	α-helix	$\alpha^1_{6,7}$	
266-275	α-helix	$\alpha^2_{6,7}$	
			283-287

278-285	α-helix	$\alpha^3_{6,7}$	290-300
312-318	α-helix	$\alpha^4_{6,7}$	
325-331	β–strand	β_7	
336–342	α-helix	$\alpha^1_{7,8}$	331-346
356–367	α-helix	$\alpha^2_{7,8}$	
372–383	α-helix	$\alpha^3_{7,8}$	
391–418	α-helix	$\alpha^4_{7,8}$	
424–430	β–strand	β_8	445-451
450–455	α-helix	$\alpha^1_{8,9}$	
467–486	α-helix	$\alpha^2_{8,9}$	
519–513	β–strand	β_9	
518–522	β–strand	β_{10}	
526–542	α-helix	α_{10}	

Conformational Search by Simulated Annealing - Since the simulation at 300°K has indicated that the loop structure is entrapped in a narrow segment of its conformational space, simulated annealing at 1000°K has been carried out. Such procedure provides the means to overcome the energy barriers separating multiple minima within reasonable simulation time-scales and has been previously applied to the definition of alternative conformations of other protein loops, of similar size (Björkstén *et al.*, 1994).

The HuAChE $L_{b3,2}$ surface loop can be classified as a Ω loop (Leszczynski and Rose, 1986) since it constitutes of a relatively long stretch of residues (28 residues) folded on itself, exhibiting limited ordered secondary structure (a single helical turn containing residue Trp86). The pronounced flexibility of such Ω loops indicates that even at 1000°K only a subset of the conformational space available to the $L_{b3,2}$ loop can be sampled within a realistic simulation time-frame. However, since the aim of this study has been to explore the consequences of the loop motions on the accessibility of the HuAChE active center and on the positioning of residue Trp86, the definition of the whole conformational space of this Ω loop, may not be necessary. Moreover, it can be expected that the range of conformations available to the $L_{b3,2}$ loop is limited by interactions with the protein core.

The solvated optimized HuAChE structure was slowly heated to 1000°K (at 50°K/3ps) and maintained at 1000°K for 60ps (for details see Methods). A wide range of different conformations was observed demonstrating the extent of the conformational space available to the $L_{b3,2}$ loop at 1000°K. During the high temperature run, the observed conformers vary in the degree of loop unwinding and in the resulting change in accessibility of the active-site gorge. In no case gross deformation of the loop structure could be observed as was also evident from the energy profile of the 1000°K MD run (not shown). Representative conformers, from two separate SA experiments, were selected and cooled to 300°K (at 50°K/3ps).

Examination of the dynamic trajectories during the entire simulation protocol revealed the following general characteristics: (a) The structures maintained the initial conformation of the solvated HuAChE model, up to 600°K. (b) During the remaining heating steps (600°-1000°K) and the constant temperature simulation at 1000°K, gradual unwinding of the loop took place. (c) During the cooling, the structures became essentially "locked" in their final conformations, around

400°K. In each case this final conformation was close to the initial structure selected from the high temperature run.

The stability of the cooled structures was assessed by subjecting them to a 300°K MD run for 60ps. Temporal analysis of the individual trajectories for changes in total energy, temperature, atomic positional displacements, backbone dihedral angles and changes in the radius of gyration, revealed only minor oscillations relative to the initial cooled structure (not shown). This allowed for averaging of structures derived from each cooling experiment, facilitating analysis and comparison of the different cooled conformers.

Conformer Analysis - The eight arbitrarily selected conformers, representing the extent of conformational change during the high temperature run (SA conformers), were further analyzed as candidate structures for the alternative $L_{b3,2}$ loop conformations. One should note that the integrity of the secondary structure elements containing the residues included in the simulation was fully preserved. Comparison of the root mean square distances (RMSD, carried out on the 96 residues included in the belly definition) of the SA conformers versus the starting structure reveals similar values for all cases (~3 Å). Of the individual structural elements, the $L_{b3,2}$ loop exhibited the largest deviation from the initial structure (RMSD>5 Å, Table 10, Fig. 17) . Minor movements were also observed for the loops surrounding the active-center , i.e. $L_{3,4}$ and $L^4_{6,7}$ (for loop assignments see Table 9). Most of the SA conformers could be grouped into two categories (A and B), according to the distance/extension of the loop from the rest of the protein. Of the eight selected conformers five can be classified in group A, two belong to group B while in the remaining SA conformer (sampled at 10ps of the high temperature MD) the main structural changes were localized in the loop helical turn $\alpha_{b3,2}$ containing residue Trp86 (Fig. 18b). In group A conformers (Fig. 18c) the loop is partially extended, with limited unwinding of its tip (residues Tyr77-Thr83). This results in an opening of a cavity extending from the surface (between residues Phe80 and Tyr341) to the active center residue Trp86. The helical turn $\alpha_{b3,2}$ is maintained, however its sequence is shorter (between Glu81 and Met85) and no longer includes residue Trp86. The side chain of Trp86, which during the heating and the early phase of the high temperature

MD assumed an extended conformation occluding the gorge, moved up and out of the active center. In group B (Fig.18d), a more extensive unwinding of the loop was observed, resulting in a more open structure. The Glu81-Asn87 helical turn disappeared and the side chain of residue Trp86 flipped outward towards the solution.

In a more detailed comparison, only the loop residues of the SA conformers were aligned with the starting structure. RMSD values were calculated for each residue (Fig. 17) ,revealing that the most mobile segment of the loop extends between residues Val73 and Arg90, involving both backbone and side chains movements. The relative displacements of the individual loop residues varied for each SA conformer but the general pattern was maintained (Fig. 19) . By comparison, dynamic fluctuations of the active site gorge residues were more restricted and limited to key residues constituting parts of loop connecting secondary structure elements and residues located on the C-terminus of helix $\alpha 1_{7,8}$ (see Table 10).

The mobile segment of the $Lb_{3,2}$ loop does not include its N and C termini (Cys69- Tyr72 and Glu91- Cys96 respectively). The C-terminus residues Ser93 to Cys96 are strictly conserved in the lipase/esterase family, probably playing a structural role in maintaining the positions of the loop ends. In particular, residue Glu94 and the conserved residue Arg46 form a salt bridge which was shown as critical for maintenance of the 3D fold of the enzyme (Bucht *et al.*, 1994). This salt bridge, which is located next to the disulfide bond of the $L_{b3,2}$ loop, was indeed maintained throughout the simulations.

In order to assess whether the $L_{b3,2}$ loop movement results from classical loop movement mechanisms, i.e. hinge bending, rigid body movement or flexible chain movement (Kempner, 1993), local structural perturbations, as reflected by changes in the backbone dihedral angles phi and psi of residues included in the simulation, were examined (Fig. 20). Visual inspection of the dynamic trajectories together with the RMSD values and changes in backbone and sidechain dihedrals reveals that throughout the simulations, the conformational changes do not result from movements of single residues but rather of a stretch of residues (Table 10). *Thus, the conformational behavior of $L_{b3,2}$ loop can be best categorized as a flexible chain movement and unlike the case for lipases does not involve a cis-trans isomerization of proline residue.* Throughout the simulations, both $L_{b3,2}$ loop proline residues (Pro78 and Pro88) retained the *trans*

conformation observed in the starting structure. Significant backbone movements ($\Delta>40^0$) were also observed for $L^1{}_{3,4}$ (containing the PAS residue Tyr124) ; in $L^4{}_{6,7}$ (connecting helices $\alpha^3{}_{6,7}$ and $\alpha^4{}_{6,7}$, in the vicinity of the acyl pocket) and in the C-terminal region of helix $\alpha^1{}_{7,8}$ (containing the hydrophobic pocket residues Tyr337, Phe338 and the PAS residue Tyr341; see Table 10).

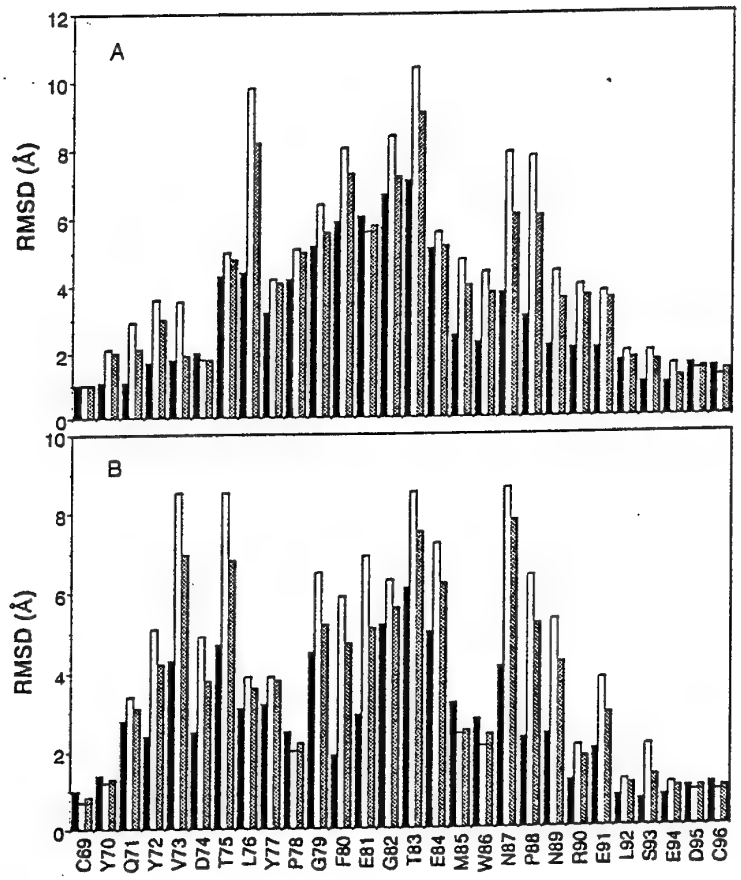

Fig.17 Plots of RMSD values for the $L_{b3,2}$ loop residues of representative SA conformers as compared to the starting model of HuAChE. The values are shown as a function of residue number. Backbone atoms (black bars) , side chain atoms (white bars) and whole residues (shaded bars). A. Representative values for group A (SA conformer sampled at 38ps) B. Representative values for group B (SA conformer sampled at 72ps).

Table 10: RMSD values and differences in torsion angles between representative SA conformers and the starting HuAChE model excluding $Lb_{3,2}$

Belly Residues	Secondary Structure	RMS Group A	RMS Group B	$\Delta\phi/\Delta\psi$ Group A	$\Delta\phi/\Delta\psi$ Group B
117-136	β_3	Y119	Y119	Y119(-3/-90)	Y119(-13/-90)
	$L^1_{3,4}$			G121(-80/3)	G121(-40/19)
			F123	F123(5/-80)	F123(6/-75)
		Y124	Y124		
				S125(15/-120)	S125(10/-108)
				G126(105/10)	G126(107/-20)
		A127		A127(-80/-60)	
			S128		
			S129		
				L130(-40/-50)	
				D131(130/-15)	D131(-25/80)
		Y133		Y133(-15/70)	Y133(19/80)
					D134(-60/40)
290-300	$L^4_{6,7}$	E292			
			V294		
		R296		R296(25/180)	R296(20/-170)
			F297	F297(-155/20)	F297(-160/20)
331-346	$\alpha 1_{7,8}$	Y337	Y337	Y337(-13/-150)	
		F338	F338	F338(136/-25)	
		Y341	F341	Y341(-25/60)	Y341(-33/60)
		G342			
	$L^2_{7,8}$	G345			

[a] Values for all residues exhibiting large deviations: RMSD>3 A and differences in torsion angles > |40°|, are listed. The corresponding values for the loop residues are presented in Fig. 17 and Fig. 20.

[b] Groups A and B are represented by SA conformers sampled at 38ps and 72 ps, respectively.

A.

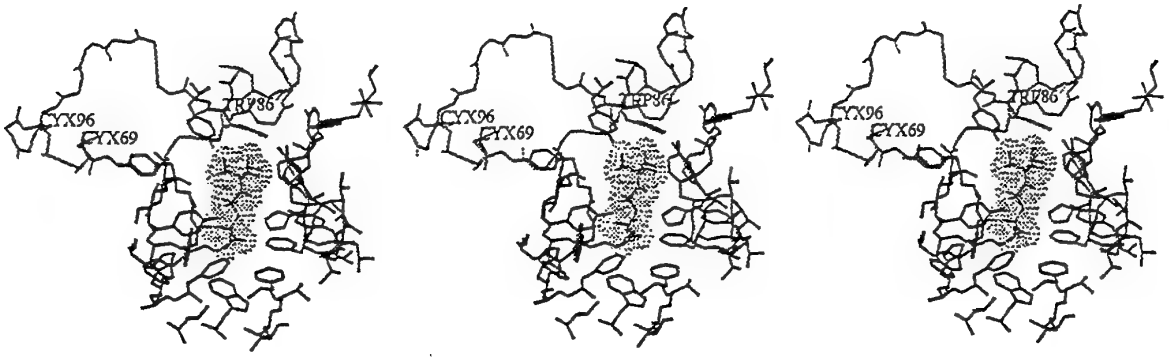
CYX96
CYX69
TRP86
CYX96
CYX69
TRP86
CYX96
CYX69
TRP86

B.

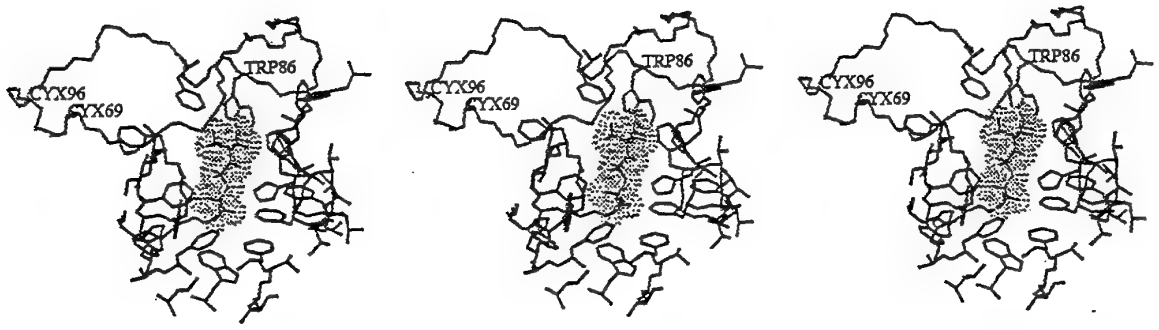
TRP86
CYX96
CYX69
TRP86
CYX96
CYX69
TRP86
CYX96
CYX69

C.

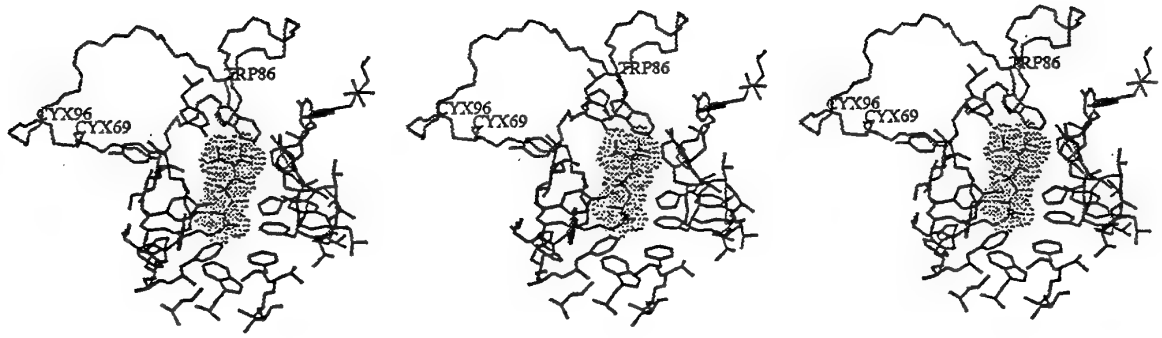
TRP86
CYX96
CYX69
TRP86
CYX96
CYX69
TRP86
CYX96
CYX69

D.

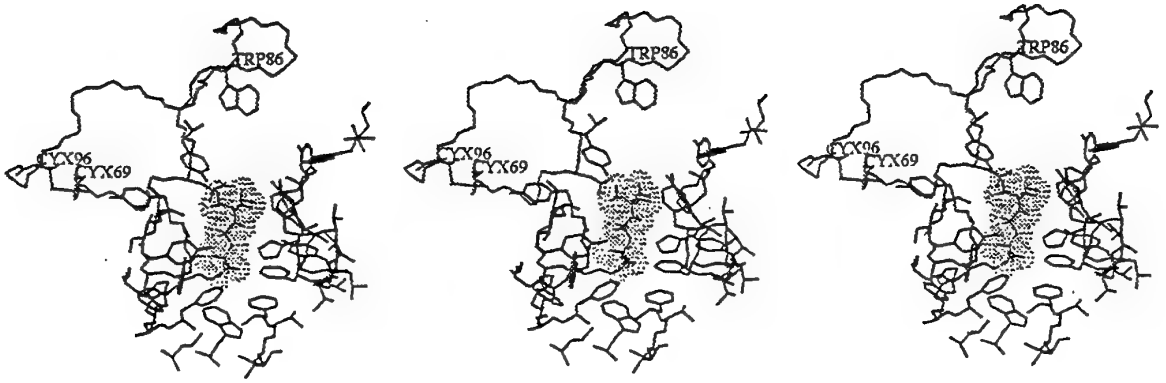
TRP86
CYX96
CYX69
TRP86
CYX96
CYX69
TRP86
CYX96
CYX69

Fig.18 Progressive conformational changes of the $L_{b3,2}$ loop in HuAChE during the high temperature MD. The loop backbone and side-chain of Trp86, as well as selected residues lining the active center gorge entrance are shown. The molecule acetylcholine (shown as dot surface) was not part of the simulations and is presented to demonstrate the location of the active center.A. represents the HuAChE model . B. SA conformer sampled at the beginning of the 1000°K run (10ps). C. SA conformer representative of group A (sampled at 42ps). D.SA conformer representative of group B (sampled at 72ps).

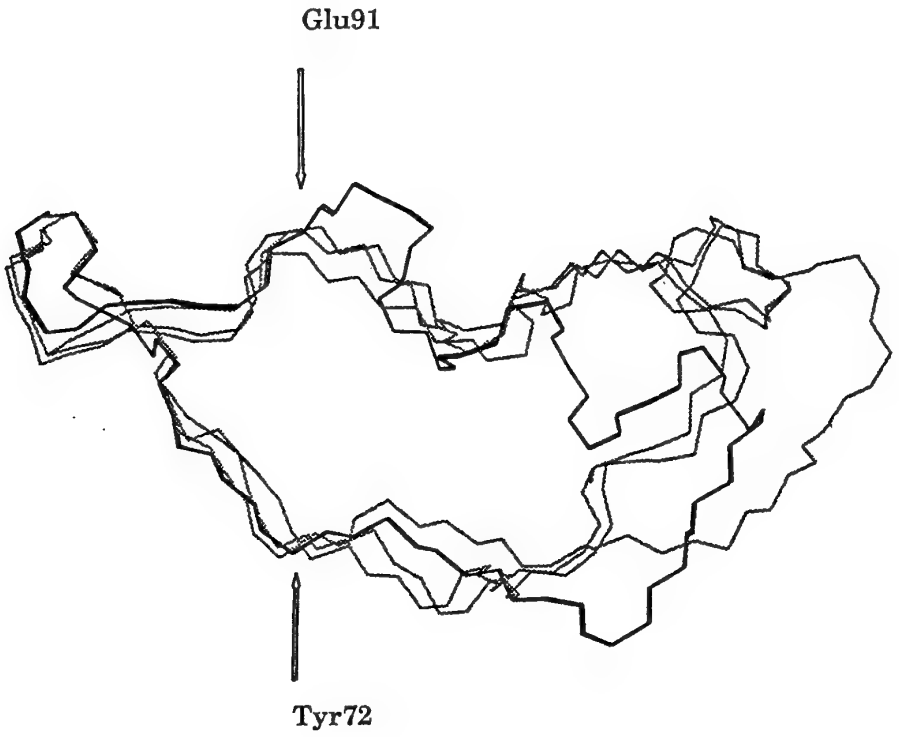

Fig. 19 α-Carbon traces of three $L_{b3,2}$ loop structures obtained from high temperature MD simulations. Structures sampled at 24ps, 38ps, and 64ps of the 1000°K run were overlaid on top of the HuAChE model (heavy line), to illustrate the regions of low and high mobility of the $L_{b3,2}$ loop. C α atoms of residues defining the mobile stretches are marked by arrows. Note that the N and C-termini of the loop (residues Cys69-Tyr72 and Glu91-Cys96, respectively), are relatively immobile.

The differences between the average energies of the eight structures are less than 5% of the total energies. Such differences are too small to allow any definite conclusions with regard to the relative stability of the SA conformers and therefore to the relative distribution. Thus, although in our simulations conformers of group A were more frequently observed than those of group B, the two groups are equally representative of the conformational subsets available to the loop and it is therefore impossible to propose any one of the examined structures as the preferred open structure of HuAChE.

Despite the similarity of the calculated conformational energies for the starting structure and the SA conformers, inspection of the specific interactions between the $L_{b3,2}$ loop residues and the protein showed considerable differences in the aromatic-aromatic and H-bonds patterns (Table 11). The HuAChE $L_{b3,2}$ loop contains four aromatic residues: Tyr72, Tyr77, Phe80 and Trp86, with the last two highly conserved within the AChE enzymes. Residue Tyr72, which was originally within aromatic-aromatic interaction distance with residues Tyr124 and Trp286, was displaced in most SA conformers to form an H-bond with residue Asp74, replacing the H-bond of the latter with residue Tyr341. Residue Tyr77 switches from aromatic-aromatic interactions with Phe80, to interactions with Tyr341 in conformers of group A and with Trp286 or Phe 338 in conformers of group B. In all The SA conformers, residue Phe80, moves outward toward the solution and no longer interacts with Trp439 and Tyr77. The anionic subsite residue Trp86, loses its H-bond to Tyr449, its stabilizing aromatic-aromatic interactions with Tyr133 weakens (in group A) or disappears (in group B) and in the latter case is replaced by interactions with residue Tyr337 (see Table 11). In the starting structure, surprisingly few H-bonds between side-chains of the $L_{b3,2}$ loop residues could be observed. The SA structures belonging to group A, contained a more extensive H-bond networks, with most of the changes occurring due to interactions of side-chains of polar residues in the loop segment Asn 87-Glu91 (see Table 11), and due to different interaction patterns with the solvent. These altered H-bond patterns, which participate in stabilization of the alternative $L_{b3,2}$ loop structures in the SA conformers, are consistent with the notion that these loop structures predominate in the solution conformations of the ligand free HuAChE.

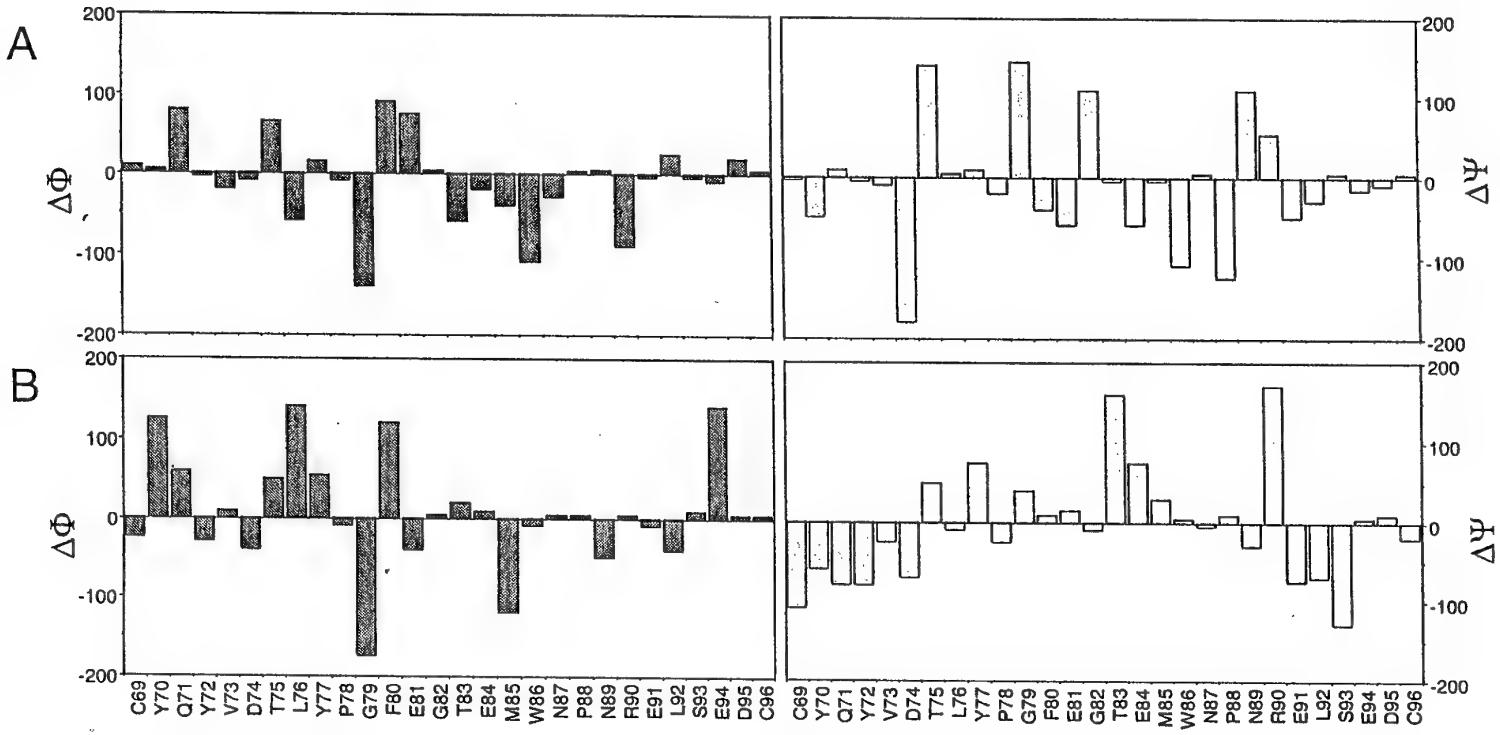

Fig. 20 Plots of differences in torsion angles Φ and Ψ of $L_{b3,2}$ loop residues between representative SA conformers and starting model of HuAChE. Values are shown as a function of residue number. **A.** Values representative of group A (SA conformer sampled at 38ps). **B.** Values representative of group B (SA conformer sampled at 72ps). Note the differences in pattern of torsion angles between conformers belonging to group A versus group B.

Table 11: Listing of hydrogen bonds of the $L_{b3,2}$ loop residues of representative SA conformers and the starting HuAChE model

	H- bonds			aromatic-aromatic interactions		
Residue	Group A	GroupB	Initial	Group A	Group B	Initial
Cys69	O, Q71 N		O, Q71 $N\varepsilon_2$			
Tyr70					Y72, F156	F156
Gln71	$N\varepsilon_2$, Y72 O	O, V73 N	N, S93 O			
Tyr72				Y124	F123	Y124,W286
Val73						
Asp74	$O\delta_1$, Y72$O\eta_1$	$O\delta_1$, T75 $O\gamma$	$O\delta_2$, L76 N			
			O, N87 $N\delta_2$			
			N, N87 $O\delta_1$			
Thr75	$O\gamma$, L76, N	$O\gamma$, L76, N				
Leu76						
Tyr77			O, T83 $O\gamma$	Y341	Y341,W286,F338	
Pro78						
Gly79	O, N E81		N, E84 $O\varepsilon_2$			
Phe80	O, N T83		O, T83 N			Y77,W439
			O, E84 N			
Glu81			O, M85 N			
Gly82						
Thr83			O, N87 N			
			O, W86 N			
Glu84	$O\varepsilon_1$,$O\varepsilon_2$ K348 $N\varepsilon$					
Met85						
Trp86				Y337		Y133,W439
Asn87	O, R90 $N\eta_1$	$N\delta_2$,N89 $N\delta_2$				
	$O\delta_2$, N89 N	$N\delta_2$, R90 $N\eta_1$				
Pro88	O, R90 $N\eta_1$					
Asn89						
Arg90	O, L92 N	$N\eta_1$, N89 $O\delta_1$,				
Glu91	$O\varepsilon_1$, E91 N					
	O, S93 $O\gamma$					
Leu92	N, R90 O					
Ser93	O, Y72 N		$O\gamma$, D95, N			
Glu94						
Asp95						
Cys96						

DISCUSSION

Mobility of the $L_{b3,2}$ loop in HuAChE (Cys69-Cys96) was recently implicated in the mechanism of catalytic activity (Barak *et al.*, 1995), based on the apparent inconsistencies between the crystallographic structure of AChE and its functional characteristics (Axelsen *et al.*, 1994; Gilson *et al.*, 1994) and on the experimental findings related to the mechanism of allosteric modulation of the enzyme activity (Ordentlich *et al.*, 1995; Barak *et al.*, 1995). The x-ray structure of AChE revealed that the active site gorge is too narrow to admit ACh, yet bulky quaternary amines can access the active center of the crystallized enzyme (Harel *et al.*, 1993; Axelsen *et al.*, 1994). In addition, the inward electrostatic field at the gorge would seem to impede the exit of the product choline (Ripoll *et al.*, 1993; Gilson *et al.*, 1994). Thus, substrate accommodation and product release must involve some measure of flexibility in the protein, including either temporal modification of the gorge dimensions or opening of an alternative route of approach to the active site. Such an alternative access route - 'back door' was indeed proposed, based on the positional shifts of residues Trp84, Val129 and Gly441 (corresponding to Trp86, Val132 and Gly448 in HuAChE) observed in the molecular dynamics simulation of TcAChE (Gilson *et al.*, 1994). However, such a mechanism is not supported by the results of mutagenesis studies designed to seal this back door in HuAChE (Kronman *et al.*, 1994). Alternatively, opening of the active site gorge may be effected through conformational change of the $L_{b3,2}$ loop (Cys69-Cys96) comprising the thin wall of the gorge and lining part of its entrance. Such function of the $L_{b3,2}$ loop is consistent with the role of surface Ω loops in many other enzymatic systems, where they participate in either spontaneous or ligand gated conformational equilibration (Fetrow, 1995).

Mobility of the $L_{b3,2}$ loop was not indicated by either the x-ray structures of AChE and its complexes with active center ligands or by molecular dynamics simulations at 300°K. In the simulation of HuAChE the relative displacements of the loop residues were comparable to those of the protein core. Similar results were obtained in the two simulations of TcAChE (Axelsen *et al.*, 1994; Gilson *et al.*, 1994), however in both cases some outstanding movement of residue Trp84 (corresponding to Trp86 in HuAChE) was noticed. Thus, although it appears that conformational transitions of the $L_{b3,2}$ loop are not evident within the time - scale of these simulations, the

structure of the helical turn containing residue Trp86 is particularly sensitive to the overall loop conformation. Similar results were obtained in the simulations of loop opening of triosephosphate isomerase, where at 298°K the loop oscillated about the closed position (Joseph *et al.*, 1990). For this enzyme, x-ray and NMR data as well as simulated Brownian dynamics indicate that the loop fluctuates between open and closed states and that this motion is not ligand gated (Lolis and Petsko, 1990; Wade *et al.*, 1993; Williams and McDermot, 1995).

The simulated annealing experiments of HuAChE at 1000°K indicate that a large segment of the $L_{b3,2}$ loop is indeed the most mobile part of the molecule. Of the 96 residues included in the simulation, movement is confined mainly to the sequence Val73-Arg90 with the loop termini and the protein core residues remaining relatively immobile. The motion of the loop is not a rigid body 'lid' movement, with residues Tyr72 and Glu91 (Fig. 19) acting as hinges, but rather an unwinding of a flexible chain. *Cis-trans* isomerization of the loop proline residues, which was implicated in the loop motion of the homologous lipases (Grochulski *et al.*, 1994), has not been observed in HuAChE. The unwinding can be observed to proceed gradually along the MD trajectory at 1000°K, with the loop moving away from the protein core. This gradual motion is exemplified by comparison of the representative conformers, sampled at different points along the trajectory and cooled to 300°K (Fig. 18). Small perturbations of the initial loop conformation have a dramatic effect on the positioning of the Trp86 side chain. In the SA conformer, originating from structure sampled at the beginning of the MD trajectory at 1000°K (10ps), the Trp86 side chain adopted an extended conformation 'dropping' into the active center cavity while the rest of the loop displayed little overall motion (see Fig. 18b). Inspection of SA conformers, in which the conformational changes of the $L_{b3,2}$ loop were more pronounced, revealed that specific interactions which maintain the proximity of the loop tip to the protein core (e.g. Tyr77-Tyr341 and Phe80-Trp439) were lost. The separation of the $L_{b3,2}$ loop from the protein core created a cavity starting from the gap between residues Tyr77 and Tyr341 and extending down to the active center. The upward motion of the loop also removed the indole moiety of Trp86 from the active center cavity. *Thus, both the gorge entrance and the active center became much more accessible in the open loop conformers* (Fig. 18c,d).

Since the calculated energy values for the different SA conformers are quite similar, it appears that all of them are accessible to the loop. Their relative stability and abundance cannot be determined

based on these simulations. Interestingly, once the loop unwinding begins (around 600°K), there is no refolding to the initial conformation of the HuAChE model. This may indicate that the extended loop conformers are more stable in solution or that the refolding path requires a much longer simulation time. Both possibilities seem to be consistent with the notion that the open loop structures are the prevalent forms of the ligand free HuAChE in solution.

The simulated annealing experiments described here provide further insight into the structure-function characteristics of HuAChE. In general, they support the notion that the unoccupied active center is more accessible to ligands than could have been estimated from the x-ray structure of TcAChE. Since the $L_{b3,2}$ loop constitutes the thin aspect of the gorge wall, the extensive loop motion results in a deformation of the gorge structure. The overall shape of the gorge changes with formation of large cavities above the gorge entrance and in the region of the $\alpha_{b3,2}$ helical turn, followed by opening of the whole gorge length (Fig. 18d). Consequently, in most of the SA conformers, and in particular in those of group B, the active center is located at the end of a narrow groove rather than at the bottom of a gorge. The possible presence of such conformational states of HuAChE in solution provides a new perspective to the issues of the active center accessibility and product release. The active center appears to be widely open to the incoming ligand, without contributions of the steric interference or the electrostatic effects implied by the x-ray derived gorge structure. Such model of ligand ingress is consistent with the experimental results from site directed mutagenesis, indicating that modifications of either the steric crowding within the gorge (Barak *et al.*, 1994) or the electrostatic properties of the enzyme (Shafferman *et al.*, 1994) are inconsequential to the catalytic activity or to the interaction with active center ligands.

Although the SA experiments did not reveal closed loop conformations of HuAChE, the x-ray structures of TcAChE complexed with quaternary ammonium ligands as well as other experimental data indicate that loop closure is essential to ligand accommodation in the active center. The crystallographic structures of the TcAChE complexes, obtained by soaking the ligands into the enzyme crystals, suggest that the loop closes after the ligand entrance. It appears that during the Michaelis complex formation the quaternary ammonium moiety of the ligand interacts with the loop mainly through residue Trp86 (Ordentlich *et al.*, 1993a,b; Barak *et al.*, 1994) and the absence of this interaction severely affects the catalytic efficiency of HuAChE toward ACh and its affinity toward charged ligands. Thus, it appears that the loop refolding and closure may be ligand

induced. The driving force for such loop closure is not clear but it does not appear to involve the ligand charge since it may take place for neutral substrates (Ordentlich *et al.*, 1995). Irrespective of the closure mechanism, we may conclude the functional significance of the loop refolding is to correctly position the indole moiety of residue Trp86 and thereby achieving the catalytically optimal architecture of the active center.

Unlike the Michaelis complex formation, the facility of the acylation/deacylation catalytic steps is not dependent upon the presence of residue Trp86 (Ordentlich *et al.*, 1993a). Therefore one can assume that the loop opens again and choline release may not be constrained by the gorge dimensions and its electrostatic field. Although the SA experiments suggest that the closed and open states are only slightly different in energy, the manner in which substrates and other active center ligands like edrophonium, contribute to the loop closure has not been addressed. Simulations of the ligand bound HuAChE can be expected to provide part of the answer, however the loop conformational transitions may be driven by interactions occurring prior to the ligation at the active center.

Another aspect of the HuAChE structure-function characteristics, that is consistent with the involvement of the $L_{b3,2}$ loop mobility in the catalytic function of HuAChE, is the mechanism of allosteric modulation of the catalytic activity through ligand interaction with the periphery. As already mentioned, upon interaction with substrate the enzyme structure may undergo an induced fit including mainly the closure of the loop. The loop closed structure, observed in the x-ray crystallography of AChE (Sussman *et al.*, 1991), shows that the side chain of residue Trp86 assumes a very unusual conformation (χ_1=-56°; χ_2=108°; for compilation of characteristic side chain conformations of tryptophan as a function of backbone geometry (see Dunbrack Jr and Karplus, 1993). Factors contributing to this unique conformation are probably the specific interactions with residue Tyr133 (Ordentlich *et al.*, 1995) and maybe also with residue Met85 (Harel *et al.*, 1995). Such a conformation of residue Trp86, has been suggested as essential for the catalytic activity towards ACh since: (a) it provides an interaction locus for the quaternary ammonium moiety of the substrate; (b) an extended conformation of Trp86 obstructs the active center preventing the proper orientation of the substrate relative to the elements of the HuAChE catalytic machinery (Ordentlich *et al.*, 1995; Barak *et al.*, 1995). On the other hand, the SA experiments indicated that almost any variation in the loop conformation, resulted in a loss of the

active conformation of Trp86 (Fig. 18), probably due to positional shifts of the $\alpha_{b3,2}$ helical turn backbone. This finding suggests that *any* modification of the $L_{b3,2}$ loop conformational space is bound to affect the conformation of Trp86 in the closed state of the loop. Such modifications may be provided by the binding of PAS ligands like propidum, which interacts with both the loop (Tyr72, Asp74) and the protein core (Trp286, Tyr124) residues (Barak *et al.*, 1994). The relative location of these four residues, comprising the major part of the PAS array (Barak *et al.*, 1994), remains almost unchanged throughout the simulation suggesting that the binding of propidium may not be significantly affected by the loop conformational mobility. Thus, the $L_{b3,2}$ loop of this complex may still be capable of undergoing the substrate induced closure, however the closed loop conformation is probably somewhat different from that of the ligand free enzyme. As a result, the side chain of residue Trp86 would not fold into its active conformation but rather remain in the extended conformation producing a steric conflict with the substrate. Such mechanism of inhibition by the PAS ligands is fully compatible with the previously proposed model of allosteric effect due to binding of propidium (Barak *et al.*, 1995), and is consistent with other experimental findings related to inhibition of AChEs by propidium like the equivalent affinity towards free and phosphonylated enzyme (Berman *et al.*, 1987); diminished affinity of the AChE-propidium complex toward edrophonium (Taylor and Lappi, 1975); the increase of inhibition constant but not of the binding constant for W86A HuAChE (Ordentlich *et al.*, 1993a; Barak *et al.*, 1995); the effect of replacement of Tyr133 by alanine on inhibition (Ordentlich *et al.*, 1995).

VII. The Ω Loop in Human Acetylcholinesterase - What is the Role of the Conserved Residues in Catalysis and Allosteric Modulation.

INTRODUCTION

Acetylcholinesterase (EC 3.1.1.7) is among the most efficient enzymes, with a turnover number of over 10^4 sec^{-1} (Quinn, 1987) . Its remarkable catalytic power is presumably determined by the unique architecture of the AChE active center, which has been recently elucidated by 3D structure analysis of *Torpedo* AChE (Sussman *et al.*, 1991), site directed mutagenesis and molecular modeling together with kinetic studies of the AChE muteins with substrates and reversible inhibitors (Gibney *et al.*, 1990; Velan *et al.*, 1991a; Velan *et a*l., 1991b; Shafferman *et a*l., 1992a,b,c; Vellom *et al.*, 1993; Ordentlich *et al.*, 1993a,b; Ordentlich *et al.*, 1995; Radic *et a*l., 1992; Radic *et al*., 1993; Barak *et al.*, 1994; Kronman *et al.*, 1994; Gnatt *et a*l., 1994; Taylor and Radic, 1994) . However, the location of the active center at the bottom of a deep and narrow 'gorge' and the crystallographic dimensions of this gorge pose an intriguing question regarding the substrate and ligand access to the catalytic site (Axelsen *et al.*, 1994). In addition, the structure reveals an uneven overall distribution of negative charge giving rise to a large electrostatic dipole, aligned along the active site gorge (Rippoll *et al*., 1993). Such a dipole would draw the positively charged substrate down the gorge, however it could also interfere with the release of the reaction product - choline. In order to reconcile the apparent steric and electrostatic impediments in the trafficking of substrate and products with the high turnover number of the enzyme, conformational adjustments of the gorge dimensions during ligand approach (Axelsen *et al*., 1994) or a possible back door path for product release have been suggested (Gilson *et al*., 1994). Subsequently it was shown, by septuple replacement of negatively charged amino acids, that electrostatic attraction does not contribute to the catalytic rate of the enzyme (Shafferman *et al.*, 1994). In addition, mutagenesis of key residues located along the putative back door channel does not support its proposed role in AChE activity (Kronman *et al.*, 1994; Faerman *et al.*, 1996).

Another intriguing feature of AChE reactivity is the allosteric modulation of its catalytic activity (Changeux *et al.*, 1966), following ligand binding to a peripheral site (PAS) at the enzyme surface (Hucho *et al.*, 1991) which is located 20 Å away from the active center and has been recently characterized by site directed mutagenesis (Shafferman *et al.*, 1992b; Radic *et al.*, 1993; Barak *et al.*, 1994). Although binding of PAS ligands was shown, over fifteen years ago, to affect the conformation of the active center (Taylor and Radic, 1994; Berman *et al.*, 1981) , the actual mechanism of this modulation was only recently proposed, suggesting the involvement of a conformational transition of residue Trp86 (Barak *et al.*, 1994). Residue Trp86 which in its active conformation is the main element of the classical "anionic subsite" (Shafferman *et al.*, 1992b; Ordentlich *et al.*, 1993a; Ordentlich *et al.*, 1995; Harel *et al.*, 1993; Harel *et al.*, 1996), essential for substrate accommodation, can occupy an alternative conformational state in which it occludes the active center (Ordentlich *et al.*, 1995). It has been further suggested that such conformational mobility of Trp86 is governed by the dynamic behavior of the cysteine loop (Cys69 - Cys96) on the protein surface and that modulation of this behavior, through occupation of the PAS, provides the means of transmission of the allosteric signal (Barak *et al.*, 1995). The HuAChE disulfide surface loop (Cys69-Cys96), which is a typical Ω loop (Lezczynski and Rose, 1986), is a structural element conserved throughout the esterase/lipase family of hydrolytic enzymes sharing the α/β hydrolase fold (Ollis *et al.*,1992), classified as the $L_{b3,2}$ variable length loop (Cygler *et al.*, 1993)). In the case of lipases, x-ray crystallographic studies of free versus complexed structures show that the $L_{b3,2}$ loop is one of the most mobile structural elements (Axelsen *et al.*, 1994; Faerman *et al.*, 1996). Simulated annealing experiments of HuAChE suggest that, also for this enzyme, a large segment of the $L_{b3,2}$ loop is the most mobile part of the molecule (see section VI). Furthermore, this mobility was shown to induce the conformational transitions of residue Trp86 and to modify the dimensions of the active site gorge rendering it more accessible to inbound ligands (Barak *et al.*, 1995).

To further test the notion that the dynamic behavior of the $L_{b3,2}$ loop is a major functional characteristic of AChE activity governing the mobility of Trp86 as well as ligand accessibility to the active center, we generated and characterized HuAChE mutants carrying replacement of residues which presumably contribute to the loop structure. Our results suggest that unlike the case of

lipases, the $L_{b3,2}$ loop in HuAChE is not involved in large lid-like displacements but more likely in specific low amplitude motions of selected loop residues. Such limited motions could be sufficient for providing access to the active center and for controlling the positioning and conformation of residue Trp86.

METHODS

Mutagenesis of Recombinant HuAChE and Preparation of enzymes - Mutagenesis of HuAChE (Soreq *et al.*, 1990) was performed by DNA cassette replacement and involved substitution by synthetic DNA duplexes (Shafferman *et al.*, 1992a). For generation of the Y77A, P78A, P85A and N87A mutants the *AccI-NruI* fragment of pACHEw4 was replaced by a synthetic fragment carrying the corresponding substitution. For generation of Y449A HuAChE, the *BstBI-BamHI* fragment of pACHEw3 was substituted. The Ala codon used in all mutations was GCC. The sequences of all new clones were verified by the dideoxy sequencing method (U.S. Biochemical Corp. sequenase kit). HuAChE mutants Y72A, D74N, E84Q, D95N and Y341A were described previously (Shafferman *et al.*, 1992a,b; Barak *et al.*, 1994). All recombinant HuAChE cDNA mutants were expressed in bipartite vectors which allow expression of the *cat* reporter gene. Human embryonal kidney 293 cells were transfected with various purified plasmids as described previously (Velan *et al.*, 1991; Kronman *et al.*, 1992). The various AChE polypeptides secreted into the medium and were quantified by AChE-protein determination relying on specific ELISA (Shafferman *et al.*, 1992a; Ordentlich *et al.*, 1993a,b).

Substrates, Inhibitors and Kinetic Studies - Acetylthiocholine iodide (ATC), 5,5-dithiobis (2-nitrobenzoic acid(DTNB) and ethyl(m-hydroxyphenyl)-dimethylammonium chloride (edrophonium), 3,8 diamino-5-3'-(trimethyl-ammonium)propyl-6-phenyl phenanthridinium iodide (propidium), di(*p*-allyl-N-dimethylamino-phenyl)-pentane-3-one(BW284C51) and1,10-bis-(trimethyl-ammonium) decane (decamethonium) were all purchased from Sigma.

Catalytic activity of the recombinant HuAChE and its mutant derivatives collected from transient transfections was assayed according to Ellman *et al.*,(1961) as described previously (Shafferman

et al., 1992a). Assays were performed with ~10^{-10}M enzymes (total volume 0.1ml) in growth medium in the presence of 0.1 mg/ml bovine serum albumin, 0.3mM (5,5-dithiobis(2-nitrobenzoic acid) in 50mM sodium-phosphate buffer pH8.0 and varying ATC (0.01-25mM) concentrations. The assays were carried out at 27°C and monitored by a Thermomax microplate reader (Molecular Devices) and corrected for background readings using medium collected from mock transfected cells. Data was analyzed according to the kinetic treatment described previously by Ordentlich *et al.* (1993a,b).

Structure Analysis and Molecular Graphics - Building and analysis of the 3D models was performed on a Silicon Graphics workstation Indigo2 using SYBYL 6.0 modeling software (Tripos Inc.). Construction of models for the HuAChE and the mutated enzymes was based upon the model structure of the enzyme obtained by comparative modeling (Barak *et al.*, 1992) from the x-ray structure of TcAChE (Sussman *et al.*, 1991). Optimization of the resulting structures was carried out as described before (Ordentlich *et al.*, 1993a,b, Ordentlich *et al.*, 1995; Barak *et al.*, 1994), using the TRIPOS force field and Kollman all - atom charges for the enzyme (Weiner *et al*, 1986).

RESULTS AND DISCUSSION

Potential Structural Modifications of the Loop: Generation and Analysis -

The HuAChE $L_{b3,2}$ surface loop constitutes of a relatively long stretch of residues (28 residues, Fig. 21) folded on itself and exhibiting a limited ordered structure (Fig. 22A,B). It has an elongated shape and lies flat on the protein surface forming the thin wall of the active site gorge. The notion that loop mobility may be important to AChE reactivity is suggested by the involvement of an equivalent loop in lipase, another member of the α/β hydrolase fold, in interfacial activation and substrate accommodation (Grochulski *et al.*, 1994). However, while the loop motion in lipases resembles a lid opening, controlled by *cis-trans* isomerization of proline (Pro92 in *Candida rugosa* lipase, Grochulski *et al.*, 1994), molecular dynamics simulations indicate that the corresponding motion in HuAChE can be best characterized as gradual unwinding (see previous chapter).

The most apparent element of secondary structure in the $L_{b3,2}$ loop of HuAChE is a helical turn (Glu81-Asn87) containing the anionic subsite residue Trp86 (Fig. 22B). Structural modifications of this element as well as other perturbations of the loop shape may be expected to affect the catalytic properties of the enzyme through relocation of the choline binding residue Trp86. Examination of molecular models suggests that such modifications could include replacement of polar residues contributing to the loop structure through salt bridges or H-bond interactions, replacement of the loop proline residues or deletion of part of the loop. Such types of modified enzymes were generated and kinetically monitored for effects on the catalytic activity as well as on reactivity toward reversible inhibitors. For the latter, three different types of reversible inhibitors were used. Affinity toward the cationic active center ligand edrophonium was determined to probe the extent of interaction with Trp86 since loop modifications were not expected to affect other elements of the active center. The inhibitory activity of a specific PAS ligand propidium was tested as it is expected to depend upon both the location of Trp86 and upon the manner by which loop mobility affects Trp86 conformation (Harel *et al.*, 1996). Inhibition by the specific bisquaternary ligands (decamethonium and/or BW284C51) which span the distance between the active center and the PAS, was examined to evaluate possible changes at both binding loci .

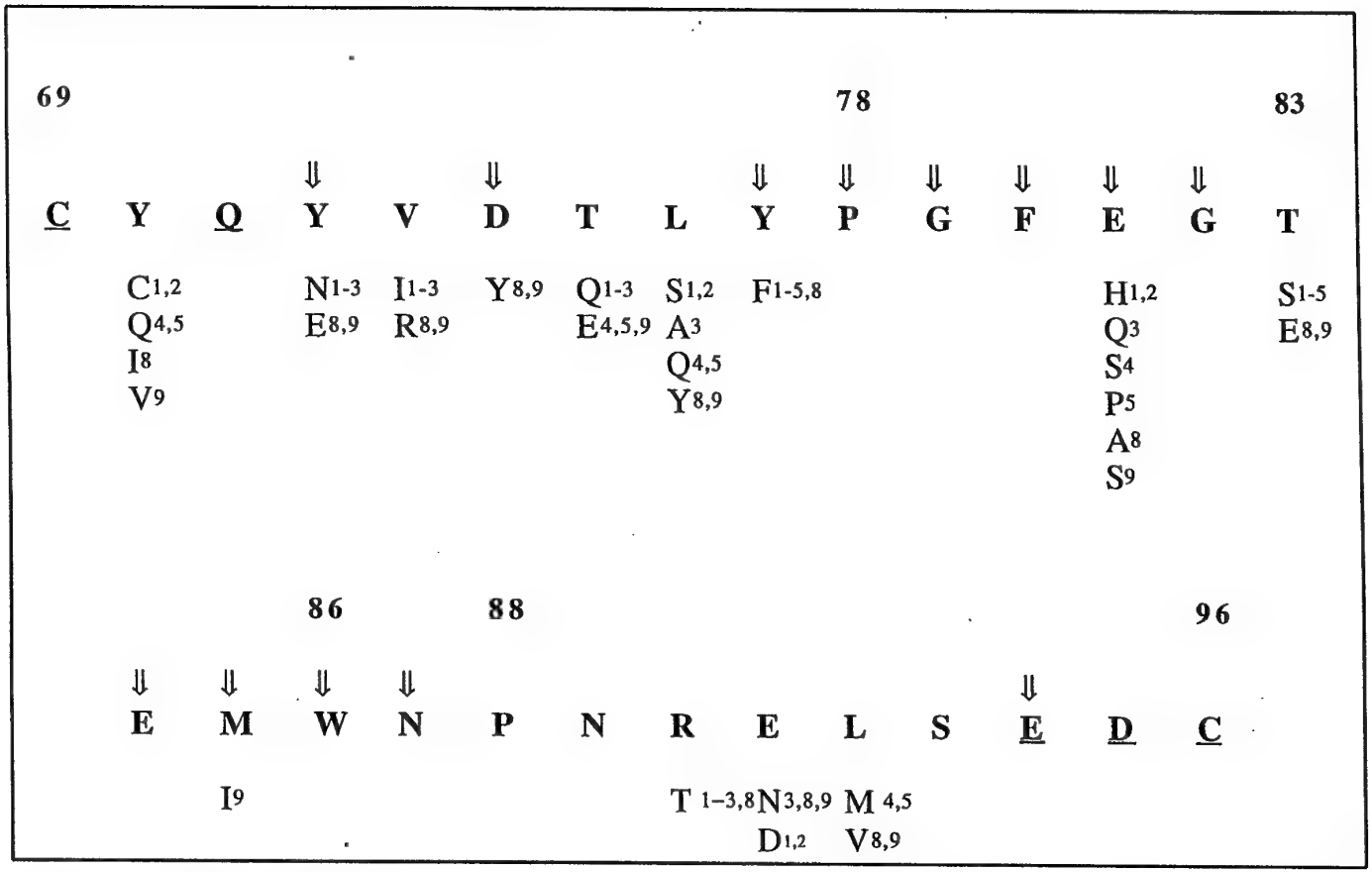

Fig. 21 Amino acid sequence of the surface Ω loop (Cys69-Cys96) in HuAChE as compared to other ChEs. Source of ChE is marked by numbers, as follows: 1. Human BuChE,2.rabbit BuChE, 3. mouse BuChE, 4. *Torpedo californica* AChE, 5. *Torpedo marmorata* AChE, 6. fetal bovine AChE, 7. mouse AChE, 8. *Anopheles stephensi* AChE, 9. *Drosophila* AChE Amino acid sequences are according to Gentry *et al.*, (1995). Residues conserved in nearly all the proteins maintaining the α/ß hydrolase fold are underlined. Positions at which replacements or deletions have been made by site directed mutagenesis, are marked by arrows.

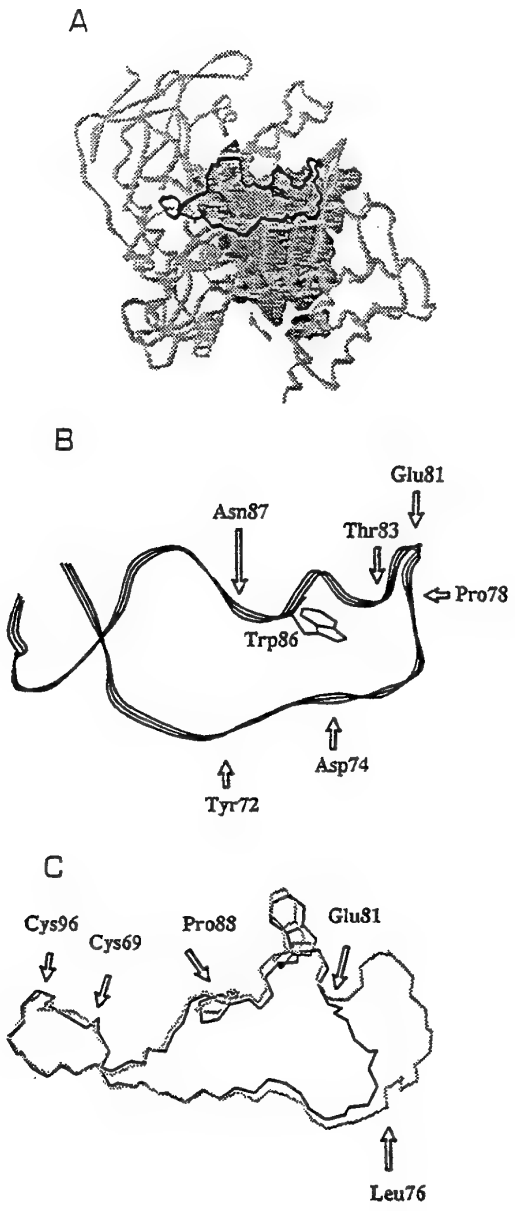

Fig. 22 Surface Ω loop (Cys69-Cys96) structure in HuAChE. A, Illustration of the Ω loop (heavy line) disposition relative to the protein core, with residues of the active site gorge shown in grid surface and the rest of the protein in line ribbon. Only the loop Cα backbone and the indole side chain of residue Trp86 are presented. B, Ribbon representation of the Ω loop main chain illustrating the α-helical turn (Glu81-Asn87), the loop tip (Pro78-Thr83) and position of the choline binding Trp86 side chain. C, Superposition of the Ω loop trace of the wild type HuAChE (light line) and that of the modeled loop structure of the Del78-82 HuAChE mutant (heavy line). The two traces diverge mainly in the vicinity of the deleted segment (between Leu76 and Glu84 of the original loop sequence), while the Cα position of residue Trp86 is nearly unchanged.Note also the slight difference in orientation of the catalytically important indole moiety in the loops of the wild type and Del 78-82 HuAChE mutant enzymes.

Structural Modifications of the Loop Ends - The $L_{b3,2}$ loop appears to be tightly fixed at its base by the Cys69-Cys96 disulfide bridge. In fact, molecular dynamics simulations indicate that the mobile segments of the $L_{b3,2}$ loops, in both lipases and cholinestrases, do not involve movement of residues at their N and C termini (in HuAChE Cys69-Tyr72 and Glu91-Cys96 respectively (Cygler *et al.*, 1993; and section VI)). Therefore, replacement of residues located near the loop termini should have only a limited effect on its shape and dynamic properties. On the other hand, the C-terminus residues Ser93 to Cys96 are strictly conserved in the lipase/esterase family and therefore may play a structural role in maintaining the loop position. In particular, residue Glu94 and the conserved residue Arg46 form a salt bridge which was shown as critical for maintenance of the 3D fold of the enzyme (Bucht *et al.*, 1994). In addition, ligand binding to the PAS array, including residue Tyr72 at the N-terminus of the loop, has been suggested to precipitate allosteric effects through modulation of the loop motion (Barak *et al*, 1995). Thus, examination of the reactivity properties of enzymes carrying replacements of the PAS residue Tyr72 and of the conserved residue Glu95, at the N and C termini respectively, may allow for a better understanding of coupling between the relatively stationary and the mobile portions of the $L_{b3,2}$ loop.

Examination of the kinetic parameters for Y72A HuAChE (Table 12) demonstrates that replacement of residue Tyr72 does not affect catalytic activity , suggesting that the positioning of residue Trp86 has not changed. The anionic subsite in the Y72A enzyme is fully functional, as indicated also by its wild type-like affinity toward the active center inhibitor edrophonium. The 4-fold decrease in the inhibition constant of propidium is probably due to the decrease in affinity toward the modified PAS of Y72A HuAChE (Barak *et al*., 1994) rather than due to effect on the conformational behavior of the loop. The affinity toward the bisquaternary ligand BW284C51 is similarly affected (2-fold). Replacement of the C terminal residue Asp95, which is conserved in all the cholinesterases, affects neither the catalytic activity nor reactivity of the D95N enzyme toward inhibitors (Table 12).

Modification of Interactions of the Potentially Mobile Part of the Loop with the Protein Core - As could be expected, the interactions of the $L_{b3,2}$ loop with the protein core are predominantly hydrophobic (Cygler *et al.*, 1993; Gerstein *et al.*, 1994; Kempner, 1993), but several polar interactions with the core can be identified. In the wild type HuAChE residue Asp74 interacts with the protein core residue Tyr341. Disruption of this interaction was already shown to affect HuAChE reactivity (Ordentlich *et al.*, 1995; Barak *et al.*, 1994) (see also Table 12). Two other residues participating in the loop-protein core polar interactions are Tyr77 (with residue Tyr341) and Glu84 (with Lys348). Both residues are located near the center of the loop, flanking its highly mobile tip (Tyr77-Thr83) (see section VI). In fact, dissociation of this tip from the protein core has been suggested, by the high temperature molecular dynamics simulations, as one of the characteristics of the $L_{b3,2}$ loop motions in HuAChE (see section VI). Another interaction of this type may involve the indole moiety of Trp86 and the adjacent side chain of residue Tyr449. However, due to the poor H-bond donating properties of the indole nitrogen, the contribution of this interaction to either the conformational stability of residue Trp86 or to the overall shape of the loop has been difficult to predict.

Examination of kinetic parameters for the Y77A; E84Q; Y341A and Y449A enzymes (Table 12) shows that neither one of these structural modifications had a significant effect on HuAChE reactivity. The fact that perturbations of polar interactions between the loop and the protein core had only a marginal effect on enzymatic activity may suggest that the coupling between loop mobility and conformation of Trp86 does not involve large loop displacements separating it from the core. The recently reported activity of TcAChE mutant, in which a disulfide bridge between the loop tip and the core has been introduced (*G80C/V431C*) (Faerman *et al.*, 1996), and our results with the similar double mutant E81C/S438C (unpublished results) appear to support such conclusion.

Modification of Interactions within the Mobile Part of the Loop - Most of the loop polar residues including Asp74, Thr75, Glu81, Thr83, Glu84, Asn87, Asn89 and Arg90 are involved in H-bond contacts within the loop. These contacts may be instrumental in maintaining the local kinks and turns characteristic to the $L_{b3,2}$ loop structure (see Fig. 22B). Among these

interactions, particularly interesting were the two in the immediate vicinity of Trp86 (Met85-Glu81 and Asn87-Thr83) since they seem to participate in maintaining the helical turn structure ($\alpha_{b3,2}$, see Cygler *et al.*, 1993), providing a flexible main chain linkage for residue Trp86. Such linkages at the tip of small loops or turns, are characteristic for residues of the catalytic machineries (e.g. those of the catalytic triad in serine hydrolases (Cygler *et al.*,1993)), allowing for minute conformational adjustments in order to achieve optimal interaction geometry. In addition, interaction of the Met85 side chain with the indole moiety has been proposed to contribute to the stabilization of Trp86 active conformation (Harel *et al.*, 1995).

Replacement of residue Met85 had no effect on the catalytic activity of the enzyme and only a minor (>3-fold) effect on affinity toward edrophonium. Although an interaction Ala85-Glu81 is still possible in the M85A enzyme, that of the methionine side chain with the indole moiety of Trp86 is certainly lost. Thus, the proximity of Met85 to residue Trp86 does not influence in a substantial way the conformation of the latter.

In the case of N87A enzyme, a small effect on the Km value (2-fold increase relative to the wild type) has been observed. This slight impairment in accommodating active center ligands is reflected also in the 5-fold decrease in affinity toward edrophonium. Interestingly, the inhibitory activity of the PAS specific ligand propidium is also about 5-fold lower. Such reactivity phenotype is shared by enzymes carrying replacements of residue Asp74 or Y133, in which the position or conformational properties of residue Trp86 have been affected, (Ordentlich *et al.*, 1993a,b; Ordentlich *et al.*, 1995; Barak *et al.*, 1994). Like in these cases, the somewhat altered properties of residue Trp86 due to the replacement of Asn87, affect both the binding characteristics of the active center and the efficiency of transmitting the allosteric signal from the PAS. This conclusion is further supported by a 10-fold increase in the inhibition constant (Ki) of BW284C51 toward N87A HuAChE, as compared to the wild type enzyme (Table 12).

Table12: Kinetic constants of catalysis and inhibition constants Ki for HuAChE Mutants of the $L_{b3,2}$ loop

AChE	K_m (mM)	k_{cat} ($x10^{-5}$x min^{-1})	k_{cat}/K_m ($x10^{-8}$ $M^{-1}xmin^{-1}$)	Edrophonium (μM)	Propidium (μM)	BW284C51 (nM)
WT	0.14	4.0	29.0	0.75	1.4	10
Y72A[a]	0.14	4.7	32.0	0.3	5.3	22
D74N[a]	0.60	2.5	4.2	3.5	7.8	2450
Y77A	0.12	2.9	24.2	0.83	1.7	3.9
P78A	0.10	3.0	30.0	0.8	0.7	7.5
E84Q[b]	0.27	4.0	15.0	1.2	2.4	78.5
M85A	0.14	4.6	33.0	2	1.3	5.2
N87A	0.23	6.1	27.0	3.4	6.5	105
P88A	0.14	5.0	37.5	1.6	0.7	14
D95N	0.13	4.4	34.0	0.43	2.2	3.2
Y341A[a]	0.30	2.5	8.3	2.0	3.4	322
Y449A	0.13	1.5	11.5	5.5	2.9	24

[a] Values for Y72A, D74N and Y341A HuAChE are cited from Barak *et al.* (1995).
[b] Some of the kinetic parameters for E84Q were determined previously (Ordentlich *et al.*, 1995)

Structural Modifications of the Loop Involving Proline Residues - The significance of proline residues in the loop mobility of lipase (from *Candida rugosa* ; CRL), was recently demonstrated by comparison of the x-ray structures of the closed and open forms (Groshulski *et al*, 1994). Transition between the two forms involves a nearly 90° rotation of the loop around hinge residues Pro92 and Glu66 (numbering according to the CRL sequence) with residue Pro65 probably providing additional rigidity to the adjacent hinge region. The corresponding $L_{b3,2}$ loops in cholinesterases also contain two conserved proline residues (Fig. 21) which may fulfill a similar function in controlling the loop mobility. However, according to the results from molecular dynamics simulations, isomerization of residues Pro78 and Pro88 does not take place in HuAChE (Barak *et al*., 1995, see previous chapter). Furthermore, while the hinge residue of CRL Pro92 is located near the C terminus of the loop sequence, the analogous HuAChE residue Pro78 (according to comparison of the lipase and cholinesterase loop sequences (Gentry *et al.*, 1995)) is located near the center of the HuAChE loop sequence and therefore may be unsuitable to function as a *cis-trans* conformational switch of the loop.

Even without being involved in *cis-trans* isomerizations, proline residues should locally restrict the conformational mobility of the adjacent residues (Yaron and Naider, 1993). In particular, this may be the case for Pro88 located at the C terminus of the $\alpha_{b3,2}$ helical turn (Glu81-Asn87). Nevertheless, replacements of both proline residues did not affect catalytic activity and had only marginal (~2-fold) effect on the affinity toward edrophonium and BW284C51 (see Table 12). These results suggest that although HuAChE and CRL share the same 3-dimensional topology, both conforming to the α/β hydrolase fold, the functional significance of analogous structural details can be very different. Namely, while proline residues in the CRL $L_{b3,2}$ loop are essential for normal enzymatic activity, the analogous residues in HuAChE appear to be devoid of any functional or even structural role. Such apparent lack of structural significance of the loop proline residues is very surprising since they are conserved in all the cholinesterases and since proline residues are recognized as major determinants of secondary structure in proteins (Gerstein *et al.*, 1994; Kempner, 1993).

Structural Modification of the Loop Through Residue Deletion - Since replacement of single residues within the loop or in its vicinity failed to produce a sizable effects on HuAChE reactivity , we turned to a more drastic way to modify the $L_{b3,2}$ loop structure, through deletions of selected loop segments. Such deletions are bound to alter the loop span and consequently the relative positions of its individual residues. Yet, a total loss of activity due to a drastic deletion would be difficult to interpret in terms of specific structural modifications.

In a preliminary experiment, designed to test whether the proper positioning of Trp86 in the active center is the only catalytically significant function of the $L_{b3,2}$ loop, deletion of most of its mobile part was attempted. However, attempts to express a protein, carrying excision of the sequence Asp74-Asn87, were not successful implying that in this case the folding process was probably affected (data not shown). To overcome this limitation we have generated and examined molecular models of truncated loop structures, looking for those in which positions of Trp86 and adjacent residues are the least affected. In construction of the truncated loop models we adjusted the geometry of residues adjacent to the excised sequence, only as necessary to reclose the loop. Several of these initial loop structures were subsequently optimized to obtain acceptable model alternatives. One such model structure has been obtained by deletion of the sequence Pro78-Gly82, resulting in a loop in which the loop tip is missing (Fig. 22C). Despite such drastic alteration of the loop sequence, the model indicated only a minor displacement of the Trp86 indole moiety relative to its position in the wild type enzyme (Fig. 22C). This is especially interesting in view of the fact that the sequence indicated for the deletion (Pro-Gly-Phe-X-Gly) is conserved in all the cholinesterases (Fig. 21).

Kinetic characterization of the Del78-82 HuAChE reveals that its reactivity toward the substrate ATC is nearly 20-fold lower compared to the wild type enzyme. Most of this decrease is due to 7-fold increase in the respective value of Km, indicating a deficient substrate accommodation in the Michaelis-Menten complex. Such destabilization is probably an outcome of an impaired interaction with residue Trp86, since structural modifications of the loop should not affect other elements of the active center. However the Michaelis Menten constants (Km) only approximate the true dissociation constants of the noncovalent complexes. Therefore it was important to examine the effects of loop deletion on the affinities toward inhibitors interacting with the active center. Indeed, the affinities of Del78-82 HuAChE toward edrophonium, BW284C51 and decamethonium were

respectively 110-fold, 230-fold and 140-fold lower (see Table 13). According to the molecular models, these suboptimal interactions are the outcome of the improper positioning of residue Trp86 indole moiety. Interestingly, a very similar reactivity phenotype was observed for the W86F enzyme where the relative 11-fold decrease in the reactivity toward ATC also originates mostly from the increase in Km (6-fold) and the affinities toward edrophonium BW284C51 and decamethonium are respectively 50-fold, 120-fold and 80-fold lower. In this case, the impaired interaction with the anionic subsite is probably effected through modification of the π-electron system rather than by repositioning of the interaction locus for the ligands charged groups. On the other hand Del78-82 HuAChE is still a highly efficient enzyme suggesting that the small relocation of Trp86 is indeed the only structural consequence of the loop deletion. This conclusion seems to be consistent with the nearly equal effects on the affinities toward the inhibitors edrophonium BW284C51 and decamethonium. For the latter, we have already shown that changes in affinity represent a combination of effects on the active center and the PAS (Barak *et al.*, 1994). Thus, loop deletion appears to have no structural effect on the PAS.

The inhibition of Del78-82 HuAChE catalytic activity by the PAS ligand propidium is about 9-fold less effective than that of the wild type enzyme. This result indicates that truncation of the loop has not abolished the mechanism of the allosteric modulation of AChE activity (Barak *et al.*, 1994) and that the lower inhibitory efficiency is due to the diminished capacity of Trp86 to block the access to the active center (Fig 23). Such interpretation is consistent with the conclusion that Trp86 is somewhat relocated in the truncated loop structure. Furthermore, similar characteristics of inhibition by propidium were observed also for the W86F enzyme, where the smaller phenyl ring could be expected to be somewhat less efficient, than the indole moiety, in blocking the active center (Fig. 23B). Thus, the reactivity characteristics of Del78-82 HuAChE appear to be consistent with the proposed involvement of the conformational mobility of Trp86 in the mechanism of allosteric modulation of AChE activity.

Table13: Kinetic constants of catalysis and inhibition constants Ki for HuAChE and its mutants

AChE Type	K_m (mM)	k_{cat} ($x10^{-5}$ min^{-1})	K_{cat}/K_m ($X10^{-8}$ M^{-1} min^{-1})	Edrophonium (μM)	Propidium (μM)	BW284C51 (nM)	Decamethonium (μM)
WT	0.14	4.0	29.0	0.75	1.4	10	6
W86A[a]	93	0.8	0.009	>45000	870	40000	90000
W86F[a]	0.8	2.1	2.6	38	3.2	1200	500
Del 78-82	1.0	1.5	1.5	84	6.6	2300	880

[a] Values for W86A and some of those reported for W86F were determined previously (Barak *et al.*, 1995; Ordentlich *et al.*, 1995)

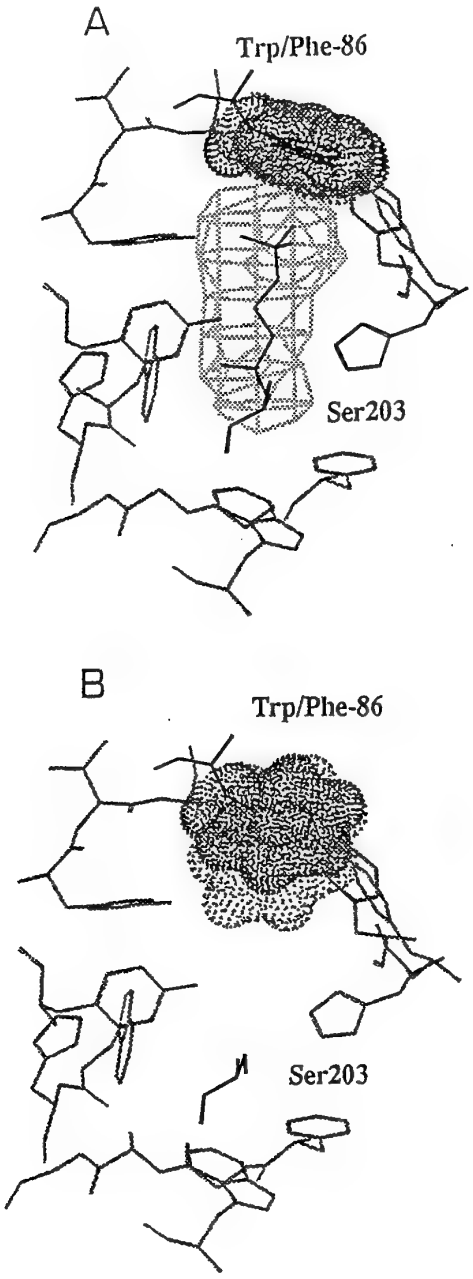

Fig. 23 Conformational transition of aromatic residue (tryptophane and phenylalanine) at position 86. A, Superposition of the catalytically functional conformations of residues Trp86 (lighter volume) and Phe86 (darker volume)in wild type and W86F HuAChE respectively with the aromatic moiety shown to accommodate the tetramethylammonium group of ACh (presented as a grid). B, Nonactive conformation of the extended aromatic side chain occluding the active center interfering with complexation of substrates and active center inhibitors. Note the greater hindrance by the indole moiety as compared to that of the phenyl ring.

Conclusions - Previous investigations of the structure-function characteristics of HuAChE demonstrated that the precise positioning of residue Trp86 in the active center is essential for the AChE catalytic activity (Ordentlich *et al.*, 1993a; Ordentlich *et al.*, 1995; Harel *et a*l., 1996). According to the x-ray structure of AChE (Sussman *et al.*, 1991), such positioning is achieved through a specific structure of the $L_{b3,2}$ loop and its juxtaposition against the protein core. Although this structural assembly is held together mainly by hydrophobic interactions, the revealed resistance of the loop 3D shape to modifications through selected replacements of its polar residues, is rather unexpected. Particularly surprising is the insensitivity of the loop structure to replacements of the conserved proline residues. Nevertheless, in cases in which enzyme reactivity was somewhat affected by modification of the loop sequence, like that of Del78-82 HuAChE, the effects were consistent with small relocations of residue Trp86. Such conclusion is also supported by the resemblance of the reactivity phenotypes of the Del78-82 and the W86F enzymes. The interdependence between the location of Trp86 and the loop structure is also consistent with the previously proposed mechanism of allosteric modulation of AChE activity (Barak *et al*, 1994). However the relative rigidity of the loop, indicated by the present results, precludes large amplitude loop motions like those observed in the lipases. It appears that the conformational transition of residue Trp86, implicated in the allosteric mechanism, takes place in response to minor and specific conformational changes of the loop. In fact, such sensitivity of the Trp86 conformation has been suggested by the high temperature dynamic simulations (see section VI), even though the minimal loop motion precipitating Trp86 conformational transition , could not be derived from these simulations. Minor motions of the central loop portion (particularly of the main chain around position 74) may also allow for relatively unrestricted ligand access to the active site. Such motion may again be a result of specific conformational changes along the loop, presenting a far more complex dynamic behavior than the flap motions in lipases which initially served as a model for the $L_{b3,2}$ loop mobility in cholinesterases.

VIII. Parameters Affecting Circulatory Residence of Recombinant Acetylcholinesterase: Biochemical or Genetic Manipulation of Sialylation Levels Improve Residence Time

INTRODUCTION

Acetylcholinesterases (AChE, EC 3.1.1.7), as well as the related butyrylcholinesterases display tissue specific variation in their structure. Assembly of catalytic and structural subunits results in formation of several classes of membrane-bound and soluble cholinesterase forms (Massoulie *et al.*, 1993). Serum derived cholinesterases represent a specific group of soluble homo-oligomeric forms which reside in the circulation for extended periods of time. When human serum butyrylcholinesterase or fetal bovine serum acetylcholinesterase are administered exogenously to experimental animals they display high serum residence and are cleared from the circulation after several hours (Douchet *et al.*,1982; Raveh *et al.* 1993; Kronman, *et al.*, 1995; Saxena, *et al.*, 1997). This high serum residence cannot be reproduced when native or recombinant AChEs from other sources are examined (Kronman *et al.*, 1995; Saxena *et al.*, 1998). Cholinesterases represent, therefore, a group of closely related proteins displaying pharmacokinetic variations and could provide a good experimental system for the analysis of molecular factors involved in clearance of proteins from the circulation.

Differences in clearance rates of proteins may originate from variations in their primary sequence or in post-translation modifications. We have explored these possibilities in the context of the acetylcholinesterase family and recently found that the difference in sequence between bovine AChE and human AChE cannot explain the difference between the clearance profiles of native bovine serum-derived AChE and recombinant HuAChE produced in HEK-293 cells. On the other hand, our studies with various glycosylation mutants of rHuAChE, indicated that N-glycosylation plays a central role in determining the circulatory residence in cholinesterases (Kronman *et al.*, 1995). Furthermore, the efficiency of N-glycan sialylation was shown to determine the rate of clearance of the AChEs and an inverse-linear relationship was shown to exist between the number

of nonsialylated glycan termini associated with the enzyme and its rate of clearance. The effect of terminal glycosylation, including sialylation, on clearance rates was demonstrated in a variety of other proteins as well (Ashwell and Harford,1982). Therefore, the distribution and abundance of various terminal glycosyltransferases (Paulson *et al.*, 1989; Paulson and Colley, 1989) in cells used to produce native or recombinant AChEs could play a key role in their pharmacokinetic profiles. This is of importance in particular for the generation of recombinant proteins whose potential therapeutic value has been impeded by their fast clearance rate (Narita *et al.* 1995a; Joshi *et al.* 1995).

Cholinesterases have been attributed a therapeutic value, by virtue of their affinity or scavenging ability of organophosphate poisons (Raveh *et al.*, 1993; Wolfe *et al.* 1987 Broomfield *et al.*, 1991; Ashani *et al.*, 1991; Cascio *et al.*, 1988). Recombinant human AChE, produced in high amounts in stably transfected cells (Velan *et al.*, 1991a; Kronman *et al.*, 1992) could be a suitable source for this bioscavenger. We have shown in the past that it is indeed possible to improve the bioscavenging performance of recombinant human AChE by site directed mutagenesis. Mutagenesis either enhanced the enzyme affinity for organophosphate compounds or prevented the aging process (Ordentlich *et al.*, 1993a; Ordentlich *et al.*, 1996 and section III-IV).

In this report, we address the role of sialylation in determining circulatory residence of rHuAChE produced in HEK-293 cells. We use refined analytical approaches to examine the sialylation state of the recombinant HuAChE and demonstrate the limited ability of the cellular glycosylation machinery to generate fully sialylated rHuAChE. We then employ *in vitro* biochemical methods as well as genetic engineering approaches to modulate the sialic acid content and circulatory clearance of AChE by 2,6 α-sialyltransferase (α2,6ST), and finally, we propose an engineered cell system for production of glycoproteins with extended circulatory residence.

METHODS

Construction of the ß-galactoside α 2,6-sialyltransferase Expression Vector - The cDNA coding for ß-galactoside α 2,6-sialyltransferase was amplified by polymerase chain reactions (PCR) from rat polyA-primed cDNA utilizing the following primers: cggggtaccATGATTCATACCAACTTGAAG (upstream primer) and ggcggatcCTCAACAACGAATGTTCCGGA (downstream primer); low case nucleotides represent the KpnI and BamHI extensions which were used for ligation. PCR was carried out using 30 cycles of the following temperature profile: denaturation for 30 seconds at 94°C, primer annealing for 30 seconds at 55°C and primer extension for 1.5 minutes at 72°C. Reactions were set up in a final volume of 100µl manufacturer-supplied Taq polymerase buffer containing template cDNA, 20pmoles of each primer, 50µM of each dNTP and 2 units of Taq polymerase (Promega). The 1210 bp PCR product was ligated into the corresponding sites of the pCEP4 vector (Invitrogen) downstream to the CMV promoter, to generate pCEP4-α2,6ST. The cloned cDNA was sequenced and its identity was verified by comparison to the published rat liver α2,6ST cDNA sequence (Weinstein *et al.*, 1987) (EMBL accession number M18769). DNA sequencing by the di-deoxy termination method, was carried out using Sequenase II (USB).

Transfection and Selection of α2,6ST Producing HEK-293 Cells - Cells of the human embryonic kidney 293 cell line (HEK-293), as well as cell clones of the same lineage which express high levels of recombinant human acetylcholinesterase (HEK-293-AChE) were transfected (Shafferman *et al.*, 1992b) with the pCEP4-α2,6ST plasmid which carries also a hygromycin resistance marker. Selection of stably transfected cells was carried out by incubating the cells in the presence of 0.3 mg/ml hygromycin; colonies of hygromycin resistant cells which appeared 3 weeks post-transfection (approx 200 colonies/2x10^{6}cells/20µg DNA) were pooled and examined for intracellular 2,6 α–sialyltransferase activity. To isolate individual cell clones expressing α2,6ST, cell pools were cloned by limiting dilution as described before (Kronman *et al.*, 1992). Twenty five individual cell clones were chosen at random, cells were expanded, and clones were tested for α2,6ST activity.

Determination of Intracellular Sialyltransferase Activity - Cell pellets (10^7 cells/sample) were washed twice with PBS, resuspended in 1ml lysis buffer containing sodium cacodylate 0.1M (pH 6) and 1% Triton X-100 and left in ice for 15 min. Cells were sonicated for 30 seconds on a Microson cell disrupter (Misonix). The cell lysate was centrifuged for 10 minutes at 3000rpm, in an Eppendorf centrifuge. The clear supernatant, containing 10-20 µg protein/µl was stored in small aliquots at -70^{0}C until determination of the sialyltransferase activity. Protein concentration was determined by the BCA kit (Sigma). Sialyltransferase activity was assayed in cellular homogenates by a modification of a method previously described (Datta and Paulson, 1995). Up to 200 µg cell extract were incubated in the presence of 50 µg acceptor bovine asialofetuin (Sigma) and 1000 pmoles of the sialic acid (NeuAc) donor CMP-[^{14}C]NeuAc (approx 100,000 cpm/assay), in a final volume of 50µl including 0.5% Triton X100 and 50mM sodium cacodylate. Incubation was carried out at 37^{0}C for up to 3 hr. The assay was terminated and the free radioactive CMP-NeuAc was removed by precipitation with a large excess of ice-cold 10% trichloroacetic acid. TCA precipitate was processed in a liquid scintillation counter to quantitate [^{14}C]NeuAc incorporation. Assays were performed kinetically; the amount of NeuAc incorporated was expressed as picomoles NeuAc transferred/hr/mg protein of cell extract to an excess of asialoprotein acceptor. Standard deviations of less than 10% were observed. Positive controls were set up using commercial pure rat liver α2,6ST (E.C.2.4.99.1, Beohringer Mannheim).

Source of rHuAChE and Enzyme Purification - Recombinant HuAChE was collected from stable G418^R cell clones expressing various levels of wild type enzyme (Kronman *et al.*, 1992) or a derivative carrying at the C-terminus the KDEL-retention signal (Velan *et al.*,1994). Pure rHuAChEs were prepared by affinity chromatography utilizing procainamide-Sepharose 4B columns as previously described (Kronman *et al.*, 1992). Eluted enzyme was extensively dialyzed against ice-cold phosphate buffered saline and quantitated by protein mass determination (BCA kit, Sigma) and by specific enzyme-linked immunosorbent assay (ELISA) based on polyclonal antibodies to rHuAChE (Shafferman *et al.*, 1992b). Purified rAChEs were used for determination of sialic acid content, ^{14}C-NeuAc incorporation assays , SDS-PAGE, glycan preparation for HAPAEC-PAD and circulatory clearance experiments.

^{14}C-sialic Acid Incorporation into rHuAChE - rHuAChE (20 pmoles) was incubated with 500 picomoles CMP-[^{14}C]NeuAc in the presence of 0.2 mU commercial α2,6ST in a buffer containing 0.5%Triton X100, 50mM Na Cacodylate and 1mg/ml BSA, in a final volume of 50µl, at 37^{0}C. Reactions were stopped at various time intervals (1-8 hr) by the addition of 1ml ice-cold 10%TCA. Usually, incorporation levels off after 1-3 hours incubation. Control experiments established that TCA precipitable radioactivity over the background level is not detected in either the absence of an acceptor protein or in the presence of an acceptor glycoprotein which does not display N-linked glycan terminating in galactose residues (such as asialomucin). Positive control experiments set up with asialofetuin as acceptor showed that once incorporated, radioactive NeuAc was not chased by an excess of nonradioactive CMP-NeuAc donor. The amount of incorporated ^{14}C-NeuAc (expressed as moles NeuAc/mole AChE) represents the number of free sites per AChE subunit which are available for the addition of NeuAc.

In vitro Sialylation and Desialylation of Recombinant AChE - Pure rHuAChE (1.8 nmoles) were incubated for 20 hrs. at 37^{0}C in the presence of 2mU α2,6ST (Boehringer) and 100 nmoles of CMP-N-acetyl-neuraminic acid/ 50mM NaCl (final volume = 800µl). The *in vitro* sialylated rHuAChE was extensively dialyzed against water for N-glycan analysis, or against PBS for *in-vivo* pharmacokinetics studies. Desialylation of rHuAChE was performed as described previously (Kronman *et al.*, 1995) by agarose-bound neuraminidase (Sigma) which was then removed by Eppendorf centrifugation. Desialylated enzyme was dialyzed against PBS to remove free sialic acid.

Glycan Structural Analysis - **(i)** Sialic acid content Determination of sialic acid contents was performed on highly purified enzyme preparations. Release and quantitation of sialic acid residues was achieved by the thiobarbituric acid method (Warren, 1959). Sialic acid extracted into cyclohexanone was quantitated at 549 nm alongside a standard curve of N-acetylneuraminic acid (Sigma) which was subjected to the same assay conditions. **(ii)** Size and charge profiles of the glycans Size and charge profiles of the glycans associated with recombinant HuAChE produced in human cells of the HEK-293 line, were determined by Oxford Glycosystems (UK). Briefly, the oligosaccharides were quantitatively released by hydrazinolysis from a 300µg pure protein sample

and recovered using GlycoPrep 1000™. The sample was fluorescently labeled by reductive amination with 2-aminobenzamide (2-AB) followed by paper chromatography purification. For the determination of charge distribution, an aliquot of the pool was subjected to HPLC anion exchange chromatography on a GlycoSep C column using acetonitrile and ammonium acetate as eluant. To determine the nature of the negatively charged substituents, an aliquot of the total pool of fluorescently labelled oligosaccharides was incubated with *Arthrobacter ureafaciens* neuraminidase and then subjected to GlycoSep C chromatography. For the determination of the size-distribution, the total pool of deacidified 2-AB labelled oligosaccharides was subjected to high resolution gel permeation chromatography using the GlycoSequencer. The material was eluted with water and on-line detection was achieved by a fluorescence flow detector (for the 2-AB labelled oligosaccharides) or by a differential refractometer (for individual glucose oligomer markers).

(iii) High pH anion exchange chromatography-pulse amperometric detection (HPAEC-PAD) analysis of N-glycans Highly purified rHuAChE preparations (100μg) were extensively dialyzed against water and lyophilized. Hydrazine-based deglycosylation of N-linked glycans and further purification steps were performed by the automated Glycoprep100 instrument (Oxford Glycosciences, Oxford UK). The purified glycans, dissolved in 4.5 ml of 1M acetic acid were dried by a rotor-vacuum evaporator. The dried glycan pool was resuspended in 100 μl solution of 4 μg/μl isomaltotriose (Sigma) in water and 90 μl were loaded on a PA-100 column (Dionex Corp., Sunnyvale , California, USA) for separation. Using the DX-500 HPAEC-PAD system (Dionex Corp., Sunnyvale, California, USA), glycans were eluted with a gradient of sodium-acetate in 100 mM NaOH, and detected by a Pulsed-Amperometric-Detector. Assignement of peaks in the resultant chromatography was achieved using standard oligosaccharide markers (Oxford GlycoSystems, Cat. No. A1, A1F, A2, A2F, NA2F, A3). Isomaltotriose served as an internal marker to ensure consistency of the various runs.

Enzyme Activity - AChE activity was measured according to Ellman *et al.* (1961). Assays were performed in the presence of 0.5 mM acetylthiocholine, 50 mM sodium phosphate buffer pH 8.8, 0.1 mg/ml BSA and 0.3 mM 5,5'-dithiobis-(2-nitrobenzoic acid). The assay was carried out at 27^{0}C and monitored by a Thermomax microplate reader (Molecular Devices). Km values for acetylthiocholine were obtained from Lineweaver-Burk plots and kcat calculations were based on

polyclonal ELISA measurements (Shafferman *et al.*, 1992b). Inhibition constants (Ki) for the specific inhibitors edrophonium, propidium, decamethonium and BW284C51 were derived as described previously (Ordentlich *et al.*, 1993a).

Pharmacokinetics - *In vivo* clearance experiments in mice (3 to 6 ICR male mice per enzyme sample) and analysis of pharmacokinetics profile were carried out as described by Kronman *et al.* (1995). The study was approved by the local ethical committee on animal experiments. Residual AChE activity in blood samples was measured and all values were corrected for background activity determined in blood samples withdrawn 1 hour before performing the experiment. The clearance patterns of the various enzyme preparations were biphasic and fitted to a bi-exponential elimination pharmacokinetic model as described previously (Kronman *et al.*, 1995).

RESULTS

Analysis of N-glycans of Recombinant HuAChE Produced by HEK-293 Cells. As an initial step towards understanding the possible contribution of N-glycans to circulatory residence of rHuAChE, the carbohydrate side-chains associated with recombinant HuAChE produced in HEK-293 cells were subjected to a structural analysis which comprised determination of size, charge, antennary branching and sialylation extent. Chromatographic size determination (Fig. 24A) establishes that the main fraction (>80%) of the deacidified glycans released from a pure preparation of the HEK-293 cell-generated rHuAChE has a size of 12.2±0.1 glucose units, in agreement with that of a biantennary glycan projection containing fucose.

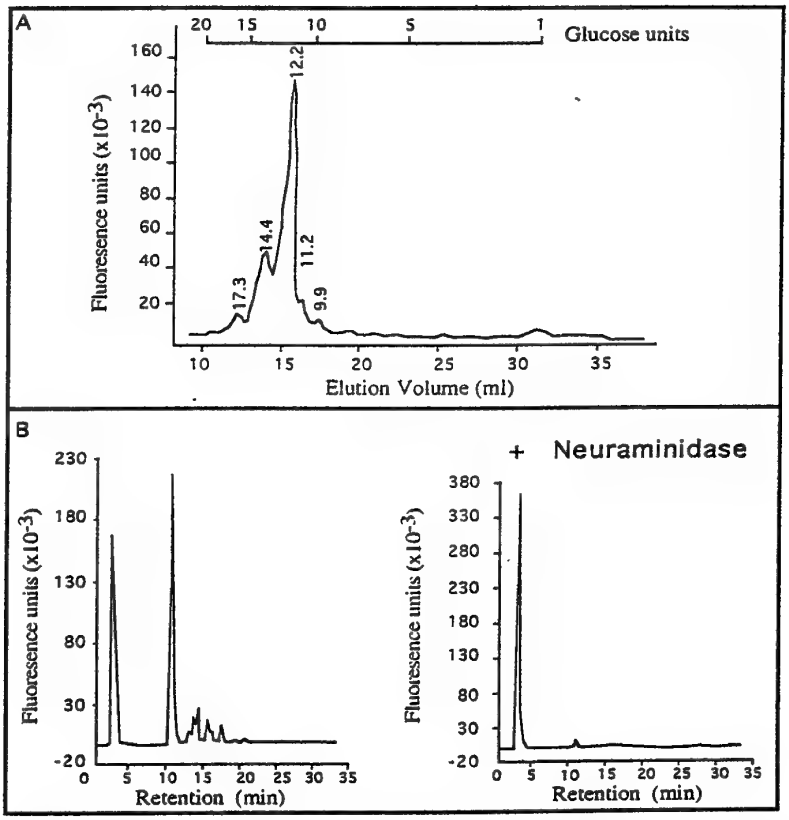

Fig. 24. Structural analysis of carbohydrates released from rHuAChE
(A) Size profile of the total pool of deacidified oligosaccharides, was determined by high resolution gel permeation chromatography on a Glyco-sequencer. Numerical superscripts represent the elution position of the co-applied glucose oligomers, expressed as glucose units and corrected for the contribution of the fluorescent label 2-aminobenzamide to the position of the elution peak. (B) Charge distribution of the total pool of oligosaccharides, before (left) and after (right) neuraminidase treatment, determined by anion exchange HPLC GlycoSep C chromatography.

The data also indicates that rHuAChE produced in this cell system does not carry significant amounts of O-glycans, as suggested by the absence of any substantial peak within the low size (1-5 glucose units) region of the chromatogram (Fig. 24A). Charge analysis of the glycan pool released from rHuAChE (Fig. 24B, left) prior to deacidification by treatment with neuraminidase, reveals that the rHuAChE associated glycans consist of a mixed population of both charged and non-charged species. Following treatment of the oligosaccharide preparation with bacterial neuraminidase, more than 99% of the material appears in the non-charged peak (Fig. 24B, right), demonstrating that nearly all of the charge is contributed by terminal sialic acid residues. To allow high resolution analysis of the N-glycans, rHuAChE was subjected to hydrazine-based deglycosylation and the released glycans were separated by High-pH-Anion-Exchange-Chromatography on a PA-100 column. The analyses (Fig. 25, upper panel) reveal the presence of four different groups of N-glycans: nonsialylated biantennary (a), monosialylated biantennary (b), disialylated biantennary (c), and trisialylated triantennary (d). Integration of peak areas of the eluted oligosaccharides, confirms that most of the glycans (>85%) correspond to biantennary forms, while only a minor fraction is triantennary.

Taken together, the carbohydrate analyses demonstrate that: (i) N-glycans associated with rHuAChE produced in HEK-293 cells are relatively homogenous both in size and in branching; this is in contrast to the heterogeneous nature of the N-glycans observed in other recombinant cholinesterases (Saxena *et al.*, 1998), (ii) N-glycans associated with 293 cell-produced rHuAChE are mostly of the biantennary type, (iii) the N-glycans are only partially sialylated, about 60% of them carrying terminal sialic acid residues. These results are in good agreement with the sialic acid measurements reported earlier (Kronman *et al.*, 1995), suggesting that the majority of glycans associated rHuAChE produced by HEK-293 cells are partially sialylated.

Recombinant HuAChE Can Serve as a Substrate for the Enzyme α2,6ST. In view of the incomplete sialylation of rHuAChE generated in HEK-293 cells, we addressed the question whether rHuAChE can act as a sialic acid acceptor in a 2,6 α-sialyltransferase reaction. This could be useful both as an analytical assay which scores the number of sites available for sialylation as well as a way to increase the sialic acid content of the recombinant enzyme.

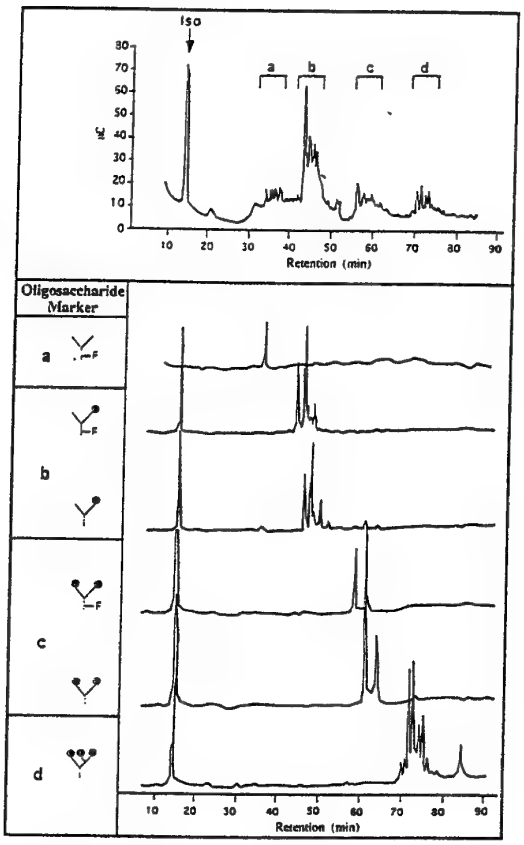

Fig. 25. HPAEC-PAD analysis of carbohydrates released from rHuAChE

Upper panel: N-glycan profile of rHuAChE. Purified N-glycans from 100μg of rHuAChE were fractionated on a PA-100 ion exchange column connected to a Dionex 500 system. Elution time regions of (a) asialoglycan, (b) monosialylated biantennary, (c) disialylated biantennary and (d) trisialylated triantennary oligosaccharide markers (see below) are denoted.The position of the isomaltotriose internal marker is also indicated.

Lower panel: Elution profiles of defined oligosaccharide standards. Elution positions of individual complex type-oligosaccharide markers with or without fucose substitutions were determined. The structures of these glycan markers are described schematically on the left side. Fucose core substitution is represented by a short projection marked F and sialic acid terminal residues are represented by a shadowed circle. Under the conditions used, all asialoglycans elute within a narrow range (32-37 min). This group is represented by the biantennary-fucosylated asialoform.

Incubation of purified rHuAChE with the radiolabeled NeuAc donor (CMP-NeuAc) in the presence of 2,6 α–sialyltransferase (α2,6ST, EC2.4.99.1, also named ST6Gall (Tsuji *et al.*, 1996) results in the addition of NeuAc residues to rHuAChE (Fig. 26A). Maximal sialylation was reached after about 2 hrs, at an incorporation of 1.8±0.3 moles NeuAc/mole acceptor rHuAChE (Fig. 26A). Since direct sialic acid measurement indicated that HEK-293-generated rHuAChE

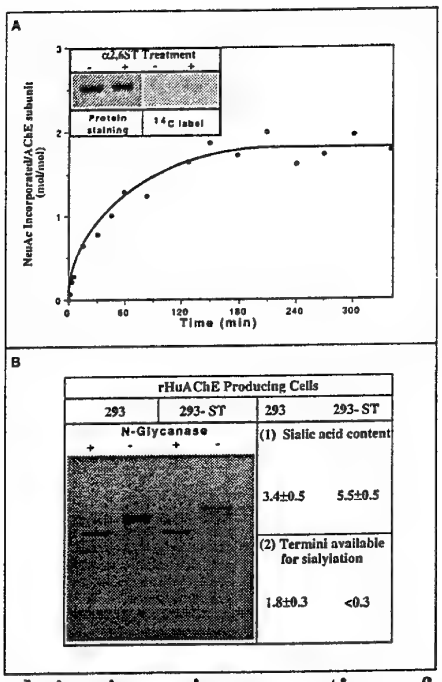

Fig. 26. *In-vitro* and *in-vivo* incorporation of sialic acid residues into rHuAChE

(A) *In-vitro* treatment of rHuAChE with 2.6 ST . Kinetics of incorporation of ^{14}C-labeled CMP-NeuAc into purified rHuAChE. The cpm values were corrected for background TCA-precipitable radioactivity observed at time 0. Inset: SDS-PAGE before and after 3 hours incubation in the presence of 2,6-ST. Commassie blue stain (left) and autoradiograph (right) of the same gel is shown. (B) Sialic acid occupancy of rHuAChE produced in HEK-293 cells and HEK-293 cells coexpressing the rat α 2,6ST gene. Pure preparations of rHuAChE produced by HEK-293 cells or α2,6ST engineered HEK-293 cells, before and after N-Glycanase treatment were analyzed by SDS-PAGE (left panel). The state of sialylation of the two preparations of rHuAChE was evaluated by: (1) Direct determination of sialic acid content by the thiobarbituric acid method and (2) Determination of termini (according to the method described in panel A).

contains 3.4±0.5 moles/enzyme subunit (Fig. 26B, right panel), the total amount of sialic acid following *in-vitro* incorporation (5.2±0.5) is close to that expected for full sialic acid occupancy of the three biantennary N-glycans associated with rHuAChE.

Sialylation of Recombinant HuAChE in HEK-293 Cells is Influenced by its Level of Expression. The partial sialylation of rHuAChE produced in HEK-293 cells may be a result of either endogenous sialidase activity which removes some of the sialic acid moieties (Drzeniek, 1973; Corfield and Schauer,1982; Gu *et al.*, 1997) or of inefficient sialylation of the recombinant product.

To distinguish between these two possibilities, we measured the level of sialylation in rHuAChE produced by two HEK-293 cell lines which exhibit a 20-fold difference in the level of expression

of the recombinant enzyme. Preparations of pure rHuAChE generated by "high" (50U/ml/24Hr) and "low" (3U/ml/24Hr) rHuAChE producer 293 cell clones were assayed for ^{14}C-NeuAc incorporation. It was found that rHuAChE from the "high" producer clone allowed incorporation of 1.8 ±0.3 NeuAc residues/AChE subunit, and rHuAChE from the "low" producer clone, displayed incorporation of only 0.5±0.1 NeuAc residues/subunit (Fig. 27B). SDS-PAGE analysis of pure rHuAChE generated by "high" and "low" producer 293 cell clones revealed that both enzymes possess similar electrophoretic migration profiles before or after N-glycanase treatment (Fig. 27A) suggesting that the overall glycosylation pattern is not affected by the rate of expression of the recombinant polypeptide. Yet, it should be noted that rHuAChE from the low producer (before N-glycanase treatment) exhibits a slightly slower mobility, consistent with its increased level of sialic acid content.

Since terminal sialylation affects the circulatory retention of rHuAChE (Kronman *et al.*, 1995), we used this indirect but sensitive pharmacokinetic assay to determine whether the dissimilarity in sialic acid content of rHuAChE from the "low" and "high" producer clones is reflected by a coinciding differential circulatory clearance. Figure 27C shows that rHuAChE synthesized by the "low producer" clone is retained longer in the circulation than rHuAChE generated by the "high producer" clone. Notably, the circulatory half-life of the "low" producer enzyme, in the second (slow) phase of the clearance curve, described by the $t_{1/2}\beta$ value, was significantly higher (133±13 minutes) than that of the "high" producer enzyme (80±4 minutes, Table 14). This result is in accordance with the ^{14}C incorporation studies which established that in the "low" producer rHuAChE more glycan termini are occupied by sialic acid residues (Fig. 27B). If cellular sialidase activity were responsible for sialic acid trimming, then rHuAChE generated by a low-level expressor clone would have displayed less terminally sialylated glycans than rHuAChE generated by a high-level expressor clone and consequently also shorter residence time. These results, therefore, strongly favor the idea that partial sialylation of HEK-293 generated rHuAChE observed in "high" producer clones is due to inefficient sialylation rather than sialidase activity.

Terminal glycan sialylation, which occurs in the *trans* -Golgi apparatus, is influenced by the residence time of the substrate glycoprotein in this compartment and by the intracellular sialyltransferase concentration (Monica *et al.*, 1997). In previous studies, we have shown that rHuAChE expressed in HEK-293 cells traverses rapidly the Golgi compartments (Kerem *et al.*,

1993) yet addition of the KDEL endoplasmic reticulum (ER) retention sequence to the C-terminus of rHuAChE, results in its sequestration in the Golgi (Velan *et al.*, 1994). However, the KDEL-modified rHuAChE, generated in a "high" producer clone (60U/ml/24h) exhibited profiles indistinguishable from that of wild type rHuAChE, in either SDS-PAGE (not shown) or circulatory clearance (Fig. 27C). Thus, the undersialylated state of the rHuAChE N-glycans was not redressed by simply altering its Golgi residence time by KDEL appendage. Taken together, the data indicate that undersialylation of rHuAChE produced by high level expressor clones, is a consequence of a quantitative limitation of endogenous sialyltransferases. Indeed, examination of sialyltransferase activity levels in HEK-293 cells (Fig. 28, inset) indicated that these are at least 20-fold lower than those found in cells of hepatic origin (Paulson *et al.*,1989; Paulson and Colley, 1989) which are known to promote efficient sialylation of glycoproteins.

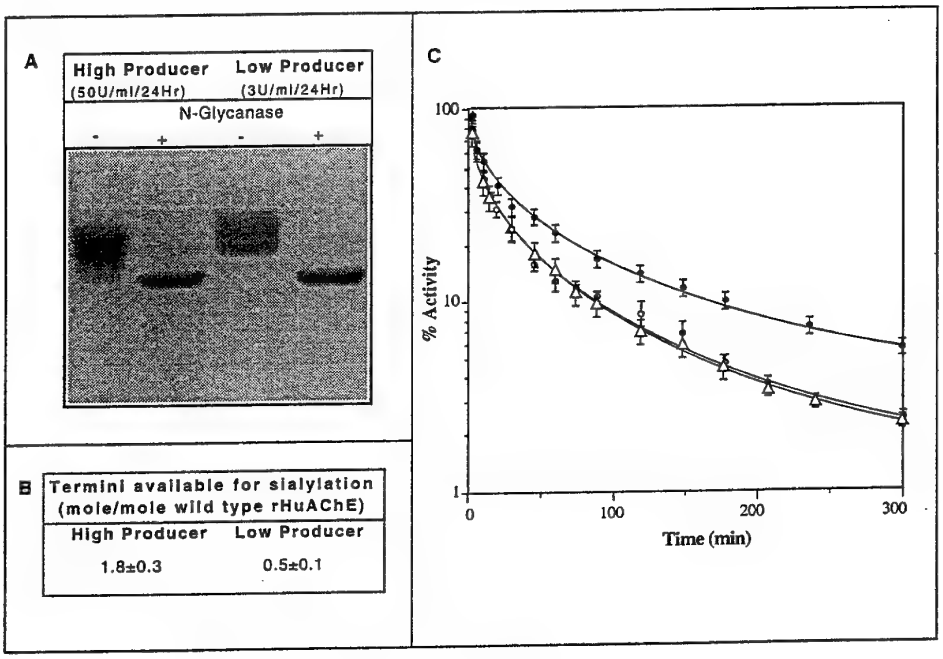

Fig. 27. Comparison of enzymes secreted from "low"and "high" producer HEK-293 cell clones. Recombinant enzyme was purified from stably transfected HEK-293 clones expressing high levels of wild type rHuAChE (50U/ml/24hr), high levels of rHuAChE-KDEL (60U/ml/24hr), and low levels of wild type rHuAChE (3U/ml/24hr). **A.** SDS-PAGE of wild-type rHuAChE nontreated or treated with N-glycanase. **B.** Evaluation of the sialic acid occupancy of rHuAChE from the two wild type clones (see Experimental Procedures). **C.** Circulation clearance profile of: wild-type rHuAChE generated by a "low" (closed circles) producer clone, wild-type rHuAChE generated by a "high" producer (open circles) clone, and rHuAChE-KDEL produced by "high" producer clone (open triangles). Values represent average of residual AChE activity determined for three independent experiments.

Table 14: Pharmacokinetic parameters of rHuAChEs expressed in HEK-293 cells, differing in their sialic acid content

Production Level (1)	Sialylation Modulation		Pharmacokinetic Parameters(4)	
	In vitro (2)	*In vivo* (3)	B(%)	$t_{1/2}$ (min)
High	-	-	**25±1.5**	**80±4**
Low	-	-	**37±5**	**133±13**
High	+	-	**37±2**	**138±14**
High	-	+	**42±2**	**129±9**

(1) Production level of rHuAChE (High = 50U/ml/24h; Low = 3U/ml/24h). (2) rHuAChE purified from high producer cell clone incubated in the presence of commercial 2,6 α-sialyltransferase. (3) Enzyme purified from HEK-293 cell lines cultures producing high levels of rHuAChE and stably transfected with the rat 2,6 α-sialyltransferase. (4) Clearance profiles conform with the biphasic elimination curve of the form: $C(t) = Ae^{-k\alpha t}+Be^{-k\beta t}$. Pharmacokinetic data refers to the B (slow) phase. In the fast phase (A), all k values were within 8-9 $x10^{-2}min^{-1}$.The fraction of enzyme cleared during the fast phase (A), was within the range of 63-74% as is reflected by the complementary B values (A+B=100). $t_{1/2} = \ln 2/k\beta$.

Engineering Cells Expressing Elevated Levels of 2,6 α-sialyltransferase. Since HEK-293 cells are limited in their sialylation ability, and rHuAChE produced by these cells can serve as a target for addition of sialic acid residues via α2,6ST activity (Fig. 26), we decided to increase the level of rHuAChE N-glycan sialylation by expressing a heterologous α2,6ST gene into cells producing high levels of rHuAChE.

A cDNA coding for ß-galactoside α 2,6-sialyltransferase was cloned by PCR amplification from rat liver cDNA. The α2,6ST sequence, spanning the entire coding segment, was confirmed by comparison to the published rat α2,6ST sequence (Weinstein *et al.*, 1987). Sequencing revealed that the cloned gene represents the liver specific version of α2,6 ST, by virtue of the characteristic cysteine residue at amino acid position 123 (Fig. 28). This α2,6 ST form is retained in the Golgi compartment (Ma *et al.*, 1997) and thereby possesses an increased ability to act upon cellular glycoproteins. The alternative α2,6ST form, which harbors a tyrosine residue at that position, should be secreted into the medium (Ma *et al.*, 1997) and therefore would not be suitable to our purpose.

The α2,6ST cDNA was cloned into an expression vector which carries the hygromycin resistance gene and used to transfect HEK-293 cells which produce and secrete high levels of rHuAChE. Selection for cells stably expressing the α2,6ST gene, was based on hygromycin resistance since

rHuAChE producing cells harbor an integrated copy of the neomycin resistance gene, which was utilized for selecting rHuAChE expressor cells (Kronman *et al.*, 1992). Stably transfected cells were subjected to limiting-dilution cloning, to allow isolation of pure cell clones expressing the α2,6ST gene.

Cell extracts of an individual α2,6ST expressor cell clone (293-AChE-ST) were prepared and tested for sialyltransferase activity. A significant increase in sialyltransferase activity over the background level (at least 20-fold higher) was observed in the 293-AChE-ST cells (Fig. 28, inset). In line with the known substrate specificity of the α2,6ST enzyme (Weinstein *et al.*,1982a; Weinstein *et al.*,1982b), asialofetuin (which contains Gal ß1-4 GlcNAc groups on N-linked oligosaccharides) but not asialomucin (which contains GalNAc groups found as O-linked oligosaccharides) could serve as a NeuAc acceptor in the assay.

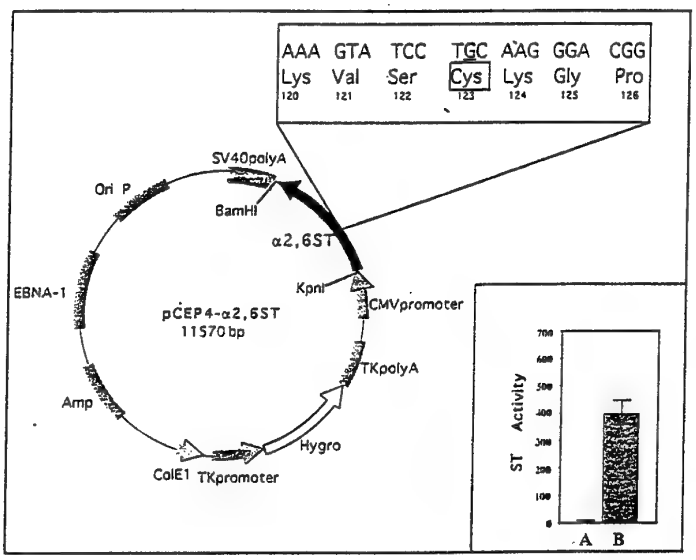

Fig. 28. The ß-galactoside α 2,6-sialyltransferase expression system. Plasmid pCEP4-α2,6ST carrying the cDNA of the "cys" version (Ma *et al.*, 1997) of rat α2,6ST. Inset shows the sialyltransferase activity (expressed as pmoles NeuAc transferred/hr/mg protein) in naive (A) or α2,6ST transfected (B) HEK-293 derived cell lines. Results represent the average activity obtained in triplicate experimental groups and are normalized to the total protein content of the cellular extract.

To determine whether or not α2,6ST activity of the transfected cells is compromised by the concomitant expression of rHuAChE, we compared the α2,6ST levels of two cell lines: HEK-293 cells transfected only with the α2,6ST gene and the previously described cells (293-AChE-ST) which coexpress both the α2,6ST and AChE genes. Sialyltransferase activity levels in these cell

clones was found to be similar, confirming that AChE production has no effect on the levels of production of α2,6ST (Fig. 28, inset). Furthermore, rHuAChE levels of cells coexpressing the α2,6ST gene together with the AChE gene was similar to that of cells transfected with the AChE gene only, determining that the ability to produce AChE was not affected by introduction of the α2,6ST gene and/or by the acquisition of hygromycin resistance.

Biochemical Characteristics of Recombinant HuAChE Produced by 2,6 α-sialyltransferase Engineered Cells. The activity and reactivity of the recombinant AChE towards various ligands were not affected by introduction of the α2,6ST gene. K_m and k_{cat} values for acetylthiocholine are 0.12mM and $3.9x10^{-5}$ x min^{-1} respectively. Inhibition constants (Ki) for the specific inhibitors edrophonium, propidium, decamethonium and BW284C51 are 0.4μM, 0.2μM, 2μM and 2.5μM respectively. These values are similar to those determined for the rHuAChE produced by HEK-293 cells which do not express the heterologous α2,6ST gene (Ordentlich *et al.*, 1995). When subjected to SDS-PAGE analysis, the 293-AChE-ST product displays a slower electrophoretic mobility than rHuAChE produced in nonmodified HEK-293 cells (Fig. 26B, left panel), consistent with an increased level of sialic acid content. Except for the apparent difference in mobility, the enzyme products of 293-AChE-ST cells and nonmodified HEK-293 cells exhibit a similar electrophoretic profile which consist of the two characteristic bands (Velan *et al.*, 1993) representing rHuAChE glycoforms which are sensitive to treatment with N-glycanase. This suggests that the overall glycosylation pattern of rHuAChE has not been affected by coexpression of the α2,6ST gene.

The sialic acid content of rHuAChE purified from 293-AChE-ST cells was found to correspond to a NeuAc/AChE molar ratio of 5.5±0.5 (Fig. 26B, right panel). In the same analyses, rHuAChE purified from HEK-293 cells non-transfected with α2,6ST exhibited a sialic acid content equivalent to a NeuAc/AChE molar ratio of 3.4±0.5. Thus, AChE produced by cells coexpressing a heterologous α2,6ST gene, are sialylated to a greater extent than that produced by nonmodified HEK-293 cells, reflecting the acquisition of a higher sialylation potential by the α2,6ST transfected cells. Notably, the increase in sialic acid content of the α2,6ST engineered cells product (1.9 moles NeuAc/mole AChE) is in very good agreement with the number of sialic acid residues which can be added *in vitro* to rHuAChE produced by HEK-293 cells not transfected with the α2,6ST

gene (Fig. 25). Moreover, when rHuAChE produced by the 293-AChE-ST cells was subjected to an *in vitro* incorporation assay (Fig. 26B, right panel), only marginal levels of NeuAc were accepted (less than 0.3 moles NeuAc/mole AChE compared to the 1.8±0.3 moles NeuAc/mole AChE incorporated into rHuAChE produced in HEK-293 cells). These results suggest that the α2,6ST engineered cells promote efficient *in vivo* sialylation of rHuAChE.

The glycans associated with rHuAChE produced by 293-AChE-ST cells were further subjected to direct oligosaccharide profiling by HPAEC-PAD and compared to the profile of rHuAChE produced in nonmodified HEK-293 cells (Fig. 29A,B, Table 15). As was noted for rHuAChE produced in HEK-293 cells not transfected with α2,6ST, the glycans associated with rHuAChE produced by 293-AChE-ST cells are predominantly of the biantennary type. However, the distribution of the various N-glycan sialoforms in the two rHuAChE preparations was markedly altered.

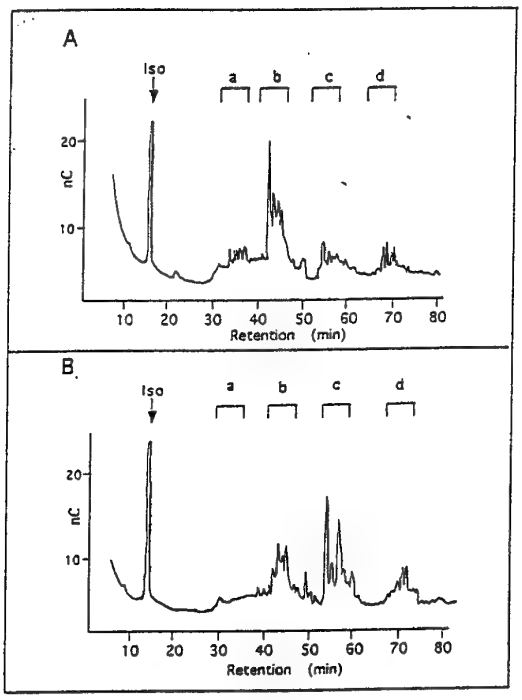

Fig. 29. Comparison of HPAEC-PAD profiles of carbohydrates released from rHuAChE produced by HEK-293 cells and α2,6ST engineered HEK-293 cells
HPAEC-PAD carbohydrate profiles of rHuAChE produced by HEK-293 cells (A) or α2,6ST engineered HEK-293 cells (B). The letters a, b, c and d denote the elution time regions of nonsialylated, monosialylated, disialylated and trisialylated glycans respectively, as described in the legend to Figure 25. The peak denoted Iso, arises from the internal marker isomaltotriose which was added to every sample. See Table 15 for the relative percent-area of each glycan in the chromatogram.

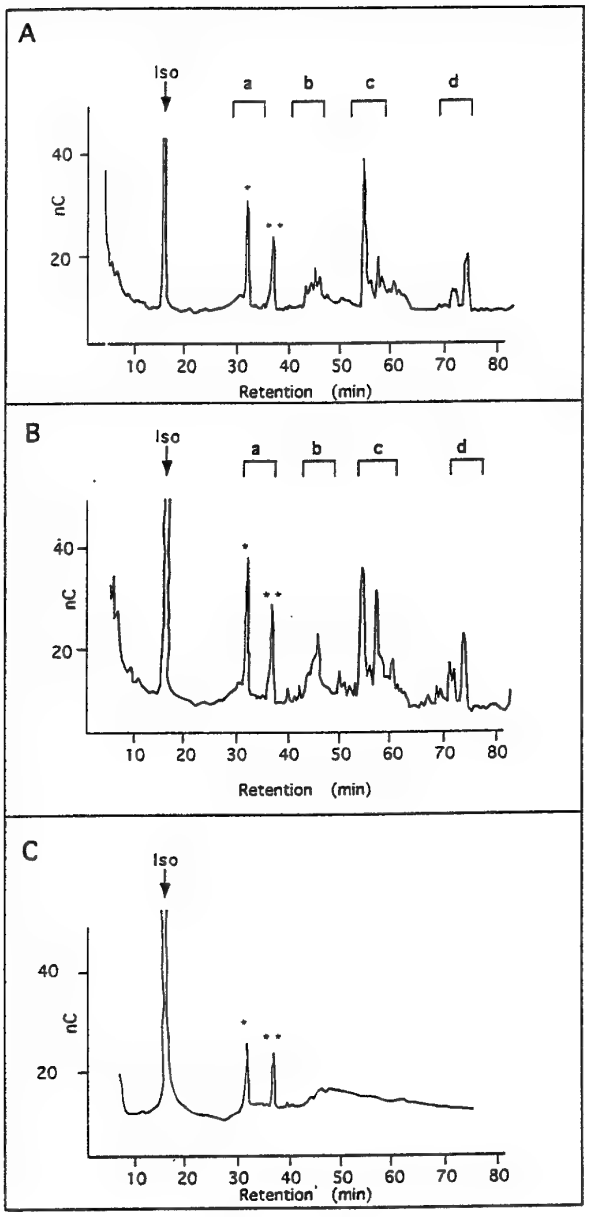

Fig. 30. Comparison of HPAEC-PAD profiles of carbohydrates released from different rHuAChE preparations following *in-vitro* treatment with α2,6ST. Purified rHuAChE (100 μg) produced by HEK-293 cells (A), or α2,6ST engineered HEK-293 cells (B), were subjected to treatment with commercial rat liver α2,6ST in the presence of excess CMP-NeuAc. The letters a, b, c and d denote the elution time regions of nonsialylated, monosialylated, disialylated and trisialylated glycans respectively, as described in the legend to Figure 25. Integration of the various peaks was used for calculating the relative percent-area of each glycan in Table 15. The peaks denoted by one or two asterisks (* or **) represent residual free NeuAc and CMP-NeuAc (NeuAC donor) which originate from the *in-vitro* α2,6ST reaction mix, as established by HPAEC-PAD of appropriate standards described in panel C. These peaks do not represent rHuAChE associated glycans and were not included in the calculations of peak areas in Table 15.

Table 15: Quantitative analysis of HPAEC percent-area of various N-glycan forms of rHuAChE

Glycan form	Source of rHuAChE			
	HEK-293	HEK-293-ST	HEK-293 + *in vitro* α2,6ST	HEK-293-ST + *in vitro* α2,6ST
(a) asialylated	15.4	4.7	4.2	5
(b) monosialylated	59.6	38.7	34.2	33.7
(c) disialylated	15.8	42.6	47.5	46.3
(d) trisialylated	9.2	14	14	15

The normalized integrated peak areas from Fig. 29 (columns 1 and 2) and Fig. 30 (columns 3 and 4) are expressed in percent (100% = total area under the curve). Note the similarity of the values in columns 2, 3 and 4.

While the biantennary glycans of rHuAChE from non-α2,6ST transfected HEK-293 cells exhibit a percent-area distribution of nonsialylated:monosialylated:disialylated forms of approximately 15: 60: 16, the respective distribution in rHuAChE produced by 293-AChE-ST cells is 5: 39: 43 (Table 15). Thus, rHuAChE produced by 293-AChE-ST cells, exhibits a significantly lower level of nonsialylated and monosialylated biantennary structures and a concomitant higher level of fully sialylated biantennary N-glycan forms. In fact, the relative percent-area of the fully sialylated biantennary form in cells coexpressing the α2,6ST gene is about three times higher than in nonmodified cells. In addition, a small increase in trisialylated forms is also displayed in rHuAChE of 293-AChE-ST cells (14% of total area, as opposed to 9% in rHuAChE of nonmodified HEK-293 cells).

Most notably, a similar alteration in the glycan chromatographic profile was observed when the rHuAChE product from nonmodified HEK-293 cells was subjected to *in-vitro* sialylation by incubation with pure α2,6ST. Following such a treatment, the percent-area distribution of nonsialylated:monosialylated:disialylated forms of the biantennary N-glycans was approximately 4: 34: 47 (compare Fig. 30A to Fig. 29A, see also Table 15). These results clearly indicate that the genetic modulation of rHuAChE producer cells by introduction of a heterologous α2,6ST gene promotes highly efficient sialylation. Moreover, when the rHuAChE product of 293-AChE-ST

cells was also subjected to *in-vitro* sialylation (Fig. 30B), the glycan pattern remained virtually unchanged (compare Fig. 30B to Fig. 29B, see also Table 15) suggesting that *in-vivo* sialylation led to almost full occupation of glycan termini that are available for sialic acid addition. Yet, a certain fraction of the biantennary N-glycans remain in the monosialylated form, suggesting that some of the N-glycan termini are refractive to sialylation. This fraction, representing approximately 20% of N-glycan termini, is observed both in the *in-vitro* oversialylated enzyme as well as in the *in-vivo* (produced by α2,6ST engineered cells) enzyme, suggesting that the inability to undergo additional sialylation is due to some structural aspect of the corresponding N-glycan termini (see Discussion).

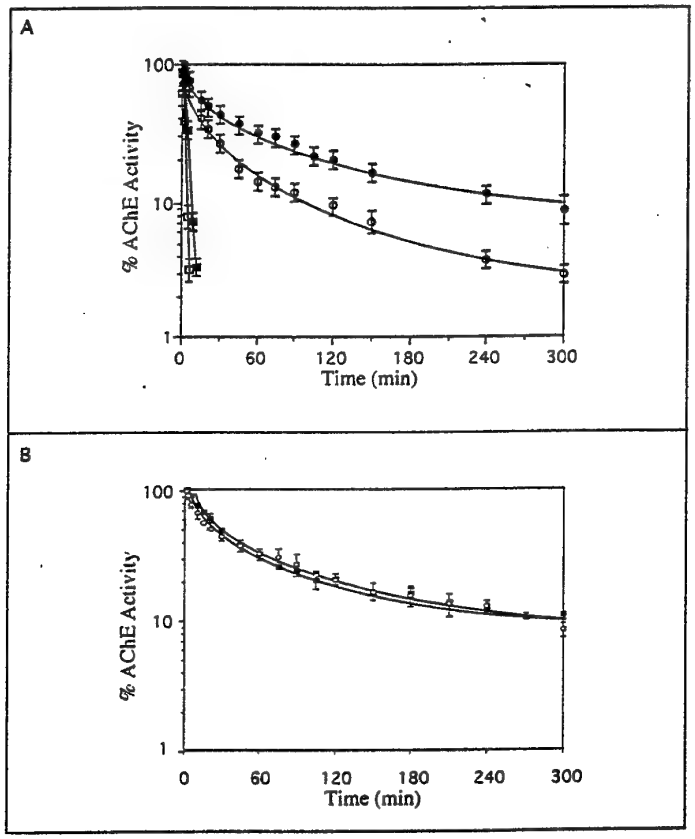

Fig. 31. Comparison of circulatory clearance rate of partially sialylated rHuAChE and oversialylated forms of rHuAChE. (A) Clearance profile of rHuAChE generated by 2,6ST engineered HEK-293 cells [before (full circles) or after (full squares) sialidase treatment) compared to rHuAChE generated by nonmodified HEK-293 cells [before (empty circles) or after (empty squares) sialidase treatment). (B) Clearance profile of rHuAChE generated by α2,6ST engineered HEK-293 cells (empty circles) compared to rHuAChE generated by HEK-293 cells and subsequently oversialylated by *in vitro* treatment with commercial α2,6ST (full squares).

Recombinant HuAChE Produced by α2,6ST Engineered Cells Displays an Enhanced Circulation Residence. Purified enzyme isolated from 293-AChE-ST cells was administered to mice and the pharmacokinetics profile was determined (Fig. 31A and Table 14). A significant enhancement of the circulatory retention, reflected by the $t_{1/2}ß$ which describes the slow phase half-life of the enzyme in circulation (129±9 minutes for the 293-AChE-ST enzyme, compared to 80±4 for the undersialylated enzyme) was observed. When subjected to *in-vitro* sialidase treatment, the 293-AChE-ST enzyme was cleared rapidly from the circulation, in a manner similar to sialidase treated enzyme of the regular HEK-293 cells (Fig. 31A), proving that the enhanced ability of the *in-vivo* oversialylated enzyme to be retained in the circulation stems from its improved NeuAc content. The pharmacokinetic profile of rHuAChE produced by the α2,6ST engineered cells was found to be virtually identical to that of *in-vitro* sialylated rHuAChE from nonmodified HEK-293 cells (Fig. 31B, Table 14) suggesting that the genetic manipulation of the HEK-293 cells glycosylation machinery by introduction of a heterologous glycosyltransferase, is highly efficient.

DISCUSSION

The Structure of Glycans of rHuAChE Expressed in Human Kidney 293 Cells

Cholinesterases differ in the number of their potential N-glycosylation sites; human and murine acetylcholinesterases carry three such sites (Massoulie *et al.*, 1993), the bovine serum acetylcholinesterase carries four sites for N-glycosylation (our unpublished results), while the human butyrylcholinesterase carries nine N-glycosylation consensus sequences (Lockridge *et al.*, 1987). Recently, studies addressing the role of N-glycans as well as other factors in determining the circulatory residence of cholinesterases from different sources, provided pertinent information on the structural characteristics of cholinesterase-associated glycans (Kronman *et al.*, 1995; Saxena *et al.*, 1997; Saxena *et al.*, 1998). Cholinesterases from various sources (Saxena *et al.*, 1998) were found to differ by a large number of variables, such as subunit oligomerization, N-glycan branching and oligosaccharide sialylation and it was therefore difficult to evaluate conclusively the contribution of N-glycan content and structure to clearance.

In the present study, we demonstrate that the major proportion of the N-glycans associated with rHuAChE expressed in HEK-293 cells are of a uniform size (Fig. 24A), belonging to the biantennary type as confirmed by gel permeation chromatography and HPAEC-PAD (Figs. 24 and 25 and Table 15). This finding is in accordance with the known propensity of HEK-293 cells to generate glycoproteins bearing complex type biantennary glycans (Smith *et al.*, 1992; Yan *et al.*, 1993). We have noted previously that only a very minor proportion of the rHuAChE molecules may contain O-glycans (Kronman *et al.*, 1995). This is also reflected, in this study, by the gel permeation chromatogram of rHuAChE associated glycans (Fig. 24A) which fails to detect any significant O-glycan-characteristic peaks in the low size range (<5 glucose units, Patel *et al.*, 1993). The structural analysis reported in the present study, establishes that though most of the N-glycan forms (>85%) exhibit negatively charged sialic acid, the major proportion of these glycans contain only one sialic acid residue per glycan unit, indicating an overall undersialylation of the N-glycans (Fig. 25 and Table 15). This limitation in sialic acid content can be relieved by adding sialic acid residues through the activity of 2,6 α-sialyltransferase, in which a significant transition of the major glycan fraction from the monosialylated to the disialylated form occurs, as attested by HPAEC-PAD analysis (Figs. 29,30).

The relatively high degree of homogeneity noted for the N-glycans released from rHuAChE produced by HEK-293 cells (Fig. 24) is in contrast to the rather heterogeneous nature observed for the N-glycans associated with murine recombinant AChE produced in the same cell line (Saxena *et al.*, 1998). This difference may be a consequence of amino acid differences, as well as variations in cell growth conditions, enzyme harvesting regime and storage conditions of the pure protein, all of which are known to affect the quality of the glycans.

Relationship Between the Extent of rHuAChE Glycosylation and Sialylation and its Circulatory Life-time. Clearance of proteins from the circulation may involve one or multiple removal systems which interact either with epitopes within the protein itself or with elements generated by post-translation modifications such as oligosaccharide appendages (Krieger and Herz, 1994); Rao Thotakura *et al.*, 1994; Narita, *et al.*, 1995b; Szkudlinski *et al.*, 1995). Cholinesterases are attributed a therapeutic potential by virtue of their bioscavenging ability. Effective exploitation of this potential requires that exogenously administered enzyme, be retained in the circulation for a considerable length of time.

However, recombinant HuAChE is removed from the circulation more rapidly than native serum-derived cholinesterases such as fetal bovine serum AChE and human serum butyrylcholinesterase (Kronman *et al.*, 1995). This differential behavior could be a consequence of the divergence in the primary amino acid sequences of these enzymes or more likely due to some post-translation modifications

To be able to discern the various parameters determining the fate of AChE in the circulation, one should rely on a system where the various AChEs are derived from the same source and each of the potential variables on the molecule can be modified separately and sequentially (eg. N-glycosylation, oligomerization, charge). We have developed such a system based on comparison of various mutated forms of recombinant AChEs, all expressed in HEK-293 cells. We have shown (Kronman *et al.*, 1995) that a mutated version of rHuAChE containing only one N-glycosylation site, as opposed to three N-glycosylation sites in the wild type enzyme, was cleared rapidly from the circulation, suggesting the involvement of N-glycans in circulatory residence. However, examination of overglycosylated rHuAChE mutants, containing four or five utilized N-glycosylation sites, revealed that the number of N-glycan appendages *per se* does not contribute to

circulatory longevity. Evaluation of an array of rHuAChE mutants differing in their sialic acid content allowed us to establish that an inverse-linear correlation exists between the number of non-sialylated N-glycan termini and circulatory residence of rHuAChE expressed in HEK-293 cells (Kronman *et al.*, 1995). In the present study, we extend these observations and show that addition of sialic acid residues to N-glycan termini of rHuAChE by coexpression of recombinant α2,6ST in HEK-293 cells, indeed results in an increased circulatory residence ($t_{1/2}\beta$ ~130 min, Fig. 31 and Table 14). Notably, the extended circulatory half-life exhibited by the oversialylated version of rHuAChE coincides with the value predicted for maximal loading of rHuAChE with sialic acid residues. This value was calculated from the inverse-linear relationship between circulatory residence and sialic acid-unoccupied glycan termini of rHuAChE expressed in HEK-293 cells (Kronman *et al.*, 1995).

In vitro treatment of the rHuAChE with commercial α2,6ST, also results in extended circulatory residence and the value obtained is very similar to that of rHuAChE produced by the α2,6ST-engineered HEK-293 cells establishing that sialylation within the modified cells is highly efficient. The fact that the extended residence time now coincides with the predicted value for maximal sialic acid loading, seemingly indicates that an upper limit for sialic acid incorporation into HEK-293 derived rHuAChE, has been reached. Yet, determination of NeuAc suggests that the sialic acid content (~5.5 sialic acid residues/rHuAChE subunit, Fig. 26B) of the oversialylated versions of rHuAChE generated either by the *in-vitro* or *in-vivo* action of α2,6ST, is somewhat lower than that expected for complete sialic acid capping of biantennary and triantennary N-glycan termini. This observation raises the possibility that though sialylation is highly efficient, a minor fraction of N-glycans remain refractive to sialylation. Furthermore, HPAEC-PAD analysis revealed that some of the N-glycan termini of the oversialylated rHuAChE preparations are indeed only partially sialylated (Figs. 29,30 and Table 15). This subset of glycan termini, which are refractive to sialylation, may provide an explanation for the fact that even oversialylated rHuAChE is cleared relatively more rapidly than native serum-derived forms of ChEs.

The observation that not all N-glycan termini may serve as acceptors for sialic acid addition, can be explained by local constraints which do not allow access to sialyltransferase (Gu *et al.*, 1997; Yeh and Cummings, 1997). Alternatively, this fraction of N-glycan termini may carry a terminal residue which precludes NeuAc capping. Elucidation of the nature of the nonsialylated form of the

N-glycans is presently under study.

Importance of Endogenous Glyosyltransferases in Cell Lines Used for High-level Expression of Recombinant Proteins. A recently proposed mathematical model of glycoprotein sialylation in the Golgi compartment has suggested that although cellular proteins are not expected to be undersialylated due to limited availability of sialyltransferase, biotechnological systems aimed at high production levels of recombinant proteins may give rise to undersialylated glycoproteins, by virtue of overloading the cellular glycosylation machinery with protein bulk (Monica *et al.*, 1997). In a recent study, analysis of N-glycans associated with overexpressed secreted recombinant α-galactosidase A in CHO cells, revealed that most of these were incompletely galactosylated and/or sialylated (Matsuura *et al.*,1998). The authors suggested that the limiting step in recombinant glycoprotein overexpression in this cell system may be the relative inefficiency of *trans* -Golgi residing glycosyltransferases. Here we show, by comparing sialylation levels of rHuAChE expressed in HEK-293 cell lines differing in the amount of rHuAChE secretion (~ 20-fold) that a higher content of sialic acid and a longer circulatory retention were indeed associated with low production levels of rHuAChE (Fig. 27, Table 14). An attempt to correct the undersialylation of rHuAChE expressed at high levels by alteration of its Golgi residence time (KDEL retention signal appendage to rHuAChE) did not result in an extended circulatory life-time of the enzyme. Yet, by genetically engineering the cells to express a heterologous α2,6ST gene, we show that it is possible to correct the relative paucity of sialyltransferase activity in the HEK-293 without affecting the yield of the recombinant product.

Since expression systems tailored for overproduction of recombinant proteins entail a concomitant compromise in post-translation modification efficiency, identification of the limiting factors and their provision by genetic modification may prove to be the method of choice for establishment of production systems in which the protein of interest is adequately processed. Several reports have documented the use of the α2,6ST gene to alter the properties of Chinese hamster ovary (CHO) and baby-hamster kidney (BHK) cells which lack the enzyme α2,6ST and therefore produce sugar chains terminating in the NeuAcα2,3Gal linkage (Grabenhorst *et al.*, 1995; Lee *et al.*, 1989; Minch *et al.*, 1995). In this study, we show that the 2,6ST *in-vivo* oversialylation system could provide a useful approach for extending the circulatory residence of recombinant proteins which are cleared

via removal pathways involving recognition of terminal galactose residues. Similar approaches may enable promotion of circulatory longevity by modulating other limiting glycosyltransferases influencing pharmacokinetic performance.

IX. CONCLUSIONS

In our studies the reactivity of a score of HuAChE mutants towards various covalent and noncovalent ligands, including organophosphorus chemical warfare agents, has been investigated. Relative to the wild type enzyme, the rates of phosphylation by some OP-agents can be enhanced through substitution of residues Phe 955, Phe297, Tyr337 and Phe338. In addition, the postinhibitory behavior of these phosphyl-HuAChE conjugates was examined with respect to reactivation and aging. We find that the aging process is retarded by replacements of aromatic residues Trp86, Phe338, the PAS residue Asp74 as well as by substitution of the H-bond network elements Tyr133, Glu202 and Glu450. However mutation of the later reduce also the rates of phosphylation and of reactivation of the phosphylated enzymes. These data provide direction for the design of an optimal OP-scavenger, based upon engineered HuAChE. Such scavenger enzyme should retain full reactivity toward organophosphorus agents combined with slowed aging and effective reactivation processes. Therefore replacements of residues which reduce the rates of aging as well as those of phosphylation and reactivation should be avoided. Our results indicate that an efficient scavenger may contain a substitution, or a combination of substitutions, of residues Asp74, Trp86, Phe295, Phe297, Tyr337, Phe338. Choice of the proper amino acid replacement and the combination of such replacements, for optimizing the OP-scavenging properties of the HuAChE enzyme, is our challenge for future study.

The use of rHuAChE as a therapeutic bioscavenger of organophosphate agents, is impeded by its relatively rapid clearance from the circulation, as compared to native serum-derived cholinesterases. Effective exploitation of the bioscavenging potential of rHuAChE therefore requires the generation of a modified version of the enzyme exhibiting extended circulatory residence.

In previous studies, we have found that though both N-glycosylation in itself as well as sialic acid content contribute to rHuAChE circulatory longevity, an inverse-linear correlation exists between the number of non-sialylated N-glycan termini and circulatory residence of rHuAChE, underlining the major role of sialylation *efficiency* in determining the pharmacokinetic properties of rHuAChE. In the present study, we indeed demonstrate that by *in-vitro* treatment of rHuAChE

with sialyltransferase, we were able to improve the sialic acid loading of the N-glycan termini and to extend the circulatory life-time of the enzyme in the circulation.

In light with these findings, we isolated the rat 2,6 sialyltransferase gene and subsequently introduced it into cells we have previously engineered to express high levels of rHuAChE. Such genetic modification (transfection with 2,6 sialyltransferase gene) of the rHuAChE producer cells indeed corrected the limitation in rHuACHE sialylation. The rHuAChE isolated from these genetically modified cells exhibited an increased sialic acid content and more significantly an extended circulatory residence. Our approach clearly demonstrates the feasibility for manipulation of intracellular post-translation pathways and thereby generation of pharmacologically improved bioscavenger. However, circulatory retention of rHuAChE produced by sialyltransferase-engineered cells is still lower than that of serum-derived cholinesterases, indicating that additional post translation factors have to be manipulated. We are currently investigating the nature of these factors in order to obtain the optimal pharmacological properties of the recombinant human AChE bioscavenger.

REFERENCES

Aldridge W.N., and Reiner E. (1972). *Enzyme Inhibitors as Substrates*, Elsevier, Amsterdam.

Amitai, G. Ashani, Y., Gafni, A. and Silman, I. (1982). Novel pyrene-containing organophosphates as fluorescent probes for studying aging-induced conformational changes in organophosphate-inhibited acetylcholinesterase. Biochemistry **21**: 2060-2069.

Andersen, J.S., Svensson, B. and Roepstorff, P. (1996). Electrospray ionization and matrix assisted laser desorption/ionization mass spectrometry: powerful analytical tools in recombinant protein chemistry. Nature Biotech. **14**:449-457.

Ashani, Y., Grunwald, J., Kronman, C., Velan, B., and Shafferman, A. (1994). The role of tyrosine 337 in the binding of Huperzine A to the active site of human acetylcholinesterase. Molec. Pharmacol. **45**:555-560

Ashani, Y., Shapira, S., Levy, D., Wolfe, A.D., Doctor, B.P., and Raveh, L. (1991). Butyrylcholinesterase and acetylcholinesterase prophylaxis against soman poisoning in mice. Biochem. Pharmacol. **41**:37-41.

Ashani, Y., Radic, Z., Tsigelny, I., Vellom, D.C., Pickering, N.A., Quinn, D.M., Doctor, B.P. and Taylor, P.(1995). Amino acid residues controlling reactivation of organophosphonyl conjugates of acetylcholinesterase by mono- and bisquaternary oximes. J. Biol. Chem. **270**:6370-6380.

Ashwell, G., and Harford, J. (1982). Carbohydrate-specific receptors. Ann. Rev. Biochem. **51**:531-554.

Axelsen, P.H., Harel, M., Silman, I., and Sussman, J.L. (1994). Structure and dynamics of the active site gorge of acetylcholinesterase : synergistic use of molecular dynamics simulations and x-ray crystallography. Prot. Sci. **3**:188-197.

Barak, D., Ariel, N., Velan, B.,and Shafferman, A. (1992). Molecular models for human AChE and its phosphonylation products. In: *Multidisciplinary Approaches to Cholinesterase Functions*. (Shafferman A. and Velan B. Eds.),pp. 195-199, Plenum Pub. Co., New York .

Barak, D., Kronman, C., Ordentlich, A., Ariel, N., Bromberg, A., Marcus, D., Lazar, A., Velan, B., and Shafferman, A. (1994). Acetylcholinesterase peripheral anionic site degeneracy conferred by amino acid arrays sharing a common core. J. Biol. Chem. **264**:6296-6305.

Barak, D., Ordentlich, A., Bromberg, A., Kronman ,C., Marcus, D., Lazar, A., Ariel ,N., Velan, B., and Shafferman ,A. (1995). Allosteric modulation of acetylcholinesterase activity by peripheral ligands involves a conformational transition of the anionic subsite. Biochemistry **34**: 15444-15452.

Barak, D., Ordentlich, A., Segall, Y., Velan, B., Benschop, H.P., De Jong, L.P.A. and Shafferman, A. (1997). Carbocation mediated processes in biocatalysts - contribution of aromatic moieties. J.Am.Chem.Soc., **119**: 3157-3158.

Benschop, H.P. and Keijer, J.H. (1966). On the mechanism of ageing of phosphonylated cholinesterases. Biochim. Biophys. Acta. **128**:586-588.

Benschop, H.P., Keijer, J.H.and Kienhuis, H. (1967). On the mechanism aging of phosphorylated cholinesterases. in: *Structure and Reactions of DFP Sensitive Enzymes* (Heilbronn,E. Ed.), pp 193-199, Forsvarets Forskninsanstalt, Stockholm.

Benschop, H.P., Konings, C.A.G., Van Genderen, J. and De Jong, L.P.A. (1984). Isolation, anticholinesterase properties, and acute toxicity in mice of the four stereoisomers of the nerve agent soman. Toxicol. Appl. Pharmacol. **72**: 61-74.

Benschop, H.P. and De Jong, L.P.A. (1988). Nerve agent stereoisomers: analysis, isolation and toxicology. Acc. Chem. Res. **21**:368-374.

Bencsura, A., Enyedy, E. and Kovach, I.M.(1995). Origins and diversity of the aging reaction in phosphonate adducts of serine hydrolase enzymes: what characteristics of the active site do they probe?. Biochemistry **34**: 8989-8999.

Berendsen , H.J.C., Postma, J.P.M., van Gunsteren, W.F., DiNola ,F., and Haak, J.R.(1984). Molecular dynamics with coupling to an external bath. J. Chem. Phys. **81**: 3684-3690.

Berman, H. A., Becktel, W., and Taylor, P. (1981). Spectroscopic studies on acetylcholinesterase : influence of peripheral-site occupation on active-center conformation Biochemistry **20**:4803-4810.

Berman H.A. and Decker M.M. (1986a). Kinetic equilibrium and spectroscopic studies on dealkylation (aging) of alkylorganophosphonyl acetylcholinesterase. J.Biol.Chem. **261**:10646-10652.

Berman, H.A. and Decker, M.M.(1986b). Kinetic, equilibrium and spectroscopic studies on cation association at the active center of acetylcholinesterase: topographic distinction between trimethyl and trimethylammonium sites. Biochem. Biophys. Acta **872**: 125-133.

Berman, H. A., Decker, M. M., Nowak, M.W., Leonard, K.J., McCauley, M., Baker, W.M., and Taylor, P. (1987). Site selectivity of fluorescent bisquaternay phenanthridinium ligands for acetylcholinestrase. Mol. Pharmacol. **31**: 610-616.

Berman, H.A. and Decker, M.M. (1989). Chiral nature of covalent methylphosphonyl conjugates of acetylcholinesterase J.Biol.Chem. **264**:3951-3956.

Björkstén, J., Soares, C,M., Nilsson, O., and Tapia, O. (1994). On the stability and plastic properties of the interior L3 loop in R.capsulatus porin. a molecular dynamics study. Protein Eng. **7**:487-493.

Bourne, Y., Taylor, P. and Marchot, P. (1995). Acetylcholinesterase inhibition by fasciculin: crystal structure of the complex. Cell **83**:503-512.

Broomfield, C.A., Maxwell, D.M., Solana, R.P., Castro, C.A., Finger, A.V. and Lenz, D.E. (1991). Protection by butyrylcholinesterase against organophosphorus poisoning in nonhuman primates. J. Pharmacol. Exp. Ther. **259**:633-638.

Brunger, A.T., Krukowski, A., and Erickson, J.W. (1990). Slow-cooling protocols for crystallographic refinement by simulated annealing. Acta Cryst. **A46**:585-593.

Bucht, G,. Häggström, B., Radic, Z,. Osterman, A., and Hjalmarsson, K.(1994). Residues important for folding and dimerization of recombinant *Torpedo californica* acetylcholinesterase. Biochim Biophys Acta **1209**: 265-273.

Cadogan, J.I.G., Eastlick, D., Hampson, F. and Mackie, R.K. (1969). The reactivity of organophosphorus compounds. Part XXIV. Acidic hydrolysis of dialkyl methylphosphonates. J. Chem. Soc. **B**, 144-146 .

Cascio, C., Comite, C., Ghiara, M., Lanza, G., and Ponchione, A. (1988). Use of serum cholinesterases in severe organophosphorous poisoning. our experience. Minerva Anastesiol. **54**:337-338.

Chambers, H.W.(1992). Organophosphorus compounds: an overview. In: *Organophosphates Chemistry,Fate and Effecs* (Chambers, J.E. And Levi, P.E. Eds.), pp.3-17, Academic Press, San Diego.

Changeux, J.P. (1966). Responses of acetylcholinesterase from torpedo marmorata to salts and curarizing drugs. Mol.Pharmacol. **2**:369-392.

Chait, B.T. and Kent, S.B.H. (1992) .Weighing naked proteins: practical high-accuracy mass measurement of peptides and proteins. Science **257**:1885-1894.

Chatonnet, A. and Lockridge, O. (1989). Comparison of butyrylcholinesterase and acetylcholinesterase. Biochem. J. **260**:625-634.

Chipot, C., Maigret, B., Pearlman, D.A. and Kollman, P.A. (1996). Molecular dynamics potential of mean force calculations: a study of the toluene-ammonium π-cation interactions. J. Am. Chem. Soc. **118**:2998-3005.

Clement, J.G., Rosario, S., Bessette, E. and Erhardt, N. (1991). Soman and sarin inhibition of molecular forms of acetylcholinesterase in mice. Biochemical Pharmacology, **42**:329-335.

Corfield, A.P. and Schauer, R. (1982). Metabolism of sialic acid. in sialic acids- chemistry, metabolism and function. Cell Biology Monographs **10**, Springer Wien, pp. 195-291.

Coyle, J.T., Price, D.L. and DeLong, M.R. (1983). Alzheimer's disease: A disorder of cortical cholinergic innervation, Science **219**:1184-1190.

Cygler, M., Schrag, J. D., Sussman, J. L., Harel, M., Silman, I., Gentry, M. K., and Doctor, B. P. (1993). Relationship between sequence conservation and three-dimensional structure in a large family of esterases, lipases, and related proteins. Prot. Sci. **2**: 366-382.

Datta, A.K. and Paulson, J. C. (1995). The sialyltransferase "sialylmotif" participates in binding the donor substrate CMP-NeuAc. J. Biol. Chem. **270**:1497-1500.

De la Escalera, S.,Backamp, E,O.,Moya, F., Piovant, M, and Jimenez, F. (1990). Characterization and gene cloning of neurotactin a Drosophila transmembrane protein related to cholinesterase. EMBO J. **9**:3593-33601.

Derewanda, U., Brzozowski, A.M., Lawson, D.M. and Derewanda, Z.S. (1992) .Catalysis at the interface: the anatomy of conformational change in a triglyceride lipase. Biochemistry **31**:1532-1541.

De Jong, L.P.A. and Kossen, S.P. (1985). Stereospecific reactivation of human brain and erythrocyte acetylcholinesterase inhibited by 1,2,2-trimethylpropyl methylphosphonofluoridate (soman). Biochim. Biophys. Acta. **830**:345-348.

Doctor, B.P., Chapman, T.C., Christner, C.E., Deal, C.C., De La Hoz, M.K., Gentry, R.K., Orget, R.A., Rush, R.S., Smyth, K.K. and Wolfe, A.D. (1990). Complete amino acid sequence of fetal bovine serum acetylcholinesterase and its comparison in various regions with other cholinesterases. FEBS Let. **266**:123-127.

Doctor B.P., Blick, D.W., Gentry, M.K., Maxwell, D.M., Miller, S.A., Murphy, M.R. and Wolfe, A.D. (1992). Acetylcholinesterase: a pretreatment drug for organophosphate poisoning. In: *Multidiciplinary Approaches to Cholinesterase Functions.* (Shafferman A. and Velan B. Eds.),pp. 277-286, Plenum Pub. Co., New York .

Douchet, J.C., Masson, P., and Morelis, P. (1982). Elimination de la cholinesterase humaine purifee injectee an rat. Trav. Sci. **3**:342-347.

Dougherty, D.A. and Stauffer, D.A. (1990). Acetylcholine binding by a synthetic receptor: Implication for biological recognition. Science **250**:1558-1560.

Dougherty, D.A. (1996). Cation-π interacions in chemistry and biology: A new view of benzene, Phe, Tyr, and Trp. Science **271**: 163-168.

Drzeniek, R. (1973). Substrate specificity of neuraminidases. Histochem. J. **5**: 271-290.

Dunbrack, R.L. and Karplus, M.(1993). Backbone-dependent rotamer library for proteins. J. Mol. Biol. **230**: 543-574.

Eastman, J., Wilson, E.J., Cervenansky, C. and Rosenberry ,T.L. (1995). Fasciculin 2 binds to the peripheral site on acetylcholinesterase and inhibits substrate hydrolysis by slowing a step involving proton transfer during enzyme acylation. J. Biol .Chem. **270**: 19694-19701.

Ellin, R.I. (1982). Anomalies in theories and therapy of intoxication by potent organophosphorus anticholinesterase compounds. Gen.Pharmacol. **13**: 457-466.

Ellman, G.L., Courtney, K.D., Andres, V. and Featherstone, R.M. (1961). A new and rapid colorimetric determination of acetylcholinesterase activity: Biochem. Pharmacol. **7**:88-95.

Eyer, P., Hagedorn, I., Klimmek, R., Lippstreu, P., Loffler, M., Oldiges, H., Spohrer, U., Steidl, I., Szinicz, L. and Worek, F. (1992). HLo dimethanesulfonate, a potent bispyridinium-dioxime against anticholinesterases. Arch. Toxicol. **66**: 603-621.

Faerman, C., Ripoll, D., Bon, S., Le Feuvre, Y., Morel, N., Massoulie, J., Sussman, J.L. and Silman, I. (1996). Site-directed mutants designed to test the back-door hypothesis of acetylcholinesterase function. FEBS Letts. **386**:65-71.

Fetrow, J.S.(1995). Omega loops: nonregular secondary structures significant in protein function and stability. FASEB J. **9**: 708-717.

Fisher, M., Ittah, A., Liefer, I., and Gorecki, M. (1993). Expression and recognition of biologically active human acetylcholinesterase from *E. coli.* Molec. Cell. Neurobiol. **13**:25-38.

Fleisher, J.H. And Harris, L.W. (1965). Dealkylation as a mechanism for aging of cholinesterase after poisoning with pinacolyl methylphosphonoflouridate. Biochem. Phamacol. **14**: 641-650.

Fournier, D., Bride, J.-M., Hoffman, F. and Karch, F. (1992). Acetylcholinesterase: two types of modifications confer resistance to insecticide. J. Biol. Chem. **267**:12470-14274.

Friedman, J.S., Cofer, C.L., Anderson, C.L., Kushner, J.A., Gray, P.P., Chapman, G.E., Stuart, M.C., Lazarus, L., Shine J. and Kushner, P.J., (1989). High expression in mammalian cells without amplification. Bio/Technology, **7**:359-362.

Froede, H.C. and Wilson, I.B. (1971). Acetylcholinesterase. In "*The Enzymes*" (Boyer P.D. Ed.), Academic Press New-York 5, pp. 87-114.

Garel, L., Lozach, B., Dutasta, J.-P. and Collet, A. (1993). Remarkable effect of receptor size in the binding of acetylcholine and related ammonium ions to water soluble cryptophanes. J. Am. Chem. Soc. **115**: 11652-11653.

Gentry, M.K. And Doctor, B.P. (1995). Amino acid alignment of cholinesterases, esterases, lipases and related proteins. In: *Enzymes of the cholinesterase family* (Quinn, D.M., Balasubarmanian A.S., Doctor, B.P. and Taylor, P., eds.) Plenum Publishing Corp.,pp. 493-505.

Gerstein, M., Lesk, M.L., and Chothia, C. (1994). Structural mechanisms for domain movements in proteins. Biochemistry **33**: 6739-6749.

Gibney, G., Camp, S., Dionne, M., MacPhee-Quigley, K. and Taylor, P. (1990). Mutagenesis of essential functional residues in acetylcholinesterase. Proc. Natl. Acad. Sci. USA. **87**:7546-7550.

Gilson, M.K., Straatsma, T.P., McCammon, J.A., Rippoll, D.R., Faerman, C.H., Axelsen, P.H.. Silman, I. And Sussman, J.L. (1994). Open "back door" in molecular dynamics simulations of acetylcholinesterase. Science **263**:1276-1278.

Gnatt, A., Lowenstein, Y., Yaron, A., Schwarz, M. and Soreq, H. (1994) . Site directed mutagenesis of active-site residues reveals plasticity of human butyryochoinesterase in substrates and inhibitors interactions. J. Neurochem. **62**:749-755.

Grabenhorst, E., Hoffmann A., Nimtz, M., Zettlmeissl, G. and Conradt, H. S. (1995). Construction of stable BHK-21 cells coexpressing human secretory glycoproteins and human Gal(β1–4)GlcNac-R α2,6 sialyltransferase α2,6-linked NeuAc is preferentially attached to the Gal(β1–4)GlcNAc Gal(β1–2)Man Gal(α1–3)–branch of diantennary oligosaccharides from secreted recombinant β–trace protein. Eur. J. Biochem. **232**: 718-725.

Gray, A.P. (1984). Design and structure-activity relationships of antidotes to organophosphorus anticholinesterase agents. Drug Metabolism Rev. **15**:557-589.

Green, A.L. and Smith, H.J. (1958). The reactivation of cholinesterase inhibited organophosphorus compounds. Biochem. J. **68**: 28-31.

Grochulski, P., Bouthillier, F., Kazlauskas, R.J., Serreqi, A.N., Schrag, J.D. Ziomek, E. and Cygler, M. (1994). Analogs of reaction intermediates identify a unique substrate binding site in *Candida rugosa* lipase. Biochemistry **33**:3494-3500.

Grunwald, J., Segal, Y., Shirin, E., Waysbrot, D., Steinberg, N., Silman, I. and Ashani, Y. (1989). Aged and non-aged pyrenebutyl-containing organophosphoryl conjugates of chymotrypsin. Biochem. Pharmacol. **38**:3157-3168.

Gu, X., Harmon, B. J. and Wang, D. I. C. (1997). Site and branch-specific sialylation of recombinant human interferon-γ in chinese hamster ovary cell culture. Biotechnol. Bioeng. **55**: 390-398.

Hall, L.M,C,. and Spierer, P. (1986). The ace locus of Drosophila melanogaster: Structural gene for acetylcholinesterase with an unusual 5' leader. EMBO J. **5**:2949-2954.

Harel, M., Su, C.T., Frolow, F., Ashani, Y., Silman, I. and Sussman, J.L. (1991). Refined crystal structure of "aged" and "non-aged" organophosphoryl conjugates of γ-chymotrypsin. J. Mol. Biol. **221**:909-918.

Harel, M., Sussman, J.L., Krejci, E., Bon, S., Chanal, P., Massoulie, J. and Silman, I. (1992). Conversion of acetylcholinesterase to butyrylcholinesterase: modeling and mutagenesis. Proc. Natl. Acad. Sci. USA **89**:10827-10831.

Harel, M., Schalk, I., Ehret-Sabatier, L., Bouet, F., Goeldner, M., Hirth, C., Axelsen, P.H., Silman, I., and Sussman, J.L. (1993). Quaternary ligand binding to aromatic residues in the active-site gorge of Acetylcholinesterase. Proc. Natl. Acad. Sci. USA **90**:9031-9035.

Harel, M., Kleywegt, G.J., Ravelli , R.B.G., Silman, I. and Sussman, J.L.(1995). Crystal structure of an acetylcholinesterase-fasciculin complex: interaction of a three-fingered toxin from snake venom with its target. Structure **3**:1355-1366.

Harel, M., Quinn, D.M., Nair, H.K., Silman, I. and Sussman, J.L. (1996). The x-ray structure of a transition state analog complex reveals the molecular origins of the catalytic power and substrate specificity of acetylcholinesterase. J. Am. Chem. Soc. **118**:2340-2346.

Harris, L.W., Fleisher, J.H., Clark, J. And Cliff, W.J. (1996). Dealkylation and loss of capacity for reactivation of cholinesterase inihibited by sarin. Science **154**: 404-407.

Harvey, B., Scott, R.P., Sellers, D.J. And Watts, P. (1968). *In vitro* studies on the reactivation by oximes of phosphylated acetylcholinesterase. Biochem.Pharmacol. **35**: 745-751.

Hobbiger, F., (1955). Effect of nicotinhydroxamic acid methiodide on human plasma cholinesterase inhibited by organophosphates containing a dialkylphosphoro group. Brit. J. Pharmacol. **10**:356-359.

Hosea, N.A., Brman, H.A., and Taylor, P. (1995). Specificity and orientation of trigonal carboxyl esters and tetrahedral alkylphosphonyl esters in cholinesterases. Biochemistry **34**: 11528-11536.

Hucho, F., Jarv, J., and Weise, C. (1991). Substrate-binding sites in acetylcholinesterase. Trends Pharmacol. Sci. **12**:422-427.

Hucho, F., Tsetlin, V.I. and Machold, J. (1996). The emerging three-dimensional structure of a receptor. The nicotinic acetylcholine receptor. Eur. J. Biochem. **239**:539-557.

Joseph, D., Petsko, G.A. and Karplus, M.(1990). Anatomy of a conformational change: Hinged "lid" motion of the triosephosphate isomerase loop. Science **249**:1425-1428.

Joshi, L., Murata, Y., Wondisford, F. E., Szkudlinski, M., W., Desai, R. and Weintraub,B.D. (1995). Recombinant tyrotropin containing a β-subunit chimera with the human chorionic gonadotropin-β carboxy-terminus is biologically active, with a prolonged plasma half-life: role of carbohydrate in bioactivity and metabolic clearance. Endocrinology. **136**: 225-230.

Karplus, M., Evanseck, J.D., Joseph, D., Bash, P.A. and Field, M.J. (1992). Simulation analysis of triose phosphate isomerase: conformational transition and catalysis. Faraday Discuss. **93**: 239-248.

Kearney, P.C., Mizoue, L.S., Kumpf, R.A., Forman, J.F., McCurdy, A. and Dougherty, D.A. (1993). Molecular recognition in aqueous media. New binding studies provide further insights into the cation-π interaction and related phenomena. J. Am. Chem. Soc. **115:** 9907-9919.

Keijer, J.H. and Wolring, G.Z. (1969). Stereospecific aging of phosphonylated cholinesterases. Biochim. Biophys. Acta 185: 465-468.

Keijer, J.H., Wolring, G.Z. and De Jong, P.A. (1974). Effect of pH, temperature and ionic strength on the aging of phosphonylated cholinesterases. Biochemica et Biophysica Acta **334**: 146-155.

Kempner, E.S. (1993). Movable lobes and flexible loops in proteins. FEBS Lett. **326**: 4-10.

Kerem, A., Kronman, C., Bar-Nun, S., Shafferman, A. and Velan, B. (1993). Interrelation between assembly and secretion of recombinant human acetylcholinesterase. J. Biol. Chem. **268**:180-184.

Kim, K.S., Lee, J.Y., Lee, S.J., Ha, T.-K. and Kim, D.H. (1994). On binding forces between aromatic ring and quaternary ammonium compound. J. Am. Chem. Soc. **116**:7399-7400.

Kirby, A.J. And Younas, M. (1970). The reactivity of phosphate esters. Reactions of diesters with nucleophiles.

Kossiakoff, A.A. and Spencer, S.A. (1980). Neutron diffraction identifies His57 as the catalytic base in trypsin. Nature **288**:414-416.

Kovach, I.M. and Bennet, A.J. (1990). Comparative study of nucleophilic and enzymic reactions of 2-propyl methylphosphonate derivatives. Phosphorus, Sulfur, and Silicon **51/52**: 51-56.

Krieger, M. and Herz, J. (1994). Structures and functions of multiligand lipoprotein receptors: macrophage scavanger receptors and LDL receptor related protein (LRP). Ann. Rev. Biochem. **63**: 601-637.

Kronman C., Velan B., Gozes Y., Leitner M., Flashner Y., Lazar A., Marcus D., Serry T., Papier Y., Grosfeld H., Cohen S., and Shafferman A. (1992). Production and secretion of high levels of recombinant human acetylcholinesterase in cultured cell lines. Gene **121**:295-304.

Kronman, C.,Ordentlich, A., Barak, D., Velan, B. and Shafferman, A. (1994). The back door hypothesis for product clearance in acetylcholinesterase challenged by site directed mutagenesis. J. Biol. Chem. **269**: 27819-27822.

Kronman, C., Velan, B., Marcus, D., Ordentlich, A., Reuveny, S. and Shafferman, A. (1995). Involvement of oligomerization, N-glycosylation and sialylation in the clearance of cholinesterases from the circualtion. Biochem. J. **311**: 959- 967.

Kumpf, R.A. and Dougherty, D.A. (1993). A mechanism for ion selectivity in potassium channels: computational studies of cation-π interactions. Science **261**:1708-1710.

Laughton, C.A. (1994). A study of simulated annealing protocols for use with molecular dynamics in protein structure predictions. Protein Eng. **7**: 235-241.

Lazar, A., Reuveny, C., Kronman C., Velan, B., and Shafferman, A. (1993). Evaluation of anchorage-dependent cell propagation system for production of human acetylcholinesterase by recombinant 293 cells. Cytotechnology **13**:115-123.

Lee, E.U., Roth, J. and Paulson, J.C. (1989). Alteration of terminal glycosylation sequences on N-linked oligosaccharides of chinese hamster ovary cells by expression of β -galactoside α 2,6-sialyltransferase. J. Biol. Chem. **264**: 13848-13855.

Leszczynski, J. F. and Rose, G.D.(1986). Loops in globular proteins: A novel category of secondary structure. Science **234**: 850-855.

Levy D., and Ashani Y. (1986). Synthesis and in vitro properties of a powerful quaternary methylphosphonate inhibitor of acetylcholinesterase. Biochem. Pharmacol. **35**:1079-1085.

Li, Y.-T., Hsieh, Y.-L., Henion, J.D. and Ganem, B. (1993). Studies on heme binding in myoglobin, hemoglobin, and cytochrome c by ion spray mass spectrometry. J. Am. Soc. Mass Spectrom. **4**:631-637.

Lin, Z and Johnson, M.E. (1995). Proposed cation-π mediated binding by factor Xa: a novel enzymatic mechanism for molecular recognition. FEBS Lett. **370**:1-5.

Lockridge, O., Bartels, C.F., Vaughan, T.A., Wong, C.K., Norton, S.E., and Johnson L.L. (1987). Complete amino acid sequence of human serum cholinesterase. J. Biol. Chem. **262**:549-557.

Lolis, E. and Petsko, G.A.(1990). Crystallographic analysis of the complex between triosphosphate isomerase and 2-phosphoglycolate at 2.5Å resolution: implications for catalysis. Biochemistry **29**: 6619-6625.

Loewenthal, R., Sancho, J. and Fersht, A.R. (1992). Histidine-aromatic interactions in barnase. Elevation of histidine pKa and contribution to protein stability. J. Mol. Biol. **224**:759-770.

Ma, J., Qian, R., Rausa III, F. M. and Colley, K. J. (1997). Two naturally occuring α2,6-sialyltransferase forms with a single amino acid change in the catalytic domain differ in their catalytic activity and proteolytic processing. J. Biol. Chem. **272**: 672-679.

Maglothin, J.A., Wins, O. and Wilson, I.B. (1975) Reactivation and aging of diphenyl phosphoryl acetylcholinesterase. Biochim Biophys Acta **403**:370-387

Main, A.R. (1964). Affinity and phosphorylation constants for the inhibition of esterases by organophosphates. Science **144**: 992-993.

Main, A.R. and Iverson, F. (1966). Measurement of the affinity of phosphorylation constants governing irreversible inhibition of cholinesterase by diisopropylphosphorofluoridate. Biochem. J. **100**: 265-275.

Main, A.R. (1976). Structure and Inhibitors of Cholinesterase. In: *Biology of Cholinergic Function* , Goldberg, A.M. and Hanin, A. (Eds.), Random Press, New York, pp. 269-353.

Masson, P., Gouet, P. and Clery, C. (1994). Pressure and propylene carbonate denaturation of native and "aged" phosphorylated cholinesterase. J. Mol. Biol. **238**: 466-478.

Massoulie, J., Pezzementi, L., Bon, S., Krejci, E., and Vallette, F.-M. (1993). Molecular and cellular biology of Cholinesterases. Prog. Neurobiol. **41**:31-91.

Massoulie, J., Sussman, J.L., Doctor, B.P., Soreq, H., Velan, B., Cygler, M., Rotundo, R., Shafferman, A., Silman, I. and Taylor, P. (1992). Recommendations for nomenclature in cholinesterases. In: *Multidisciplinary Approaches to Cholinesterase Functions.* (Shafferman A. and Velan B. Eds.), pp.285-288, Plenum Pub. Co., New York.

Matsuura, F., Ohta, M., Ioannou,Y.A. and Desnick, R.J. (1998). Human α-galactosidase A: characterization of the N-linked oligosaccharides and secreted glycoforms overexpressed by Chinese hamster ovary cells. Glycobiology. **8**: 329-339.

McCurdy, A., Jimenez, L., Stauffer, D. A., and Dougherty, D. A. (1992). Biomimetic catalysis of S_N2 reactions through cation-π interactions. The role of polarizability in catalysis. J. Am. Chem. Soc. **114**: 10314-10321.

Méric, R., Vigneron, J.-P. and Lehn J.-M. (1993) Efficient camplexation of quaternary ammonium compounds by a new water-soluble macrobicyclic receptor molecule. J. Chem. Soc. Chem. Commun. 129-131.

Michel, H.O., Hackley Jr, B.E., Berkowitz, L., List, G., Hackley, E.B., Gilliam, W.and Paukan, M., (1967). Aging and dealkylation of soman-inactivated eel cholinesterase. Arch. Biochem. Biophys. **121**:29-34.

Minch, S. L., Kallio, P.T. and Bailey, J. E. (1995). Tissue plasminogen activator coexpressed in chinese hamster ovary cells with α(2,6)-sialyltransferase contains NeuAc α(2,6)Gal β(1,4)Glc-N-AcR linkages. Biotechnol. Prog. **11**: 348-351.

Monard, C. and Quinchon, R. (1961). Preparation and physical properties of isopropyl methylfluorophosphonate I. J. Bull. Soc. Chim. Fr. 1084-1087.

Monica, T. J., Andersen, D. C. and Goochee, C. F. (1997). A mathematical model of sialylation of N-linked oligosaccharides in the trans-Golgi network. Glycobiology. **7**: 515-521.

Mullner, H. and Sund, H. (1980) Essential arginine residues in acetylcholinesterase from Torpedo californica. FEBS Lett. **119**:283-287.

Nakagawa, S., Yu, H.-A., Karplus, M. and Umeyama, H.(1993). Active site dynamics of acyl-chymotrypsin. Proteins:Struct.Func.Genet. **16**: 172-194.

Narita, M., Bu., G., Herz, J. and Schwartz, A. L. (1995a). Two receptor systems are involved in the plasma clearance of tissue-type plasminogen activator (t-PA) J. Clin. Invest. **96**: 1164-1168.

Narita, M., Bu, G., Olins, G. M., Higuchi, D. A., Herz, J., Broze Jr., G. J. and Schwartz, A.L. (1995b). Two receptor systems are involved in the plasma clearance of tissue-type plasminogen inhibitor. J. Biol. Chem. **270**: 24800-24804.

Norin, M., Olsen, O., Svendsen, A., Edholm, O. and Hult, K.(1993). Theoretical studies of Rhizomucor miehli lipase activation. Protein Eng. **6**: 855-863.

Norvall, G. and Hacksell, U. (1992) Binding-site modeling of the muscarinic m1 receptor: a combination of homology-based and indirect approaches. J. Med. Chem. **36**:967-976.

Ollis, D.L., Cheah, E., Cygler, M., Dijkstra, B., Frolow, F., Franken, S.M., Harel,M., Remington, S.J., Silman, I., Schrag, J., Sussman, J.L., Verscchueren, K.H.G., and Goldman, A. (1992). The α/ß hydrolase fold. Protein Eng.: **5**, 197-211.

Olson,P.F., Fessler,L.I., Nelson R.E., Cambell,A.G., and Fessler J.H. (1990). Glutactin, a novel Drosophila basement membrane-related glycoprotein with sequence similarity to serine esterase.EMBO J. **9**: 3593-3601.

Ordentlich A., Barak D., Kronman C., Flashner Y., Leitner M.,Segall Y., Ariel N., Cohen S., Velan B.,and Shafferman A. (1993a). Dissection of the human acetylcholinesterase active center - determinants of substrate specificity: Identification of residues constituting the anionic site, the hydrophobic site, and the acyl pocket. J. Biol. Chem. **268**:17083-17095.

Ordentlich, A., Kronman, C., Barak, D., Stein, D., Ariel, N., Marcus, D., Velan, B., and Shafferman, A. (1993b). Engineering resistance to 'aging' in phosphylated human acetylcholinesterase - role of hydrogen bond network in the active center. FEBS Lett. **334**:215-220.

Ordentlich, A., Barak, D., Kronman, C., Ariel, N., Segall, Y., Velan, B., and Shafferman, A. (1995). Contribution of aromatic moieties of tyrosine 133 and of the anionic subsite tryptophan 86 to catalytic efficiency and allosteric modulation of acetylcholinesterase. J. Biol.Chem. **270**: 2082-2091.

Ordentlich, A., Barak, D., Kronman, C., Ariel, N., Segall, Y., Velan, B., and Shafferman, A. (1996). The architecture of human acetylcholinesterase active center probed by interactions with selected organophosphate inhibitors. J. Biol.Chem. **271**: 11953-11962.

Ortiz, A.R., Pisabarro, M.T., Gallego, J. and Gago, F. (1992). Implications of a concensus recognition site for phosphatidylcholine separate from the active site in Cobra venom phospholipases A_2. Biochemistry **31**:2887-2896.

Patel.T., Bruce, J., Merry, A., Bigge, C., Wormald, M., Jaques, A. and Parekh, R. (1993). Use of hydrazine to release intact and unreduced form both N- and O- linked oligosaccharides from glycoprotein. Biochemistry. **32**: 679-693.

Paulson, J. C., Weinstein, J. and Schauer, A. (1989). Tissue-specific expression of sialyltransferases. J. Biol. Chem. **264**:10931-10934.

Paulson, J. C., and Colley, K. J., (1989). Glycosyltransferases: structure, localization and control of cell type-specific glycosylation. J. Biol. Chem. **264**: 17615-17618.

Pearlman, D.A., Case, D.A., Caldwell, J.C., Seibel, G.I., Singh, U.S., Weiner, P. & Kolmann, P.A. (1991). AMBER 4.0, University of California, San Fransisco.

Prody, C.A., Zevin-Sonkin, D., Gnatt, A., Goldberg, O., and Soreq, H. (1987). Isolation and characterization of full length cDNA clones coding for cholinesterase from fetal human tissues. Proc. Natl. Acad. Sci. USA. **84**:3555-3559.

Qian, N. and Kovach, I.M. (1993). Key active site residues in the inhibition of acetylcholinesterases by soman. FEBS lett. **336**: 263-266.

Quinn, D.M. (1987). AChE: Enzyme structure, reaction dynamics and virtual transition states. Chem. Rev. **87**:955-979.

Rachinsky,T.L., CampS.,Li, Y.,Ekstrom, T,J.,Newton, M.,and Taylor P.(1990). Molecular cloning of mouse acetylcholinesterase: Tissue distribution of alternatively spliced mRNA species. Neuron **5**:317-327.

Radic, Z., Reiner, E., and Taylor, P. (1991). Role of the peripheral anionic site on acetylcholinesterase: inhibition by substrates and coumarin derivatives. Mol. Pharmacol., **39**: 98-104.

Radic, Z., Gibney, G., Kawamoto, S., MacPhee-Quigley, K., Bongiorno, C., and Taylor, P. (1992). Expression of recombinant acetylcholinesterase in Baculovirus system: kinetic properties of glutamate 199 mutant. Biochemistry **31**:9760-9767.

Radic, Z., Pickering, N.A., Vellom, D.C., Camp, C., and Taylor, P. (1993). Three distinct domains in the cholinesterase molecule confer selectivity for acetyl and butyrylcholinesterase inhibitors. Biochemistry **32**:12074-12084.

Radic, Z., Duran, R., Vellom, D. C., Li, Y., Cervenansky, C., and Taylor, P. (1994). Site of fasciculin interaction with acetylcholinesterase. J. Biol. Chem. **269**: 11233-11239.

Radic, Z., Quinn, D.M., Vellom, D.C., Camp, S. and Taylor, P. (1995). Allosteric control of acetylcholinesterase catalysis by fasciculin. J. Biol. Chem. **270**: 20391-20399.

Raine, A.R.C., Yang, C.-C., Packman, L.C., White, S.A., Mathews, F.S. and Scrutton, N.S. (1995). Protein recognition of ammonium cations using side-chain aromatics: a structural variation for secondary ammonium ligands. Protein Sci. **4**:2625-2628.

Rao Thotakura, N., Szkudlinski, M. W. and Weintraub, B. D. (1994). Structure- function studies of oligosaccharides of recombinant human thyrotrophin by sequential deglycosylation and resialylation. Glycobiology. **4**: 525-533

Raveh, L., Ashani, Y., Levi, D., De La Hoz, D., Wolfe, A.D. and Doctor, B.P. (1989). Acetylcholinesterase prophylaxis against organophosphate poisoning: Quantitative correlation between protection and blood-enzyme level in mice. Biochem. Pharmacol. **38**:529-534.

Raveh, L., Grunwald, J., Marcus, D., Papier, Y., Cohen, E., and Ashani, Y. (1993). Human butyrylcholinesterase as a general prophylactic antidote for nerve agent toxicity. Biochem. Pharmacol. **45**:2465-2472.

Ripoll, D.L., Faerman, C.H., Axelsen, P.H., Silman, I., and Sussman, J.L. (1993). An electrostatic mechanism for substrate guidance down the aromatic gorge of AchE. Proc. Natl. Acad. Sci. USA **90**:5128-5132.

Rosenberry, T.L. (1975). Acetylcholinesterase. Adv. Enzymol. Relat. Areas. Mol. Biol. **43**:103-219.

Rosenberry, T.L. and Berhnard, S.A. (1972). Studies of catalysis by acetylcholinesterase: synergistic effects of inhibitors during the hydrolysis of acetic acid esters. Biochemistry **11**:4308-4321.

Roufogalis, B. D., and Quist, E. E. (1972). Relative binding sites of pharmacologically active ligands on bovine erythrocyte acetylcholinesterase. Mol. Pharmacol. **8**: 41-49

Roussaux, C.G. and Dua, A.K. (1989). Pharmacology of HI-6 an H-series oxime. Can. J. Physiol. Pharmacol. **67**:1183-1189.

Ryckaert ,J.P., Ciccoti , G and Berendsen, H.J.C. (1977). Numerical integration of the cartesian equations of motion of a system with constraints: molecular dynamics of n-alkanes. J. Comput. Phys **23**: 327-341.

Saxena, A., Doctor, B.P., Maxwell, D.M., Lenz, D.E., Radic, Z. and Taylor, P. (1993). The role of glutamate-199 in the aging of cholinesterase. Biochem. Biophys. Res.Comm. **197**: 343-349.

Saxena, A., Raveh, L., Ashani, Y. and Doctor, B. P. (1997). Structure of glycan moieties responsible for the extended circulatory life time of fetal bovine serum acetylcholinesterase and equine serum butyrylcholinesterase. Biochemistry.**36**: 7481-7489.

Saxena, A., Ashani, Y., Raveh, L., Stevenson, D. and Doctor, B.P. (1998). Role of oligosaccharides in the pharmacokinetics of tissue-derived and genetically engineered cholinesterases. Mol. Pharmacol. **51**: 112-122.

Schumacher, M., Camp, S., Maulet, Y., Newton, M., MacPhee-Quigley, L., Taylor, S.S., Friedman, T., and Taylor, P. (1986). Primary structure of Torpedo californica acetylcholinesterase deduced from its cDNA sequence. Nature **319**:407-409.

Schwartz, T.W. (1994). Locating ligand-binding sites in 7TM receptors by protein engineering Curr. Opin. Biotechnol. **5**:434-444.

Segall, Y., Waysbort, D., Barak, D., Ariel, N., Doctor, B.P., Grunwald, J. and Ashani, Y. (1993). Direct observation and elucidation of the structures of aged and nonaged phosphorylated cholinesterases by 31P NMR spectroscopy. Biochemistry **32**:13441-13450.

Selwood, T., Feaster, S.R., States, M.J., Pryor, A.N. and Quinn, D.M. (1993). Parallel mechanisms in acetylcholinesterase- catalyzed hydrolysis of choline esters. J. Am. Chem. Soc. **115**: 10477-10482.

Shafferman, A. and Velan, B. Eds. (1992a). "*Multidisciplinary Approaches to Cholinesterase Functions*". Plenum Pub. Co., New York .

Shafferman, A., Kronman, C., Flashner, Y., Leitner, S., Grosfeld, H., Ordentlich, A., Gozes, Y., Cohen, S., Ariel, N., Barak, D., Harel, M., Silman, I., Sussman, J.L. and Velan. B., (1992b). Mutagenesis of human acetylcholinesterase: identification of residues involved in catalytic activity and in polypeptide folding. J. Biol. Chem. **267**:17640-17648.

Shafferman, A., Velan, B., Ordentlich, A., Kronman, C., Grosfeld, H., Leitner, M., Flashner, Y., Cohen, S., Barak, D., and Ariel, N. (1992c). Substrate inhibition of acetylcholinesterase: residues involved in signal transduction from the surface to the catalytic center. EMBO J. **11**:3561-3568.

Shafferman, A., Velan, B., Ordentlich, A., Kronman, C., Grosfeld, H., Leitner, M., Flashner, Y., Cohen, S., Barak, D., and Ariel, N. (1992d). Acetylcholinesterase catalysis-protein engineering studies. In: *Multidisciplinary Approaches to Cholinesterase Functions*. (Shafferman A. and Velan B. Eds.),pp. 165-175, Plenum Pub. Co., New York .

Shafferman, A., Velan, B., Barak, D., Kronman, C., Ordentlich, A., Flashner, Y., Leitner, M., Segall, Y., Grosfeld, H., Stein, D. and Ariel, N.(1993). Recombinant human acetylcholinesterase - enzyme engineering. Proc. Med. Def. Biosci. Rev. **3**:1111-1124

Shafferman, A., Ordentlich, A., Barak, D., Kronman, C., Ber, R., Bino, T., Ariel, N., Osman, R., and Velan, B. (1994). Electrostatic attraction by surface charge does not contribute to the catalytic efficiency of acetylcholinesterase. EMBO J. **13**:3448-3455.

Shafferman, A., Ordentlich, A., Barak, D., Kronman, C., Ariel, N., Leitner, M., Segall, Y., Bromberg, A., Reuveny, S., Marcus, D., Bino, T., Lazar, A., Cohen, S. and Velan, B. (1995). Molecular aspects of catalysis and of allosteric regulation of acetylcholinesterase. In: *Enzymes of the Cholinesterase Family*. (Balasubarmanian, A.S., Doctor, B.P., Taylor, P. and Quinn, D.M., Eds). pp 189-196, Plenum Publishing Co. , New York.

Shi, Z., Buntel, C.J. and Griffin, J.H. (1994). Isolation and characterization of the gene encoding 2,3-oxidosqualene-lanosterol cyclase from Saccharomyces cerevisiae Proc. Natl. Acad. Sci. USA **91**: 7370-7374.

Sikorov, J.L., Krejci E. and Massoulie J. (1987). cDNA sequence of *Torpedo marmorata* acetylcholinesterase: Primary structure of the precursor of a catalytic subunit: existence of multiple 5' untranslated regions. EMBO J. **6**:1865-1873.

Smith, P.L., Skelton, T.P., Fiete, D., Dharmesh, S.M., Beraneck, M.C., MacPhail, L., Broze, G.J. and Baenzinger, J.U. (1992). The asparagine-linked oligosaccharides of tissue factor pathway inhibitor terminate with SO_4-GalNac-beta1,4GlcNAc-beta1,2Man.J. Biol. Chem. **267**:19140-19146.

Soreq, H., Ben-Aziz, R., Prody, C., Gnatt, A., Neville, A., Lieman-Hurwitz, J., Lev-Lehman, E., Ginzberg, D., Seidman, S., Lapidot Lifson, Y. and Zakut, H. (1990). Molecular cloning and construction of the coding region for human acetylcholinesterase reveals a G+C reach attenuating structure. Proc. Natl. Acad. Sci. USA. **87**:9688-9692.

Staufer, D.A., Barrans, R.E. and Dougherty, D.A. (1990). Concerning the thermodynamics of molecular recognition in aqueous and organic media. Evidence for significant heat capacity effects. J. Org. Chem. **55**:2762-2767.

Steinberg, N., van der Drift, A.C.M., Grunwald, J., Segall, Y., Shirin, E., Haas, E., Ashani, Y. and Silman, I. (1989). Conformational differences between aged and nonaged pyrenebutyl-containing organophosphoryl conjugates of chymotrypsin as detected by optical spectroscopy. Biochemistry **28**: 1248-1253.

Sussman J.L, Harel M., Frolow F.,Oefner C. Goldman A. and Silman I.(1991). Atomic structure of acetylcholinesterase from *Torpedo californica*: A prototypic acetylcholine binding protein.Science. **253**:872-879.

Szkudlinski, M. W., Rao Thotakura, N., Tropea, J. E., Grossmann, M. and Weintraub,B.D. (1995). Aspargine-linked oligisaccharide structures determine clearance and organ distribution of pituitary and recombinant thyrotropin. Endocrinology. **136**: 3325-3329.

Taylor P. and Lappi S. (1975). Interaction of fluorescent probes with acetylcholinesterase : the site and specificity of propidium binding.Biochemistry **14**:1989-1997.

Taylor P. (1990). In: "*Pharmacological Basis of Therapeutics*" (Gilman A.G., Goodman L.S., Rall T., and Murad F. Eds.); MacMillan New York, pp 131-149.

Taylor, P., and Radic, Z. (1994). The cholinesterases: from genes to proteins. Ann. Rev. Pharmacol. Toxicol. **34**:281-320.

Thompson, C.M., Ryu, S. and Berkman, C.E. (1992). Consequence of phosphorus stereochemistry upon the postinhibitory reaction kinetics of acetylcholinesterase poisoned by phosphorothiolates. J. Am. Chem. Soc. **114**:10710-10715.

van Tilbeurgh, H., Egloff, M.P., Martinez, C., Rugani, N., Verger, R. and Cambillau, C.(1993). Interfacial activation of the lipase-procolipase complex by mixed micelles revealed by X-ray crystallography. Nature **362**: 814-820.

Trumpp-Kallmeyer, S., Hoflack, J., Bruinvels, A. and Hibert, M. (1992) Modeling of G-protein coupled receptors: Application to dopamine, adrenaline, serotonin, acetylcholine and mammalian opsin receptors. J. Med. Chem., **35**:3448-3462.

Tsuji, S., Datta, A. and Paulson, J. C. (1996). Systematic nomenclature for sialyltransferases. Glycobiology. **6**: pp. v-xiv

Van der Drift, A.C.M., Beck, H.C., Decker, A.G., Hulst, A.G. and Wils, E.R.G. (1985). ^{31}P NMR and mass spectrometry of atropinesterase and some serine proteases phosphorylated with a transition-state analogue. Biochemistry **24**:6894-6903.

Velan, B., Kronman, C., Grosfeld, H., Leitner, M., Gozes, Y., Flashner, Y. Serry, T., Cohen, S., Benaziz, R., Seidman, S., Shafferman, A. and Soreq, H. (1991a). Recombinant human acetylcholinesterase is secreted from transiently transfected 293 cells as a soluble globular enzyme. Cell. Mol. Neurob. **11**:143-156.

Velan B.,Grosfeld H.,Kronman C.,Leitner M.,Gozes Y.,Lazar A.,Flashner Y.,Marcus D., Cohen S., and Shafferman A. (1991b). The effect of elimination of intersubunit disulfide bonds on the activity, assembly and secretion of recombinant human acetylcholinesterase. J.Biol.Chem. **266**:23977-23984.

Velan, B., Grosfeld, H., Kronman, C., Flashner, Y., Leitner, M., Cohen, S., and Shafferman, A. (1993a). N-glycosylation of human acetylcholinesterase : efects on activity, stability and biosynthesis. Biochem. J. **296**:649-656.

Velan, B., Kronman, C., Lazar, A., Ordentlich, A., Flashner, Y., Leitner, M., Marcus, D., Reuveny, S., Grosfeld, H., Cohen, S. and Shafferman, A. (1993b). Recombinant human acetylcholinesterase - production and post-translational pocessing. Proc. Med. Def. Biosci. Rev. **3**:1097-1108.

Velan, B., Kronman, C., Ordentlich, A., Flashner, Y., Ber, R., Cohen, S., and Shafferman, A. (1994). Post translational processing of acetylcholinesterase - cellular control of biogenesis and secretion . In: *Enzymes of the Cholinesterase Family*. (Balasubarmanian, A.S., Doctor, B.P., Taylor, P., and Quinn, D.M., Eds.). pp. 269-276. Plenum Publishing Co.

Vellom , D.C., Radic, Z., Li, Y., Pickering, N.A., Camp, S. and Taylor, P. (1993). Amino acid residues controlling acetylcholinesterase and butyrylcholinesterase specificity. Biochemistry **32**:12-17.

Wade, R.C., Davis, M.E., Luty ,B.A., Madura, J.D.and McCammon, J.A.(1993). Gating of the active site of triose phosphate isomerase: Brownian dynamics simulations of flexible peptide loops in the enzyme. Biophys. J. **64**: 9-15.

Warren, L. (1959). The thiobarbituric acid assay of sialic acids. J. Biol. Chem. **234**:1971-1975.

Warshel, A. in: *Computer Modeling of Chemical Reactions in Enzymes and Solutions*. 1991, Ch. 6, Wiley-Interscience Pub., New York.

Weiner, S.J., Kolman, P.A., Nguyen, D.T. And Case, D.A. (1986). An all-atom force field for simulations of proteins and nucleic acids. J. Comput. Chem. **7**:230-252.

Weinstein, J., Lee, E.U., McEntee, K., Lai, P.-H. and Paulson, J.C. (1987). Primary structure of β-galactoside α2,6-sialyltransferase. J. Biol. Chem. **262**: 17735-17743.

Weinstein, J., de Souza-e-Silva, U. and Paulson, J. C. (1982a). Purification of a Galβ1--> 4GlcNac α2-->6 sialyltransferase and a Galβ1-->3(4)GlcNacα2-->3 sialyltransferase to homogeneity from rat liver. J. Biol. Chem. **257**: 13835-13844.

Weinstein, J., de Souza-e-Silva, U. and Paulson, J. C. (1982b). Sialylation of glycoprotein oligosaccharides N-linked asparagine. J. Biol. Chem. **257**: 13845-13853.

Weise C. Kreienkamp h-J.,Raba R.,Pedak A., Aaviksaar A., and Hocho F. (1990). Anionic subsites of the acetylcholinesterase from Torpedo californica : affinity labelling with the cationic reagent N,N-dimethyl-2-phenyl-aziridinium. EMBO **9**:3885-3888.

Whiteley, C.G. And Ngwenya, D.S. (1995). Protein ligand interactions: alkylated pyridinium salts as inhibitors of acetylcholinesterase from *Electrphorus Electricus*. Biochem. Biophys. Res. Comm. **211**: 1083-1090.

Williams, J.C. and McDermott, A.E.(1995). Dynamics of the flexible loop of triosphosphate isomerase: The loop motion is not ligand gated. Biochemistry **34**: 8309-8319.

Wilson, I.B. (1967) in: Drugs affecting the peripheral nervous system (Burger A. Ed.) pp.381-397, Marcel Dekker, New York.

Wilson, B.W., Hooper, M.J., Hensen, M.E. And Neiberg, P.S.(1992). Reactivation of organophosphorus inhibited ache with oximes. In: organophosphates chemistry,fate and effecs (Chambers, J.E. And Levi, P.E. Eds.), pp.107-137, Academic Press, San Diego.

Winstein, S. and Marshall, H. (1952). Neighboring carbon and hydrogen. IV. Formolysis and other solvolysis rates of some simple secondary and primary benzenesulfonates. J. Am. Chem. Soc. 74:1120-1126.

Wolfe, A.D., Rush, R.S., Doctor, B.P., Koplovitz I., and Jones, D., (1987). Acetylcholinesterase prophylaxis against organophosphate toxicity. Fundam Appl Toxicol. 9: 266-270.

Yan, S.B., Chao, Y.B., and van Halbeek, H. (1993). Novel Asn-linked oligosaccharides terminating in GalNac beta (1,4) the (alpha1,3)GlcNac are present in recombinant human PKC expressed in HEK293 cells. Glycobiol. 3:597-608.

Yaron, A. and Naider, F. (1993). Proline-dependent structural and biological properties of peptides and proteins. Criti. Rev. Biochem. Molec. Biol. 28: 31-81.

Yates, C.M., Simpson,J., Moloney, A.F.J., Gordon, A. and Reid, A.H. (1980). Alzheimer like cholinergic deficiency in Down Syndrome, Lancet, 2:979-980.

Yeh, J.-C. and Cummings, R. D. (1997). Differential recognition of glycoprotein acceptors by terminal glycosyltransferases. Glycobiology. 7: 241-251